# ENERGY EFFICIENCY ANALYSIS AND IMPROVING PERFORMANCE OF LIGHT EMITTING DIODES

Master Thesis

by

Halil İbrahim Kahvecioğlu

Submitted to the

Graduate School of Sciences and Engineering

in Partial Fulfillment of the Requirements for

the degree of

Master of Science

in the

Department of Mechanical Engineering

**Özyeğin University**

December 2018

# ENERGY EFFICIENCY ANALYSIS AND IMPROVING PERFORMANCE OF LIGHT EMITTING DIODES

**Approved by:**


**Prof. Dr. Mehmet Arık (Advisor)**
Department of Mechanical Engineering
Özyeğin University

**Prof. Dr. Taylan Akdoğan**
Departmant of Natural and Mathematical Sciences
Özyeğin University

**Assist. Prof. Dr Mete Budakli**
Department of Mechanical Engineering
Turkish-German University


Date Approved: December 2018

*Dedicated to all human beings*

# ABSTRACT

Energy efficiency of light sources continually increases as the technology advance. Traditional light sources have inefficiency, large sizes, short life times and poisonous mercury vapor. On the other hand, the improvements in solid state lighting like light emitting diode caused them to take place of traditional light sources because they have small sizes, high color quality, long life, high efficiency and low power consumption. Despite such benefits, LEDs' performance can still be improved. In this study, some packaging elements of white light emitting LEDs have been studied about energy gain and loss such as chip, phosphor, encapsulant, and optical elements (lenses and reflectors). Moreover, elevated temperatures in LEDs can decrease the chip's external quantum efficiency and light conversion efficiency of the phosphor. Although, remote phosphor technique can provide better thermal performance in LED systems, high power requirements have needed better application. Hence, dielectric liquid coolant integrated remote phosphor used LED package has been proposed for an experimental and computational research. Experiments, which contain the combined optical and thermal effects, have been performed with the proposed dielectric liquid cooled remote phosphor coated LED. The total light extraction enhancement has been achieved about 25-26% with the aid of liquid injection. Then, problem has been computationally simulated for optical effects. The overall optical flux performance has reached about 13% for remote phosphor used LED package with a liquid injection. Hence, the rest of the improvements about 12-13% have been induced by thermal effects.

# ÖZETÇE

Işık kaynaklarının enerji verimliliği gelişen teknoloji ile artmaktadır. Geleneksel olarak kullanılan ışık kaynakları düşük verimli olup, aynı zamanda boyutça büyük ve kısa ömürlüdür ve civa gibi bazı zehirli gazları içermektedirler. Fakat, yarı iletken teknolojisinin gelişmesiyle ışık yayan diyotlar küçük yapıları, uzun ömürlü olmaları, yüksek verim ve düşük enerji tüketimi gibi nedenlerle geleneksel olarak kullanılan ışık kaynaklarının yerini almaya başlamışlardır. Bu tür avantajlarına rağmen, henüz LED'lerdeki enerji verimi yeterince yüksek olmayıp, çok daha arttırılabilir bir potansiyele sahiptir. Bu çalışmada, beyaz ışık yayan LED ışık kaynaklarında bulunan çip, fosfor, silikon muhafaza, lens ve reflektör gibi bileşenlerindeki enerji kazanç ve kayıplar çalışılmıştır. Buna ek olarak, yüksek LED sıcaklıkları çip ve fosfor verimini olumsuz etkilemektedir. LED'lerde fosforun uzağa yerleştirilmesi sıcaklıkların düşmesi yönünde olumlu sonuçlar vermesine rağmen, yüksek güçte çalışan LED'ler için soğutma işlemi problem olmaya devam etmektedir. Bu nedenle, uzak fosfor kullanılan LED'lerde dielektrik sıvı eklenmesi yoluyla verimi arttırmaya yönelik bir LED modeli çalışması yapıldı. Sıvı kullanımı ile soğutma ve optik nedenlerden dolayı LED paketinde ışık çıkış artışı elde edildi. Bütünleşik ışık veriminde bu yöntem ile %25-26 artış sağlanmış oldu. Deney ve simülasyonların karşılaştırılması yoluyla ise, lumen artışın %13'lük kısmının optik nedenlerden kaynaklandığını, geri kalan %12-13'lük artışın ise soğuma ve ısı iletimi yoluyla olduğu gösterildi.

# ACKNOWLEDGMENTS

Firstly, I would like to thank to my mother Firdevs, my father Ismail, my grandmother Nimet and my grandfather Raşid for always supporting me with their prayers. I also want to thank to my son Ali Kağan for being the joy in our home and I want to extend my gratitude to my wife Ayşe for her unbounded love and support during this research.

Then, I would like to express my sincere appreciation to my advisor, Prof. Dr. Mehmet Arık, for advising me in this thesis study in Evateg Center. I should also thank him again for educating new engineers, new scientist with wider visions.

Moreover, I am grateful to all of my friends (Mete Hoca, Enes T., Thamer, Burak, Mete, Nasır, Muhammed, Omid, Umut, Gökçe, Enes O., Ulaş, Songul, Mert) in Evateg Center for their ideas, and friendship. You will always have a special place in my life.

Lastly, I would like to thank to all unnamed brains and hearts for improving the knowledge since time began.

I see I have made myself a slave to Philosophy

– Newton, Isaac

# TABLE OF CONTENTS

# LIST OF TABLES

# LIST OF FIGURES

# CHAPTER I

# INTRODUCTION

## *1.1. What Is Light*

Philosophers have argued for centuries about the light that what is the nature of it. In the sacred text the most well-known is that God created light in the universe by this word: Let there be light. Hindu and Greek philosophers believed world was based on atoms of earth, water, fire, air, and light was brought out from these elements. Around 300 BC, Euclid described the laws of reflection of light, Ptolemy wrote about refraction. Later, in the 11$^{th}$ century Ibn al Haytham established the laws of refraction in this book Kitab al Manazir. He is known as the father of optics. In 984, the Persian mathematician Ibn Sahl correctly described refraction of light equivalent to Snell's law.

In the 17$^{th}$ century Johannes Kepler wrote about reflection by curved mirrors lenses, inverse square law determining the intensity of light. He also set out the theory of telescope. In the second half of the 17$^{th}$ century, Isaac Newton determined that white light was a mix of colors that separated by a prism. In 19$^{th}$ century, Young and Fresnel conducted experiments on the interference of light that shows the wave nature of light. For centuries, philosophers and scientists tried to understand the nature of light if it is particle, wave, both particle or wave, or neither.

Under the leadership of UNESCO, the organization IYL2015 (International Year of Light 2015) has gathered hundreds of international organizations together in order to raise awareness of light science in areas such as energy, health, education, sustainable development, climate-change [1].

Photons can be explained very well by quantum physics. They have particle wave duality. They have the properties of wave when their position is not measured. Whenever they interact with a matter, they behave like a particle. They do not have any mass. In the lower figure, we can see the wave property of photons occurring in a propagation of Young's Double Slit Experiment. This experiment proves the particle wave duality of photons (Figure 1-1).

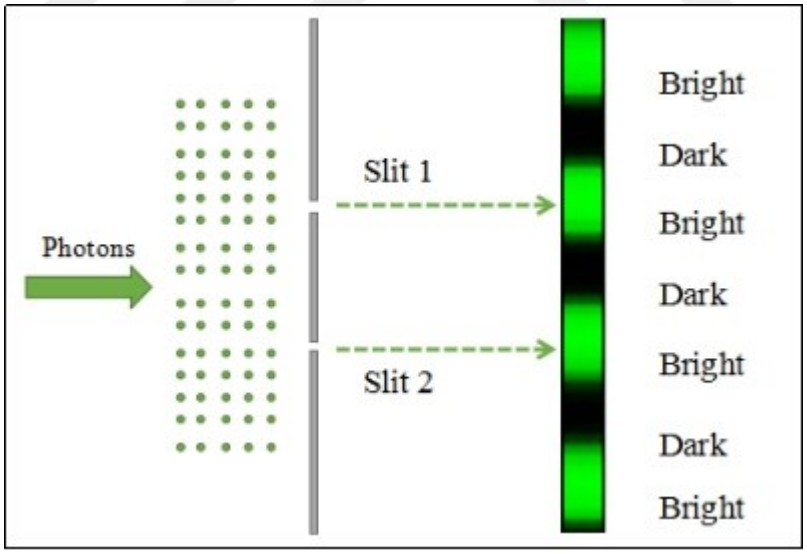


**Figure 1-1:** Double slit experiment showing particle wave duality

In the beginning of 20$^{th}$ century, physicists were thinking that emission of an electron depends on the light intensity from a metal surface. Einstein performed an experiment on photoelectric effect which light comes on a metallic surface and electrons are emitted from

surface. In some materials, red light with low frequency cannot break off electrons on a metal due to their lower energies. However, blue light causes to emit electrons in the metal surface. To emit an electron, atom in the material absorbs a single photon whose energy is higher than the ionization energy of the outer shell electrons. A blue photon has enough energy to do that, but a red photon does not to exceed this energy in the cesium plate no matter how it is intense.

This experiment had shown the relation between energy and frequency of a photon. After this experiment, it is found that energy and photons is quantized and depends on the frequency of the light. Einstein showed this photoelectric effect in 1905 and later won the Nobel Prize [2]

## *1.2. Electromagnetic Spectrum of Light*

Electromagnetic spectrum in the universe contains gamma rays, x-rays, ultraviolet rays, visible light, infrared rays, radar rays, radio waves (FM, TV, shortwaves and AM frequency) (Figure 1-2). It would be good to explain where we observe those kinds of rays in order to understand the nature of photons [3].

Gamma rays are created in nuclear decay, nuclear reactions, pulsars, black holes, supernova explosions and even in electron positron annihilation. Gamma rays have very high energy MeV (mega electron volts). The wavelength of gamma rays is shorter than atomic nuclei ($10^{-11}$ m) and because of that they are very dangerous for our health.

X-rays are known as Rontgen rays and they are used in X-ray imaging in order to identify cracks in body. X-rays are also essential in inspection of cargo and luggage in airports. Their wavelength is in the atomic scale ($10^{-9}$m).

Ultra-violate (UV) rays are the electromagnetic spectrum with a wavelength from 10 nanometer (nm) to 380 nm. UV rays consist of 3 regions in spectrum: UV-A (320-380 nm), UV-B (290- 320 nm), UV-C (220-290 nm). Ozone layer absorbs the wavelengths less than 320 nm, yet UV-A rays can penetrate into the earth's atmosphere. UV light exposure relatively increases with sun light intensity. In order to protect human skin UV-A and UV-B sun creams are used. Sun tan is an effect of UV rays. UV rays are used in the insect killer lamps, sterilizing surgical equipments, sterilizing foods, also in the security marker pens which is invisible unless UV light exposure [4].

In the longer wavelength of the visible spectrum, infrared rays (IR) extend from 1 micro meter (μm) to100 μm. IR rays are used in thermal cameras, night vision cameras. In military technology aircrafts and its smoke leaves behind IR rays due to heat and can easily be detected.

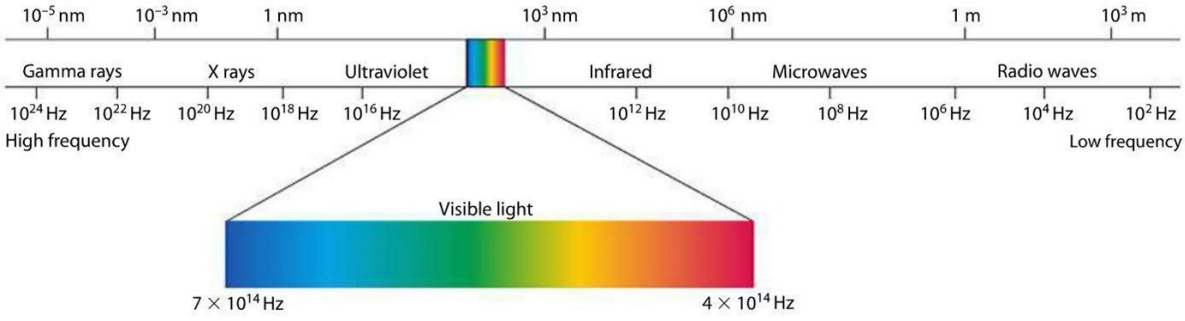


**Figure 1-2:** Electromagnetic spectrum[3]

In the spectrum after IR region microwaves takes place which has the order of millimeter. Microwave ovens which water highly absorbs in this frequency operate at 2.45 GHZ, and cellular phones operate at 1 GHz.

In the order of meter to kilometer radio waves region takes place. FM and AM radio frequencies, satellite communications, TV broadcasting and radar are the samples of this kind of electromagnetic spectrum of photons. The amount of energy of a photon can be found by Planck's constant ($6.6\times10^{-34}$ j.s) and frequency. Equation 2 gives the relationship between wavelength and frequency with respect to speed of light ($3\times10^{8}$ m).

$$E = hf = {}^{hc}/_{\lambda} \tag{1-1}$$

Light is a very narrow portion of the electromagnetic spectrum that takes place between infrared and ultraviolet regions (380 and 780 nanometers). Each nanometer (nm) in that region represents a wavelength of light or band of light energy. Light is the visible photons that human eye has the highest sensitivity at the highest solar radiation.

The visible spectrum of 380-780 nm range contains the colors which are violate, dark blue, blue, green, yellow, orange, and red. Violate is the most energetic photons; while red is the least energetic in the visible spectrum. Violate photons have about 3.2 electron volt (eV) energy, and red photons have 1.8 eV.

Violate, blue and green photons have higher energy than yellow, orange, and red due to their vibration frequency. Thus, some materials like phosphor absorb photons in the higher frequency and emits them in lower frequency. A wider electromagnetic spectrum (more

colors) can be achieved by such materials [5]. In this thesis, blue and yellow colors have been mostly used in the simulations or measurements.

## *1.3. Basic Concepts in Photonics*

When photons encounter a surface, it can be reflected, refracted, transmitted or absorbed. At the surface of the material, if photon is not reflected back, it will refract and be transmitted into medium. Then, it can be absorbed through the material.

### 1.3.1. Reflection

Reflection is the change of direction of a photon at an interface between two different medium, thus changing the medium is the main reason of reflection of light. Condensation of medium determines the speed of photon and reflection angle. Incoming photon reflect off the surface at same angle as the incoming photon's angle. Thus, incident angle becomes equal to reflected angle. When the interface is polished, light only obeys this rule, and reflection becomes at specular angle when the interface is similar to mirror, so image is not corrupted.

Unpolished and uneven surfaces cause spread reflection more or less the same as the incident light. When the surface is matte it reflects the light at many different angles, this is called diffused reflection. The distribution of light on surface becomes Lambertian distribution with a cosine function, because of that it is sometimes called as cosine distribution.

### 1.3.2. Refraction

When photons are transmitted from one material to another, they bend and their speed in this new medium changes as well. That is called as refraction in optics. The refractive index is the ratio of the speed of light in vacuum ($c=2.997\times10^8$ m) to the speed of light in the transmitted medium, see Equation (1-1).

$$n = {}^{c}/_{v} \tag{1-1}$$

The speed of light in air is very close to the speed of light in free space (vacuum). Thus, the index of refraction in air is considered to be 1 ($n_{air}$ =1.0003). Due to the refraction index formula, speed of light in a medium is less than the speed of light in vacuum, and the index of refraction for all other materials is greater than 1.

Snell's law of refraction explains well how photons refract in the interface of the medium. Refraction depends on two factors: the index of refraction (n), and the incident angle, see Equation (1-2).

$$n_1 sin\theta_1 = n_2 sin\theta_2 \tag{1-2}$$

In the equation, $n_1$ and $n_2$ are the refractive index of mediums, and θ's are incident and refracted light respectively. Light with a normal incident angle does not refract at the surface. Snell's law results that incident light coming from a lower refractive index bends towards the normal in the medium with a higher refractive index. Vice versa, when photons transmit to lower refractive index they bend away from the normal angle.

Refractive index of water is 1.333, which means the speed of light in water will be 1.333 times slower than vacuum. When we see rainbow in the sky, it results from different

refraction angles of different wavelengths in rain drops. Thus, light particles with different wavelengths refract with different angles. That is called dispersion of light in optics. For example, the indices of refraction are 1.337 and 1.333 for blue light and yellow light respectively in water. In rain drop longer wavelengths like yellow and red bend less than violate and blue. Colors coming out of rain drop thus refract with different angles, and we see these 7 colors in the visible spectrum.

Moreover, with an aid of nonparallel surface like prism dispersion pattern can be seen too. As previously mentioned, light particles of different colors have different speeds in different mediums.

**Table 1-1:** Refractive indices of some materials used in lighting technology

| Substance | Refractive index ($n_r$) | Imaginary refractive index ($n_k$) (589 nm) |
|---|---|---|
| Water | 1.333 | 0 |
| Ice | 1.309 | 0 |
| Borosilicate glass | 1.52 | 0 |
| Diamond | 2.417 | 0 |
| $SiO_2$ | 1.55 | 0 |
| PMMA | 1.489 | 0 |
| Carbon | 1.95 | -0.79 |
| GaAs | 3.927 | 0 |
| InGaN/GaN | 2.4 | 0 |
| Phosphor YAG | 1.8 | -1.00E-06 |

Glass materials are mostly used for protection and covering in light sources. The index of refraction of glass is about 1.518 (550 nm). Almost all liquids and solids have refractive

index more than 1.3. Most plastic materials have in the range of 1.3 and 1.7. Most gases have refractive index close to 1 due to low densities. Some material's refractive indices used in the lighting equipments are given in Table 1-1 [6].

In the table, elemental carbon has high imaginary refractive index, so light in the atmosphere is highly absorbed. GaN semiconductors which are mostly used as light source in LEDs have a refractive index of 2.4 with a complex part is zero. In YAG:Ce phosphor refractive index is about 1.8 and the imaginary index is in the order of minus 7. More details will be given in the following chapter.

### 1.3.3. Total Internal Reflection (TIR)

If angle of a beam in a higher density material goes away from the normal angle, it reaches a critical angle that light reflects back into the higher density medium. At the higher angles of incidence than critical angle, all incoming light reflects back with the same angle of incidence according to Snell's law of refraction. This is called total internal reflection (TIR). This particular angle can be calculated using Snell's law. When the refracted angle is 90 degree (see Figure 1-3), TIR at the critical angle happens, and at angles larger than the critical angle sinus function should be higher than 1, that means we get a total internal reflection. Critical angle can be found by Equation (1-3).

$$\theta_c = \sin^{-1}(\frac{n_2}{n_1}) \tag{1-3}$$

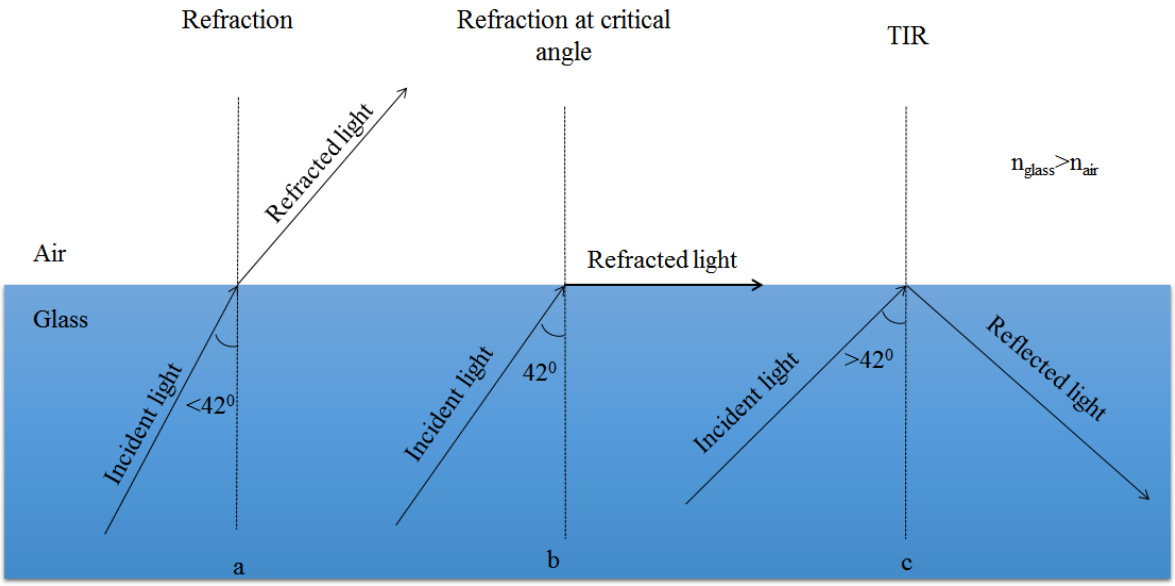


**Figure 1-3**: a) Refraction, b) Refraction at critical angle, c) Total internal reflection

The critical angle of water to air is thus found 48.6 degree, and it is 42 degree for glass to air respectively (see Figure 1-3). An important example of total internal reflection is diamond which has very high refractive index of 2.417 (Table 1-1), light is mostly confined in the diamond and diamond looks very bright. Another example of TIR is fiber optic cables that light is reflected back into the medium without light loss except for absorption.

### 1.3.4. Fresnel Reflection

When light travels through a medium with different refractive index, some of light reflects back regardless of higher or lower refractive indices. That is called Fresnel loss or Fresnel reflection. In Figure 1-4, incident light is transmitted into higher density medium, and it refracts toward the normal of surface. Yet, some of them are reflected off with the same angle.

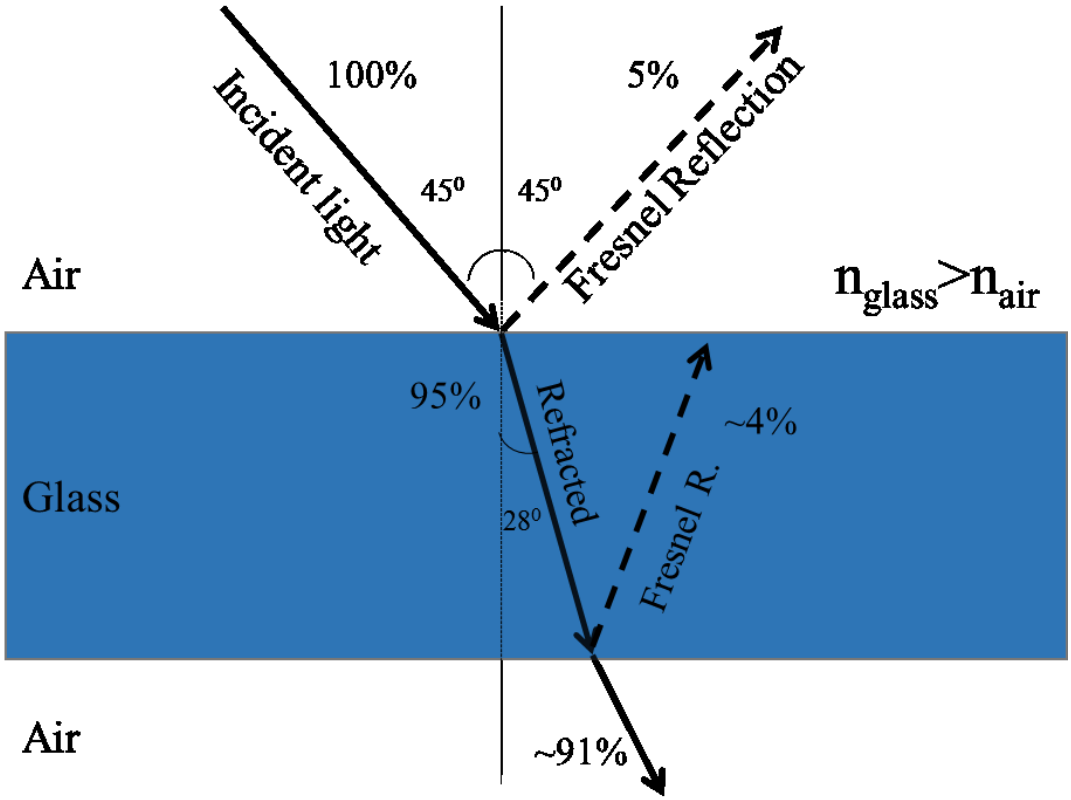


**Figure 1-4:** Reflected and refracted light

Reflection loss for the normal incidence can be found via Equation (1-4). R stands for Fresnel reflection, n's are the refractive indices. When the difference between refractive indices increases, Fresnel reflection ratio increases. For example, between water and air, Fresnel reflection loss is about 2% for normal incidence. From air to glass at normal angle of incidence, this loss is about 4% for only one surface. You can see the reflections of 45 and 28 degrees in Figure 1-4.

$$R = \frac{|n_1 - n_2|^2}{|n_1 + n_2|^2} \tag{1-4}$$

Fresnel reflection, refraction, reflection are applicable not only for the visible light but for the full electromagnetic spectrum. In light emitting diodes (LED) Fresnel reflection takes very important place to cause optical losses.

### 1.3.5. Polarization Angle

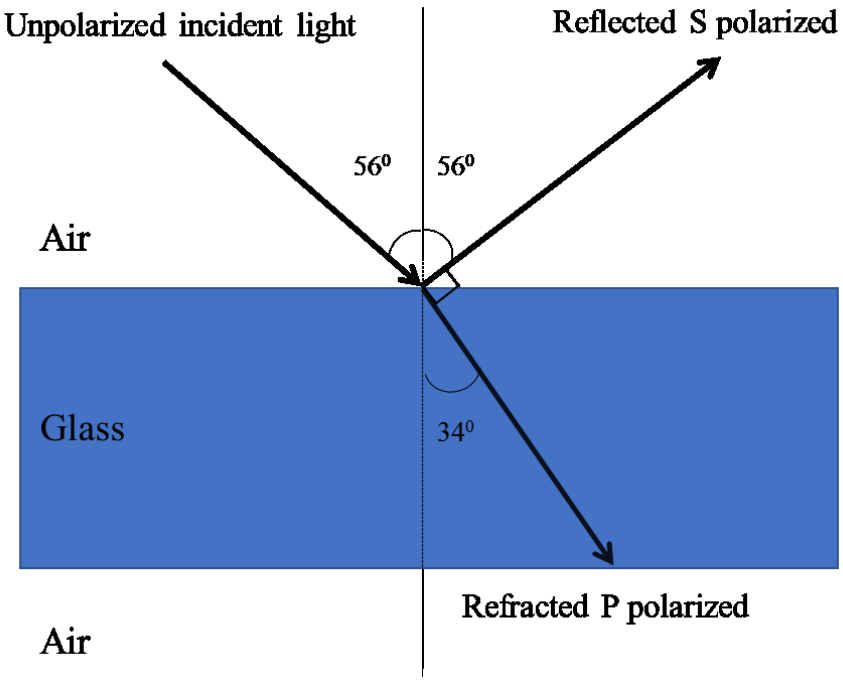


**Figure 1-5:** At polarization angle, reflected S polarized and refracted P polarized rays

At a certain angle (Brewster angle), light which is polarized in the plane of incidence is transmitted totally into second medium. In that case light does not reflect back to the first plane. That angle is called polarization angle in optics (photonics). For the glass in Figure 1-5, polarization angle is about 56 degree (summation of $\theta_i$, $\theta_t$ should be 90 degrees at this special angle). Polarizing sun glasses are the applications to cut off the reflected S polarized light from water and roads. For water air interface it is $53^0$. Polarization calculation is given in Equation (1-5).

$$\theta_{pa} = \tan^{-1}(\frac{n_2}{n_1}) \quad (1\text{-}5)$$

### 1.3.6. Transmission

A material's ability to transmit light is known as transmission in optics. It is measured for a material with a thickness, and defined by Equation (1-6) where $I_0$ is intensity of light entering the material. *I* is the intensity of transmitted light from the material.

$$T = \frac{I}{I_0} \quad (1\text{-}6)$$

Fresnel reflections should be discarded at the both surfaces of material in order to calculate transmission of material (see Figure 1-6).

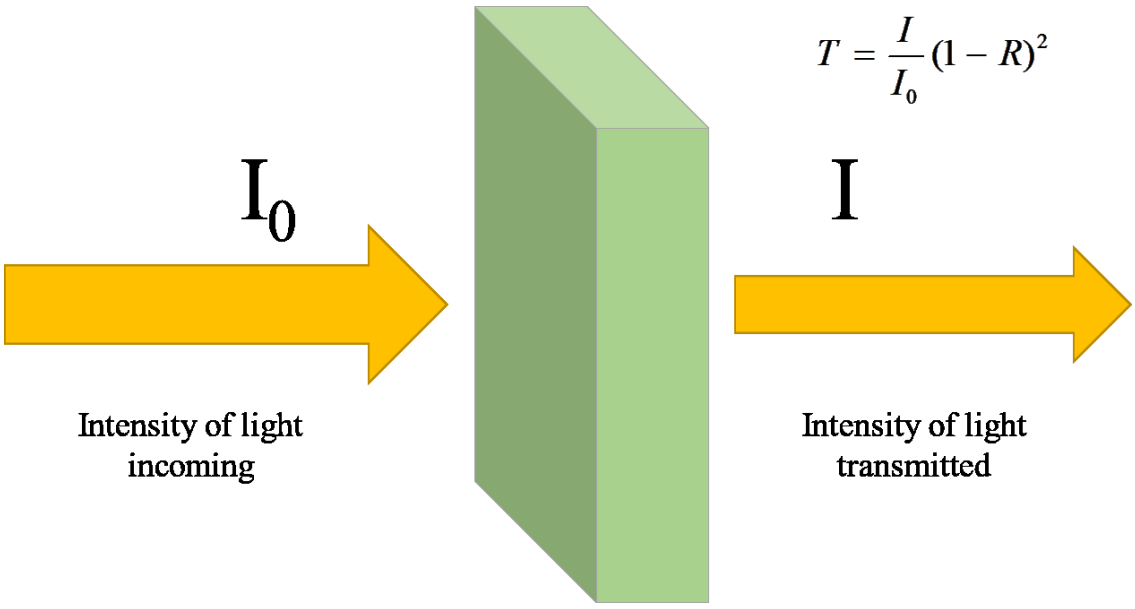


**Figure 1-6:** Transmission of light

### 1.3.7. Absorption

A beam of light can be absorbed in a material and converted into heat. That is called absorption. Some wavelengths are absorbed in many materials while transmitting other wavelengths. For example the rate of absorption of visible light region is very little in glass and water. Absorbance of the material can be calculated by Equation (1-7).

$$I = I_0 e^{-\alpha L} \tag{1-7}$$

### 1.3.8. Spatial Distribution

Light distribution pattern of light sources is important when modeling luminaries and simulating indoor and outdoor places. Spatial distribution information is generally given with polar diagrams in data sheets or with Eulumdat files that taken from the goniophotometer systems. A light emitting material with a planar surface typically radiates with Lambertian emission pattern seen in Figure 1-7. At an angle of nearly $60^0$ the light intensity becomes half of the maximum value at the normal incidence. Therefore, this kind of distribution has a view angle of 120 degree.

However, light emission pattern can be changed by using epoxy or silicon encapsulants. Non-planar surfaces exhibit light emission with various different patterns. Narrow angle light emission can be achieved with a parabolically curved surface. For example, light emission with 10 degree or less beam angle can be obtained with the aid of such parabolic encapsulants. Moreover, isotropic light emission can be achieved with a hemispherically shaped LED (see Figure 1-7).

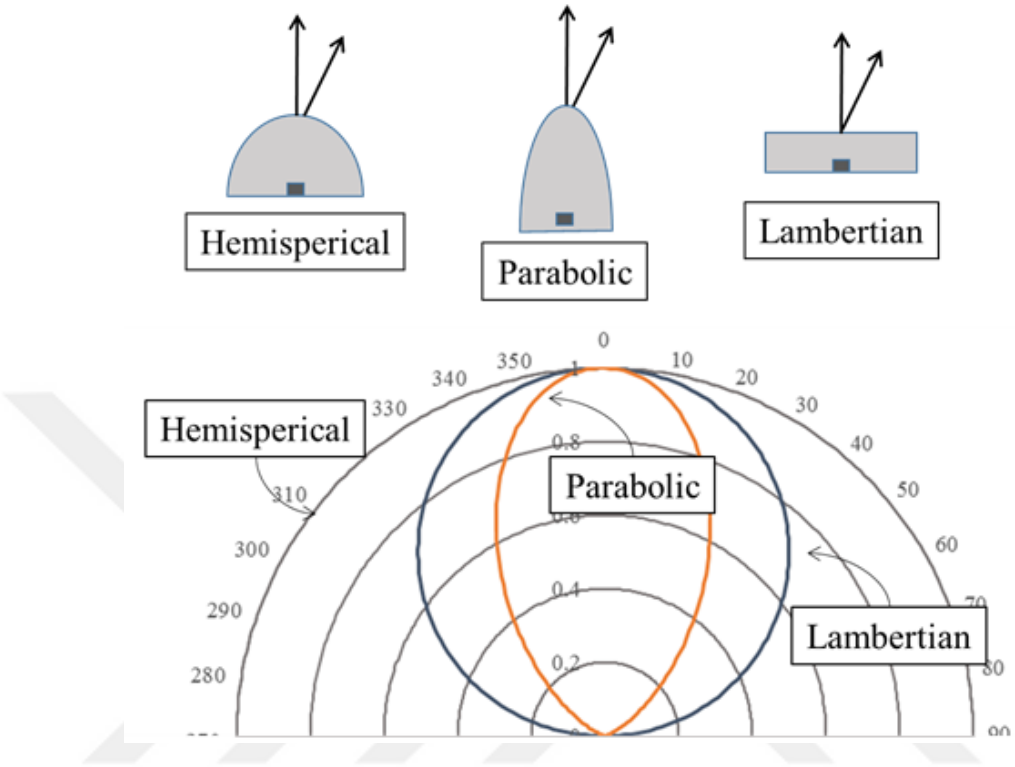


**Figure 1-7:** Sample of emission pattern with different encapsulants

## *1.4. Scattering of Photons*

Some optical interactions (Reflection, refraction) are actually results of scattering. When photons interact with a material, they change their original direction, so we can define scattering as the redirection from the previous direction. Electromagnetic (EM) waves perturb the particle's molecules periodically with the same frequency. That creates an oscillation and induced dipole moment in the molecules, thus resulting the scattering of photons. The majority of light scattered in the medium is emitted at the same frequency of incident light. Thus, energy of photon remains same and this kind of scattering is called elastic scattering.

Rayleigh and Mie scattering are the samples of elastic scattering that energy does not change. In Rayleigh scattering incident rays scatter on the particles of which are relatively small against wavelength, yet Mie scattering is applicable for the particles that particle size is close to wavelength (see Figure 1-8). Rayleigh and Mie scattering focus on the visible region in this thesis. In inelastic collisions, energy of incoming photon decreases in scattering. The wavelength of incident light thus changes. Raman scattering is the sample of that kind of scattering.

$$a = \frac{2\pi d}{\lambda} \tag{1-8}$$

The parametric size equation of scattering particle is given in Equation (1-8). In the equation, a is size parameter, d is the diameter of particle and λ is wavelength of photon.

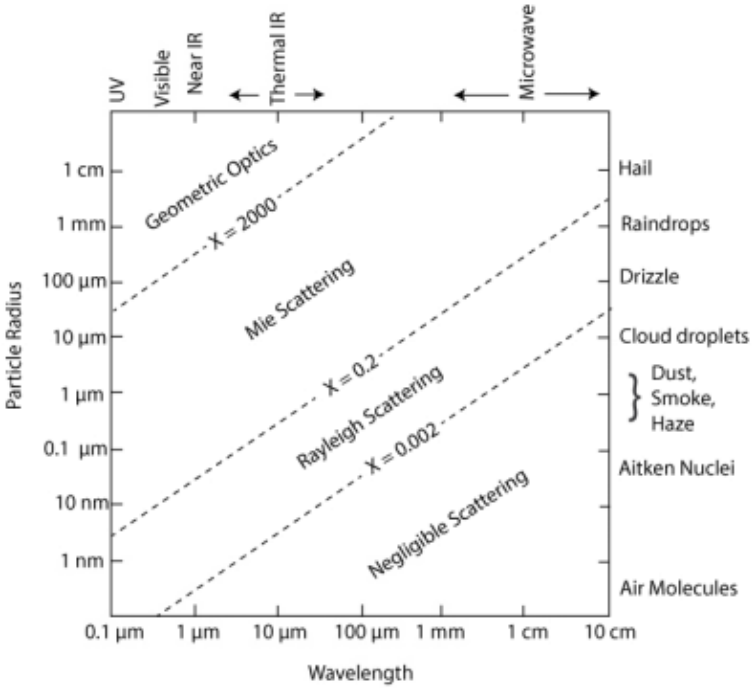


**Figure 1-8:** Type of scattering as a function of wavelength and particle radius [7]

### 1.4.1. Rayleigh scattering

When the size parameter in Equation (1-8) is much smaller than 1, ray path of Rayleigh scattering is applicable. Rayleigh scattering is applicable in the atomic scale of solids, liquids, and gases which have refractive index close to 1.

In atmosphere blue color is more dominant because of Rayleigh scattering. Light with higher frequency (like violate and blue) undergoes more scattering than light with lower frequencies. Lord Rayleigh calculated the scattered intensity from a dipole scatterer. The amount of scattering is inversely related with the fourth power of the wavelength as can be seen in Equation (1-9). Therefore, the blue light of 450 nm can scatter 8 times more than the red light of 650 nm in the particles at the atomic scale.

$$I = I_0 \left( \frac{1 + cos^2\theta}{2R^2} \right) \left( \frac{2\pi}{\lambda} \right)^4 \left( \frac{n^2 - 1}{n^2 + 2} \right)^2 \left( \frac{d}{2} \right)^6 \quad (1\text{-}9)$$

In the equation, I is intensity of scattered light, d is the diameter of particles, n is refractive index, R is the distance to the particle, θ is the scattering angle, and λ is the wavelength of photon. The intensity distribution of Rayleigh scattering is close to spherical in all direction with respect to other scatterings (Figure 1-9). Yet, at the right angles, scattering is half of the forward and backward intensity for Rayleigh scattering.

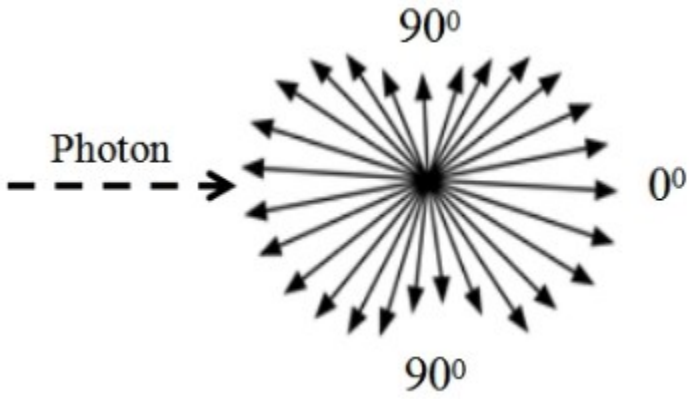


**Figure 1-9**: Distribution of Rayleigh scattering

$N_2$ and $O_2$ gases which have the radius about 0.3 nm constitute the 99% of the atmosphere. Light scattering becomes mostly at every direction around the molecules. As previously mentioned, blue color scatters more than other colors like orange and red colors in atmosphere and we see that atmosphere is blue due to Rayleigh scattering.

During sunset and sunrise sun light passes through longer path in the atmosphere than at noon. Blue color is scattered more in all directions and orange and red color remains in the forward direction. Therefore, at sunset and sunrise weather turns into orange and red colors.

Moreover, the yellowish color of the sun is related with this kind of scattering at noon time. At the edge of ultra-violate region, oxygen absorbs the incoming electromagnetic radiation and blue photons are mostly scattered in all directions resulting color of the sun becomes yellow. However, at the sunset and sunrise yellow wavelength undergoes Rayleigh scattering in the long path of atmosphere and the color of the sun seems reddish. In fact, the sun seems white and space seems black when there is no air like in free space. In Table 1-2, some of the radii of the atmospheric particles are given with the types of scattering [8].

**Table 1-2:** The radius of atmospheric particles and scattering type for visible light

| Type | Size | Scattering Type |
|---|---|---|
| $N_2$ molecule | 0.3 nm | Rayleigh |
| $O_2$ molecule | 0.3 nm | Rayleigh |
| Smoke, haze | 0.1-2 μm | Mie |
| Cloud droplet | 5-50 μm | - |
| Drizzle drop | 100 μm | - |
| Ice crystal | 10-100 μm | - |
| Rain drop | 0.1-3 mm | - |
| Hailstone | 1 cm | Optic |

### 1.4.2. Mie Scattering

Mie scattering (Lorenz-Mie-Debye solution to Maxwell's equations of electromagnetic radiation) explains how an incoming wave scatters from a dielectric spherical element. When the size parameter is close to wavelength, Mie scattering occurs between the electromagnetic wave and the collided particle. For the size parameter close to 1 scattering produces a pattern that most of the photon goes in the direction of forward scattering (see Figure 1-10).

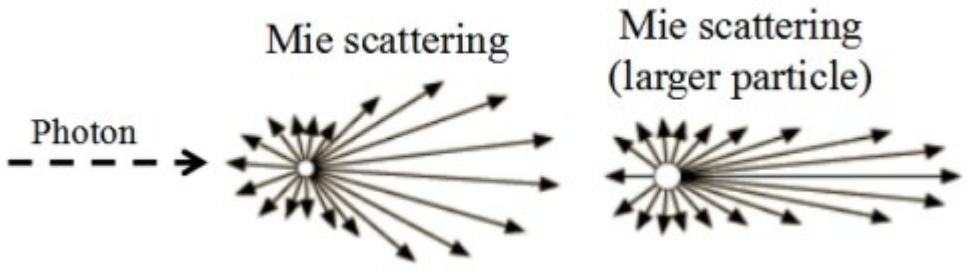


**Figure 1-10:** Mie Scattering from small and larger particles

As we mentioned previously that Rayleigh scattering mostly depends on the wavelength of the incoming light, but Mie scattering is not affected too much by the wavelength of incoming light. Therefore, white light coming from the sun and moon scatters and produces white circular glare around them in foggy weather due to mostly going into direction of forward. Dust particles, smoke and haze in the atmosphere are the reasons of white glare. Another example is that we see such glare around outdoor lighting fixtures in foggy weather.

Phosphor material used in the light emitting diode packages has diameter of 5-20 μm and its size parameter is close to 1. Mie scattering thus occurs in the phosphor particles. Some more information will be given about Mie scattering in the experiment and simulation parts.

## *1.5. Basics of Radiometry and Photometry*

Radiometry is the measurement and detection of electromagnetic spectrum which contains ultra-violate, visible, and infrared. Photometry, on the other hand, is concerned with the visual response of human eye to photons in the visible region. Radiometric units (Watt, $W/m^2$, etc.) are physical quantities and calculated via the relationship between Planck's constant and frequency with the help of Equation (1-1). However, photometric units (e.g. lm, lx, cd) are calculated by the luminosity function of eye.

In Table 1-3, most common concepts of radiometry and photometry can be seen with their units. The family of photometric concepts has been given in a manner analogous to the display of radiometric concepts.

**Table 1-3:** Units of radiometric and photometric quantities with their notations and units.

| Radiometry | | | Photometry | | |
|---|---|---|---|---|---|
| Concept | Notation | Unit | Concept | Notation | Unit |
| Radiant power | $\Phi_e$ | W | Luminous power | $\Phi_v$ | lm |
| Radiant intensity | $I_e$ | W/sr | Luminous intensity | $I_v$ | lm/sr |
| Irradiance | $E_e$ | $W/m^2$ | Illuminance | $E_v$ | $lm/m^2$ |
| Radiance | $L_e$ | $W/m^2$-sr | Luminance | $L_v$ | $lm/m^2$-sr |

Radiant power is calculated by the spectral radiant distribution in Equation (1-10). Radiant energy can be calculated in ultra-violate, visible, and infrared region. Some examples of radiant energy are micro ovens, x-ray machines, UV light sources, IR lasers, radio and TV signals, etc.

$$P_R = \int_{\lambda} P(\lambda) d\lambda \tag{1-10}$$

Luminosity function of eye (eye sensitivity function) is in the range of 380 nm and 780 nm -violate and red-. Spectral radiant energy function *P(λ)* is multiplied by the luminosity function *V(λ)*, and the sum is integrated over wavelength with the aid of Equation (1-11). Thus, the most common unit of photometry which is luminous flux $\phi_v$ (or mostly called as lumen) can be calculated. The highest value of 683 luminous efficacy is obtained by the

photopic function. Eye sensitivity function *V(λ)* has a maximum value at 555 nm green color and at other wavelengths the luminous efficacy slightly decreases [9].

$$\phi_V = 683lm/W \int_\lambda P(\lambda)V(\lambda)d\lambda \tag{1-11}$$

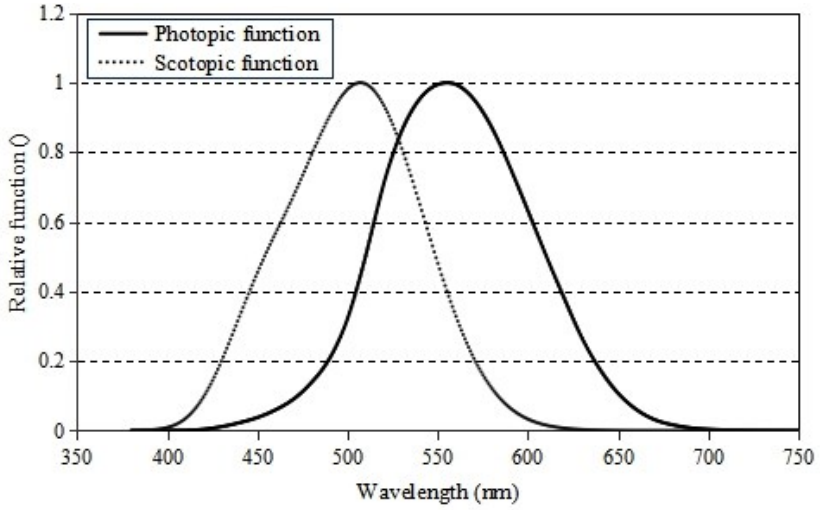


**Figure 1-11** Normalized photopic luminosity function and scotopic luminosity function

However, human eye has two kinds of photo-receptors which are cones and rods corresponding to photopic and scotopic visions. Light measurement is generally calculated by the photopic luminosity function as in Equation (1-11). The brightness of light determines which vision is active and be used in the calculation of lumen. When the eye receives light level of which luminance is greater than 3cd/m$^2$, photopic vision is dominant and cones are operative at this brightness, but the rods are operative in scotopic vision at the luminance level below 0.001cd/m$^2$. At the scotopic vision luminosity function has a maximum at 507 nm with 1700 lm/W efficacy [10] (see Figure 1-11). That does not imply that lamps would be more efficient in scotopic vision. The rods are insensitive to colors in the visible spectrum and they can only be active at the lower luminance levels. Both

receptors are active between these two luminance levels which is called mesopic vision [11].

Intensity in radiometry and photometry is calculated by dividing power or lumen by solid angle which the unit is steradian (Equation (1-12) and (1-13). In the equation, $\phi_e$ and $\phi_v$ are radiant flux and luminous flux respectively and Ω is solid angle [12].

$$I_e = \frac{\phi_e}{\Omega} \tag{1-12}$$

$$I_V = \frac{\phi_V}{\Omega} \tag{1-13}$$

Solid angle can be calculated with the help of Equation (1-14). In the equation, θ is the half peak angle of distribution of light source. A is spherical area, and r is spherical radius of solid angle. Light emitting chips have generally Lambertian distribution (Cosine distribution) which is about 120 degree. Then, solid angle becomes π steradian. Typical devices which intensity measurement is done are light emitting diodes, UV and IR sources.

$$\Omega = 2\pi\left(1 - \cos\frac{\theta}{2}\right) = \frac{A}{r^2} \tag{1-14}$$

Irradiance and illuminance are the measurement of flux incident on a surface per unit area, Equation (1-15) and (1-16).

$$E_e = \frac{\phi_e}{\mathrm{A}} \tag{1-15}$$

$$E_V = \frac{\phi_V}{\mathrm{A}} \tag{1-16}$$

Irradiance measurements are important in medical systems and remote sensing in recent years. Most radiometric and photometric sensor heads have a 1 $cm^2$ detector area or the detector area is controlled by an aperture with a known area. Illumination levels are important to have optical comfort in each work space. The recommended light levels are given for different work spaces in Table 1-4 [13].

**Table 1-4:** Recommended light levels of different work spaces.

| *Activity* | *Illumination (lx)* |
|---|---|
| Houses | 150 |
| Offices, Classrooms | 250 |
| Laboratories, PC Work Places, Groceries, Show Rooms, | 500 |
| Supermarkets, Mechanical Workshops | 750 |

As a surface is drawn away from a light source, the surface appears to be less bright. Hence it becomes dimmer when it goes away from the light source. Inverse square law can be applied to illuminance calculation. It relates illuminance and light intensity with Equation (1-17).

$$E_V = \frac{I_V}{d^2} \tag{1-17}$$

Radiance and luminance are the intensities emitted per unit area of an electromagnetic source (Equation (1-18) and (1-19). Radiance and luminance levels can generally be seen in display units to state the brightness levels of electromagnetic spectrum. For example, a

typical liquid crystal display (LCD) TVs have luminance levels of 200-300 cd/m$^2$ and HD TV systems range from 450 to 1200 cd/m$^2$ [14]. Solar disk has $10^9$ cd/m$^2$, clear sky $10^3$ cd/m$^2$, clear sky at moonlit night $3x10^{-2}$ cd/m$^2$, clear sky without moonlit $3x10^{-5}$ cd/m$^2$.

$$L_e = \frac{\phi_e}{\Omega A} \tag{1-18}$$

$$L_V = \frac{\phi_V}{\Omega A} \tag{1-19}$$

The luminous efficiency ($\eta_v$) is the most known definition to determine effectiveness of light source. It can be found by luminous flux dividing by the electrical input power (Equation (1-20) and (1-21) [5]. In Equation (1-20), P is electrical power, $I$ is driving current and $V$ is voltage. Moreover, luminous efficacy ($k$) is calculated by luminous flux dividing by the radiant power given in Equation (1-22).

$$P = IV \tag{1-20}$$

$$\eta_V = \frac{\phi_V}{P} = \frac{lm}{W} \tag{1-21}$$

$$k = \frac{\phi_V}{P_R} = \frac{lm}{W_R} \tag{1-22}$$

Luminous efficiency of common light sources is given in Table 1-5 [5]. Incandescent light sources have efficiencies of 15-25 lm/W, fluorescent light sources have 50-60 lm/W, discharge lamps have 50-140 lm/W. Semiconductor based light sources have highest efficiencies among light sources and take over the lighting industry due to their efficiency, compact size, and long life in recent years [15],[16],[17],[18]. During this thesis GaN-based

LEDs have been used in the experiments and simulations. Light emitting diodes will be discussed in the next chapter.

**Table 1-5:** Luminous efficiencies of incandescent (a), fluorescent (b), discharge (c), and LED sources.

| *Light source* | *Luminous efficiency (lm/W)* |
|---|---|
| Tungsten filament (a) | 15-20 |
| Halogen (a) | 20-25 |
| Fluorescent (b) | 50-80 |
| Mercury vapor (c) | 50-60 |
| High pressure sodium (c) | 100-140 |
| LED (d) | 100-200 |

# CHAPTER II

# LIGHT EMITTING DIODES AND LIGHT CONVERTERS

## *2.1. Semiconductors of Light Emitting Diodes*

Semiconductor materials are used in LEDs to produce light in or near visible region. Their electrical conductivity is between conductors (like gold, copper) and insulators (like glass), so semiconductors are used in some mechanical devices as well with the help of that property e.g. transistors, solar cells. Traditional semiconductor samples which have been used more than 30 years are silicium that have been used in transistors, solar cells, photo-detectors, and rectifiers; germanium (solar cells, laser diode), and gallium arsenide (infrared light emitting diode, lasers, solar cells). They are compound materials with a chemical formula of AB (e.g. SiC, GaAs) which they are trivalent(5A), tetravalent (6A) or pentavalent (7A) elements in the periodic table [11].

Their physical structure consists of layers on top of each other, and they include n-layer of high concentration free electrons, p-layer which has a high concentration of holes (known as positive charges), and in addition smaller band gap compounds take place between n-layer and p-layer at the junction point. This mid-layer with lower band gap between the layers of higher band gap materials spatially traps electrons and holes, allowing them to recombine efficiently. Combination of electrons and holes in these quantum wells generate light at the wavelength of the smaller band gap material.

LED modules also include substrates and DC current contact points. The contact points are located in the corners of the LED so that the photons should not be obstructed by the DC electric contacts. Additionally, bottom surface of substrate can be coated with silver to reflect photons in order to increase reflection from back side. Schematic drawing of LEDs can be seen in Figure 2-1.

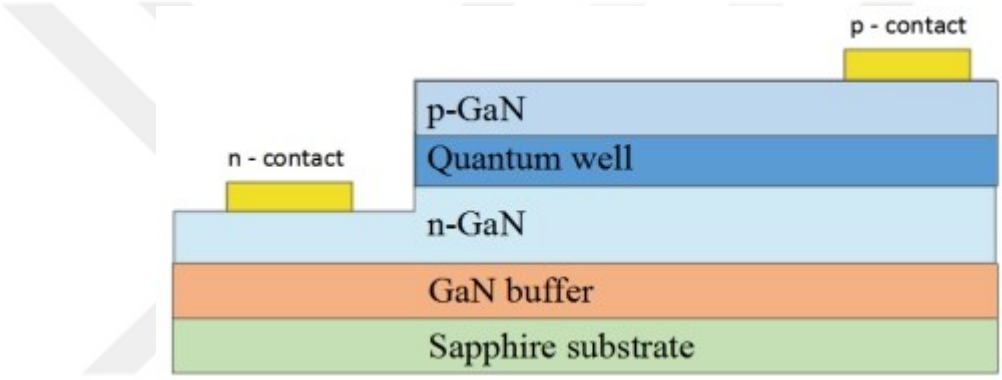


**Figure 2-1:** Schematic of blue light emitting LEDs

Gallium nitride based semiconductors have been mostly used to directly generate blue light and indirectly produce white light in the past decade. Gallium nitride semiconductors were drawn attention because of their direct band gap properties and wide spectrum ranges. Direct band gap of GaN semiconductor is about 3.2 eV and wide spectrum range between 200-1500 nm which covers UV, visible, and IR regions can be achieved by varying the amount of elements [19] (e.g. Aluminum, Indium). During this thesis, GaN based LED chips have been used in the experiments and simulations.

In a direct band gap material like GaN, the energy is directly transacted between the minimum of the conduction band and the maximum of the valance band. However, for an indirect band gap semiconductor energy is transferred by vibrations (also called as

phonons) between molecules. It results in an excess heat production and less efficiency in light emitting diodes (LEDs).

The luminous efficiency development of visible range semiconductors and conventional light sources are given in Figure 2-2 including the Edison's first light bulb. It is assumed that the luminous efficiency has doubled every 4 years for light emitting diodes, heat loss is decreased accordingly.

Gallium arsenide (GaAs) and gallium phosphide (GaP) semiconductors emit red color, yet GaP semiconductors can also emit orange and yellow colors. Moreover, GaP semiconductors can provide higher luminous efficiency due to the high eye sensitivity in this wavelength range. Furthermore, GaP based semiconductors have lower manufacturing cost compared with GaN (gallium nitride) based chips. Therefore, if amber and yellow colors are needed, GaP semiconductors are used in such applications where low brightness is desired with respect to GaN based semiconductors, e.g. highway signage applications [5].

However, GaP diodes have strong temperature dependence than GaN diodes. Thus, GaN based blue-green diodes are used in high-brightness applications. Lastly, over 200 lm/W luminous efficiency has been achieved in nitride based semiconductors.

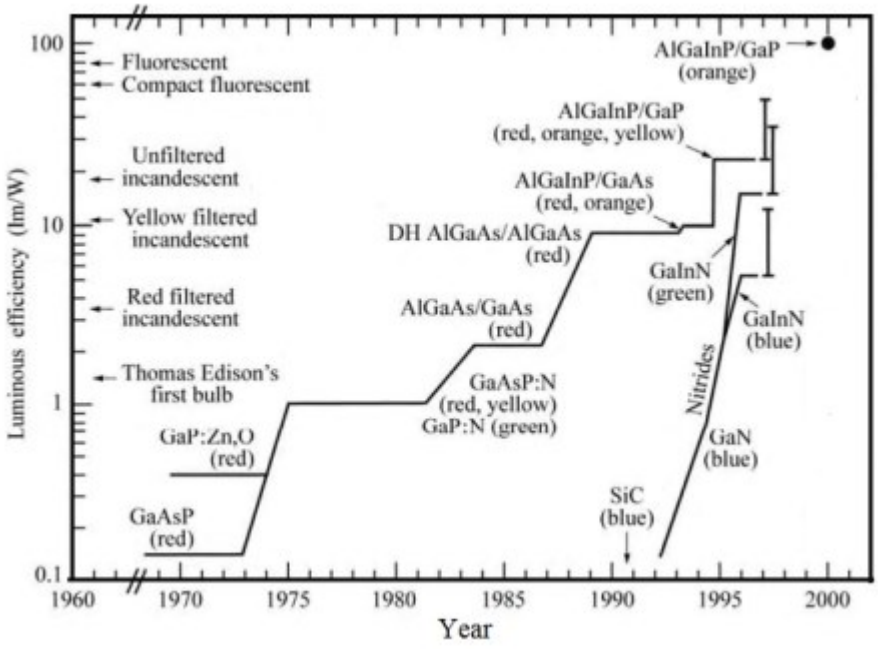


**Figure 2-2:** Development of semiconductor LEDs and conventional light sources[5]

The most of the energy loss occurs in semiconductor layers of LED packages. Improvements are still required to advance efficiency in these diodes. Semiconductor efficiency which is known as external quantum efficiency (EQE) is the proportion of the number of photons emitted and escaped from semiconductor to the number of electrons coming to the semiconductor material. This ratio includes in sub-categories electrical efficiency, internal quantum efficiency of quantum wells (IQE) and light extraction efficiency of the semiconductor chip (LEE). Electrical efficiency is the ration of the electrons coming to the device to the injected ones into the active region. IQE can be described by the ratio of all recombinations in the quantum wells that are radiative. IQE of semiconductors has greatly improved in recent years due to use of good quality crystals.

However, the light extraction is still inefficient in semiconductors due to the high refractive indices. In the previous chapter, Fresnel losses were mentioned about that approximately 96% of internal light reflects back in the upper surface of a semiconductor like GaN, see Equation (2-1). Escape cone of photons is about 23 degree for GaN chips and the rest of photons outside the escape cone is imprisoned in the semiconductor [5].

$$\frac{P_{escape}}{P_{source}} = \frac{1}{4}\frac{{n_{air}}^2}{{n_{sem}}^2} \tag{2-1}$$

Thus, LEE is the main reason for heat production and reflection losses in LEDs. Improving the LEE is significant, and various methods are studied in order to accomplish this, such as surface textures [20], [21], [22], [23]. Moreover, Fresnel reflection can be reduced by using a dome-shaped package. This thesis study aims to increase LEE and luminous efficiency using similar methods. Refractive indices are given for the most common semiconductors used in LEDs in Table 2-1.

**Table 2-1:** Most common semiconductors with refractive indices [24]

| *Material* | *Refractive index* |
|---|---|
| GaAs | 3.4 |
| GaP | 3 |
| GaN | 2.4 |
| Ge | 4 |
| Si | 3.3 |
| InAs | 3.5 |
| InP | 3.4 |
| $SiO_2$ | 1.46 |

## *2.2. Phosphors Converted White Light Emitting Diodes*

### 2.2.1. LED Phosphors

Most commonly there are 3 methods to obtain white light with the help of light emitting semiconductors, but 3 methods have their own advantages and disadvantages. The first method is to use individual monochromatic LEDs of red (R), green (G), and blue (B) which is mostly used in display screens, such as TVs and mobile phones. Combination of these RGB LEDs results in white light from LEDs. However, the luminous efficiency in green LEDs is not very high and the lifetime of red LEDs is not long enough. In this method, green phosphor can be pumped with blue LEDs in order to solve those problems [5], [12], [25].

The second option is to use yellow phosphors with blue LEDs in order to get white light. This bi-chromatic way of blue and yellow colors is highly efficient and easy to use. However, medium color rendering index (70-80) can be achieved due to bi-chromaticity. To achieve a higher CRI higher than 90, two or more phosphor blends of green and red are used at the same time instead of using yellow phosphor. When high efficiency is necessary, phosphor converters are generally optimized to achieve high luminous efficiency [26].

The third option is pumping a UV or near UV-LED and down-convert by using phosphor blends for white light. In this method a semiconductor of band gap at UV is used to generate photons and with the help of 2 or more phosphors photons are down-converted to visible region. In this process, efficiency is less than the second method due to wavelength shift of photons. In this thesis, the second method is used to get white light in the experiments and simulations.

In order to down-convert from blue or UV region, wavelength shift is very important. This process which includes absorption and re-emission of photons is called Stokes shift. In the phosphor converted LEDs (pcLEDs), GaN based blue light emission is generally at 450 nm and yellow phosphor emission spectrum is at 550 nm. That wavelength shift causes almost 20% loss in the radiant power of the blue LED (see Figure 2-3).

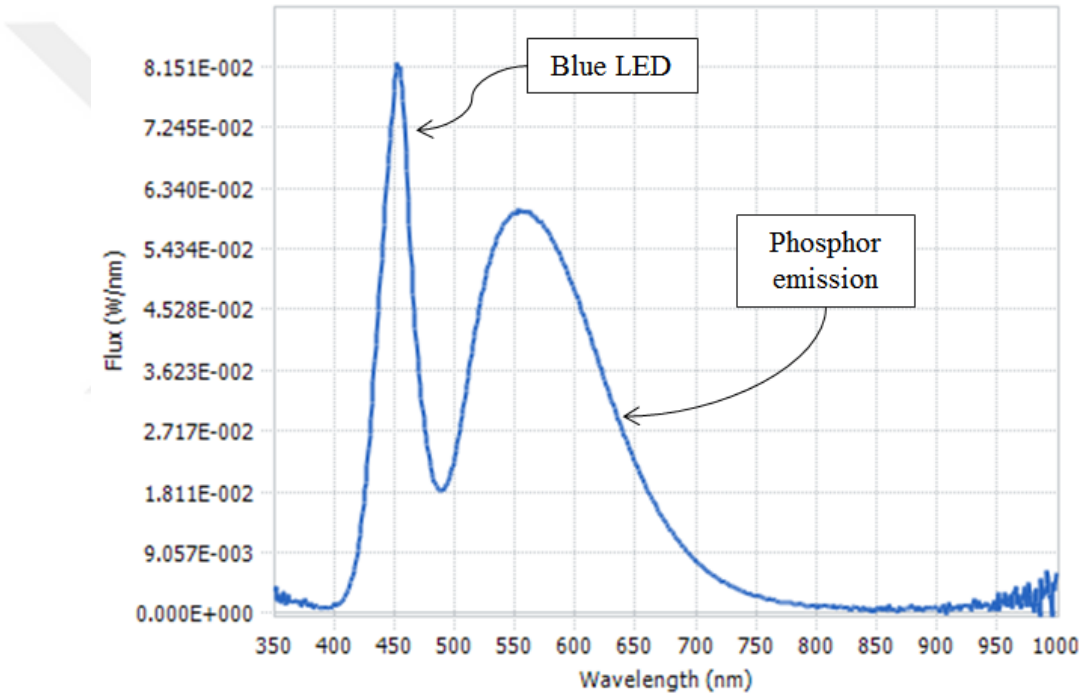


**Figure 2-3:** Spectrum of phosphor converted LEDs

On the other hand, this process reduces the radiant power, but it increases the luminous power. It can be considered as gain due to the luminosity efficiency at the yellow and green region of the spectrum. Stoke shift can be calculated by Equation (2-2) [27], [28].

$$n_{stokes} = \frac{\lambda_{blue}}{\lambda_{yellow}} \tag{2-2}$$

### 2.2.2. Selection of Phosphor Mixtures for pcLEDs

It is quite important to choose appropriate phosphor for pcLEDs in order to get higher luminous efficiency, optimized CRI, and appropriate color temperature. Although there are many types of phosphors that have been developed for fluorescent light sources, CRT display screens, and sensors, only limited number of phosphors is suitable to use in pcLEDs. The selection of phosphor for white light generally acquires the parameters of excitation spectrum, emission spectrum, quantum efficiency, sustainability at higher temperatures, stability, and non-saturation at high fluxes [29], [30].

Firstly, the excitation spectrum of phosphor should be high and it should cover the spectrum of semiconductor emitter. Selected phosphor should also match the variations of the emission spectrum of LED with the changing temperatures. In fluorescent light sources, phosphors have high excitation at 254 nm which is the emission of mercury vapor. Thus, this kind of phosphor has no use due to Stokes shift rates of almost 50%. In pcLEDs, appropriate phosphors have high excitability between 400-500 nanometer wavelengths, and blue LEDs have radiation at 450 nm. Hence, phosphors with high excitation rates are required in the blue region of spectrum in order to get highly efficient light sources.

Other phosphor parameter is the emission spectrum of phosphor which should be broad enough to cover visible spectrum in order to obtain high color rendering white light. However, emission spectrum should not overlap with the excitation spectrum of phosphor in order to prevent re-absorption. The total spectrum of semiconductor and phosphor emission should include 3 main colors which are blue, green, and red. This combination can be achieved by blue LEDs and yellow phosphor. In LED backlights, wide color

spectrum is necessary and the number of phosphors can be 2 or 3. In that case, high color rendering costs of luminous energy efficiency. Phosphors are thus selected for energy efficiency or color rendering accordingly in indoor and outdoor lighting.

The quantum efficiency of phosphor is the ratio of the number of emitted photons to the number of incoming photons, so a higher radiative emission rate leads to higher luminous efficiency. Non-radiative process after absorbing a photon is the initial reason to decrease quantum efficiency in phosphors. Non-radiative energy may also cause lower luminous efficiency and heat generation. As a result, it will induce degradation, delamination, and even local stress which leads to decrease of life time and reliability significantly [31]. It is hard to find the quantum efficiency of phosphor in the datasheets and internet, but measuring quantum efficiency is straightforward. It can be found by the relation with the intensity of incoming, converted, and scattered photon as given in Equation (2-3).

$$Q = \frac{n_{converted}}{n_{incoming} - n_{scatterred}} \tag{2-3}$$

Phosphor also requires a sustainable performance for excitation, luminous spectra, and quantum efficiency at the elevated operating temperatures during their lifespan. Current commercially available pcLEDs promise lifetime of 15.000 to 50.000 hours. That corresponds to more than 15 years of operation for 8 hours daily usage [11]. At the end of their lifespan, pcLEDs can suffer from altering the emission color and lowering the luminous flux. In addition, phosphor requires stability against moisture, oxygen, and UV lights [29].

Saturation time is another effect that cannot be underestimated for phosphors. When a color conversion element like phosphor with a long decay time of electrons exposes to high light flux, they cannot efficiently convert all incoming photons. Hence, it results inefficiency in phosphors.

### 2.2.3. Chemical Compositions of Phosphors

Chemical compositions of phosphors have 2 main parts including hosts and dopants. Firstly, some host components are garnets, aluminates, silikates and nitrides. Generally, hosts are chosen from garnets. The common formula of the garnets is $X_3Y_5O_{12}$. Yttrium aluminum garnets ($Y_3Al_5O_{12}$) are most preferred phosphors because of their quantum efficiency, emission spectrum, shorter decay times etc.

Dopants are rare earth materials. Such elements are optically active. Cerium is mostly used in white light emitting YAG:Ce phosphors. Neodymium (Nd) dopants are used in YAG:Nd doped lasers.

Moreover, the concentration of the phosphor particles and the thickness of phosphor in the epoxy can shift up or down the emittance spectrum of photons. As the concentration and the thickness increases, the down-converted light amount increases, additionally efficiency and color temperature decrease.

For the bluish white light, phosphor thickness and concentration can be lower, but to get reddish light these rates can be increased or we can add another phosphor type which has a different spectrum.

Furthermore, we need to give information about a special type of phosphor and its characteristics. YAG:Ce is most common phosphor type in pcLEDs, and it has a very broad emission spectrum with a FWHM of typically 100 nm. YAG:Ce can easily be excited by the blue pumping at 450-460 nm. It has high quantum efficiency near to 90% [29][30]. In addition, YAG:Ce has an excellent thermal behavior and chemical stability. Its decay constant is about 63 nanosecond which is hard to be saturated.[29]

# CHAPTER III

# EXPERIMENTAL STUDY

Gallium nitride based phosphor converted LEDs (pcLEDs) are widely used in indoor and outdoor lighting due to energy efficiency, low energy consumption, compact size, long life, high color rendering, and low production cost [16],[17],[18].

Blue LED chips which are semiconductor materials are driven by DC power source, and they need to exceed their stopping potential to emit light in the multi quantum well layer. This stopping potential starts at 2 volts, and they operate up to 4 volts. Moreover, LEDs are temperature dependent devices that the efficiency drops as a function of linearity with the increasing temperature. Light intensity decreases 25% with an increasing temperature of 100 degree of Celsius in LEDs. Their light distributions generally are in the pattern of Lambertian distribution [32].

Phosphor converted light emitting diodes (LEDs) and packaging elements have been studied in the experiments. Radiant flux, luminous flux, gain and loss rates will be shown in this part of thesis. Moreover, the effects which increase and decrease lumen will be studied, and then they will be compared with the simulation results in order to distinguish optical and thermal effects.

## *3.1. Experiments with Blue Light Emitting GaN Chip*

The experiments have started with a blue GaN chip. Gallium nitride dies (CREE EZ1000) were used as light source in the experiments. It has peak wavelength of between 450-460 nm and 980x980x100 micrometer dimensions (μm=$10^{-6}$) with the top gold bond pads of 130x130 μm [32].

Blue GaN based LED chip was mounted to metal core aluminum PCB which is 3x3 cm with a 1.6 mm thickness. Around the LED chip, a 3x3 mm ceramic enclosure surrounds the LED chip for the protection. Moreover, 2 holes on the PCB will be used for injecting liquid. One is used to inject, and second one is used to circulate the liquid during injection procedure Figure 3-1.

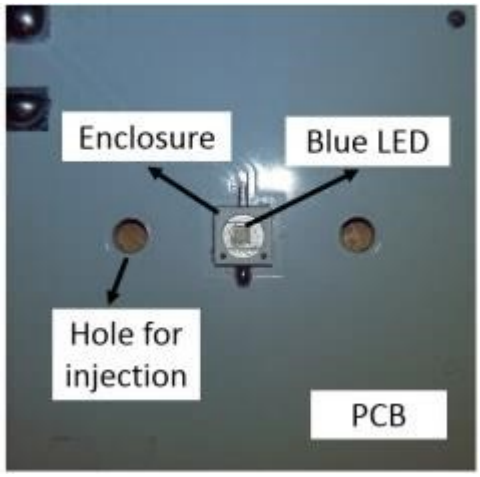


**Figure 3-1:** GaN based blue LED and PCB

Blue light emitting diodes were driven by a direct current (DC) power supply of Agilent. A set of temperature sensors of T type were used to control the experimental system, and an integrating sphere (LabSphere Illumia Plus 610) was used for the optical measurements

[33] . That integrating sphere, which can measure the wavelength region of 350 nm and 1000 nm, can measure up to 45000 lumens. The sensitivity is 0.04 lumens. Our experimental region starts at about 400 nm and goes up to 700 nm. The integrating sphere can be seen in Figure 3-2.

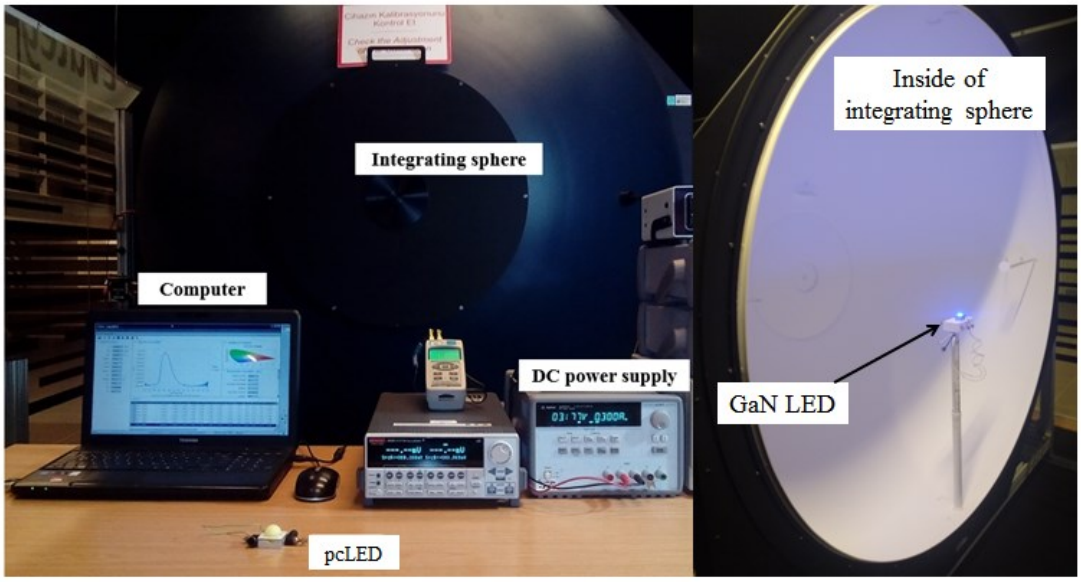


**Figure 3-2:** Experimental system for optical tests

In our study, we mostly focus on luminous flux (lumen) and radiant power. Lumen is a photo-metric unit which can be used to obtain human light sensation. However, radiant power is the physical quantity and can only be used for energy efficiency analysis in such studies. Moreover, color rendering index (CRI), correlated color temperature (CCT), spatial distributions, and scotopic lumens were also evaluated in both experimental and theoretical research chapters.

Experimental have been carried out in 2 different driving currents in order to get gain and loss factors. First, blue bare chips were driven at 300 mA, and 10 measurement results were

taken in the integrating sphere at the steady state conditions, then the average lumen is calculated from those measurements. In the second part of experiments, the blue bare chips were driven at 450 mA current, and 10 measurement results were taken at the steady sate, then the average is calculated for the given current.

### 3.1.1. Measurements at 300 mA

In Figure 3-3, the spectral power distribution was given for the blue bare chip at 300 mA DC. The radiometric measurements have a peak wavelength of 455.2 nm, CCT of 22000, CRI of -51.9, center wavelength at 452.3 nm, and full width half maximum (FWHM) 24.7 nm. Its chromaticity results are 0.1453 x, 0.0409 y, 0.1817 u, 0.0766 v.

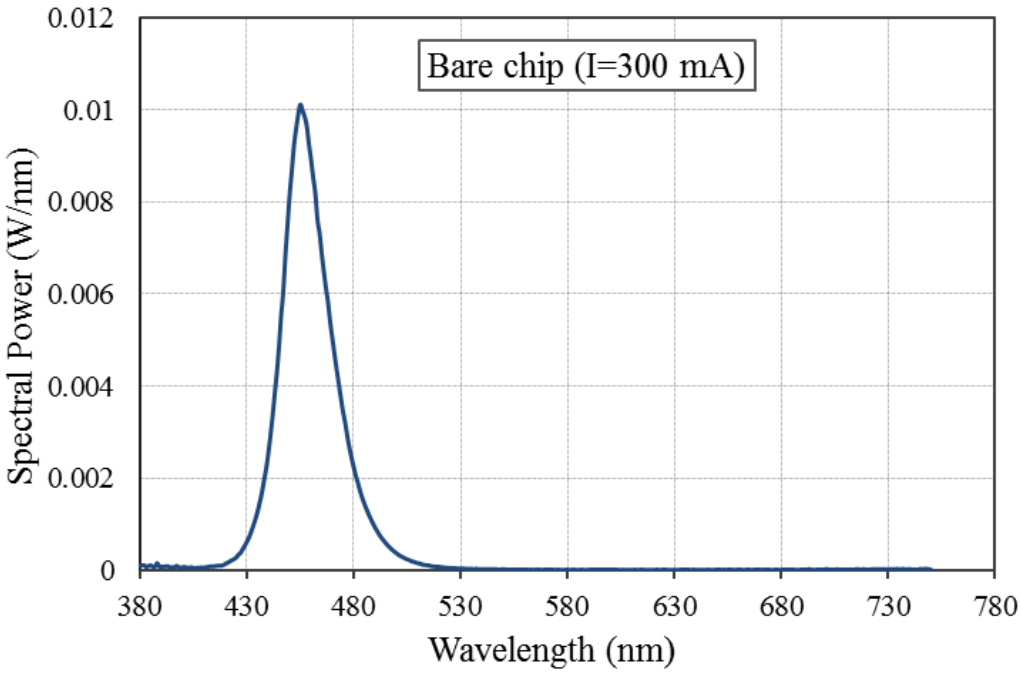


**Figure 3-3:** Spectral power distribution of blue LED for 300 mA DC

In Table 3-1, the radiant and luminous fluxes are given for the driving current of 300 mA. Average luminous flux for the blue bare chip is 15.5±0.04 lm, and radiant power is 298.6±0.5 mW.

**Table 3-1:** Measurement results for blue LED chip at 300 mA

| | *1* | *2* | *3* | *4* | *5* | *6* | *7* | *8* | *9* | *10* |
|---|---|---|---|---|---|---|---|---|---|---|
| Luminous Flux (Lm) | 15.6 | 15.6 | 15.6 | 15.6 | 15.6 | 15.5 | 15.6 | 15.6 | 15.5 | 15.6 |
| Radiant power (W) | 0.299 | 0.299 | 0.299 | 0.299 | 0.299 | 0.298 | 0.299 | 0.299 | 0.298 | 0.298 |

### 3.1.2. Measurements at 450 mA

In Figure 3-4, the spectral power distribution is given for the blue bare chip at 450 mA DC. The radiometric measurements have a peak wavelength of 455.1 nm, CCT of 22000, CRI of -51.9, center wavelength at 456.9 nm, and FWHM 25.5 nm. Its chromaticity results are 0.1456 x, 0.0402 y, 0.1826 u, 0.0756 v.

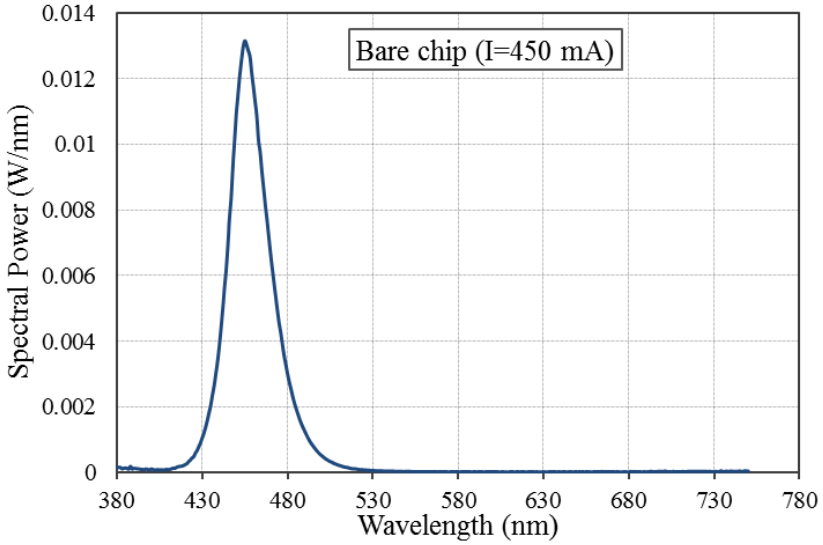

**Figure 3-4:** Spectral power distribution of blue LED for 450 mA DC

In Table 3-2, the radiant and luminous fluxes are given for the driving current of 450 mA. Average luminous flux for the blue bare chip is 20.98±0.05 lm, and radiant power is 405.33±0.4 mW.

**Table 3-2**: Measurement results of blue LED at 450 mA

| | *1* | *2* | *3* | *4* | *5* | *6* | *7* | *8* | *9* | *10* |
|---|---|---|---|---|---|---|---|---|---|---|
| Luminous Flux (Lm) | 21.0 | 21.0 | 20.9 | 21.1 | 21.0 | 21.0 | 21.0 | 21.0 | 20.9 | 21.0 |
| Radiant power (W) | 0.405 | 0.405 | 0.404 | 0.405 | 0.405 | 0.405 | 0.405 | 0.405 | 0.404 | 0.404 |

## *3.2. Experiments with Glass Dome over a Blue LED*

A special type of glass (borosilicate, Schott BK7) was used as in order to perform protection, remote phosphor coating, and liquid injection in LED package. Borosilicate glass consists of silica ($SiO_2$ > 60%) and boric oxide (boron trioxide $B_2O_3$) as the main glass-forming constituents. Borosilicate glasses have very low thermal expansion coefficients ($3\times10-6\ K^{-1}$). Hence, borosilicate glasses are resistant to thermal shock more than any other glasses, and it is less subject to thermal stress [34].

Borosilicate glass is used as lenses in flashlights in lighting industry. Hence, the transmittance of light is increased in the lens compared to lower quality glass. Borosilicate glass has refractive index of 1.525 for 450 nm blue light, 1.518 for 550 nm [35]. Highest working temperature of borosilicate glass is 268 °C. Hence, borosilicate glasses are

generally used in high intensity discharge mercury and metal halide lamps as the outer envelope material due to higher temperatures. In addition to discharge lamps, organic light-emitting diodes (OLEDs) use borosilicate glass (BK7). BK7 is generally used as a common substrate in OLEDs because of its optical and mechanical characteristics in relation to cost.

### 3.2.1. Measurements at 300 mA

In the second phase, the blue chip with a glass dome which has a radius of 10 mm and a thickness of 1.5 mm has been measured. Glass dome mounted over the PCB as in the figure below. 10 measurement results have been taken at the steady state for 300 and 450 mA driving currents.

**Figure 3-5:** Blue LED chip with a glass dome

In Figure 3-6, the spectral power distribution is given for the blue bare chip at 300 mA DC. The radiometric measurements have a peak wavelength of 455.2 nm, CCT of 22000, CRI

of -51.9, center wavelength at 452.3 nm, and FWHM 24.7 nm. Its chromaticity results are 0.1453 x, 0.0409 y, 0.1817 u, and 0.0766 v.

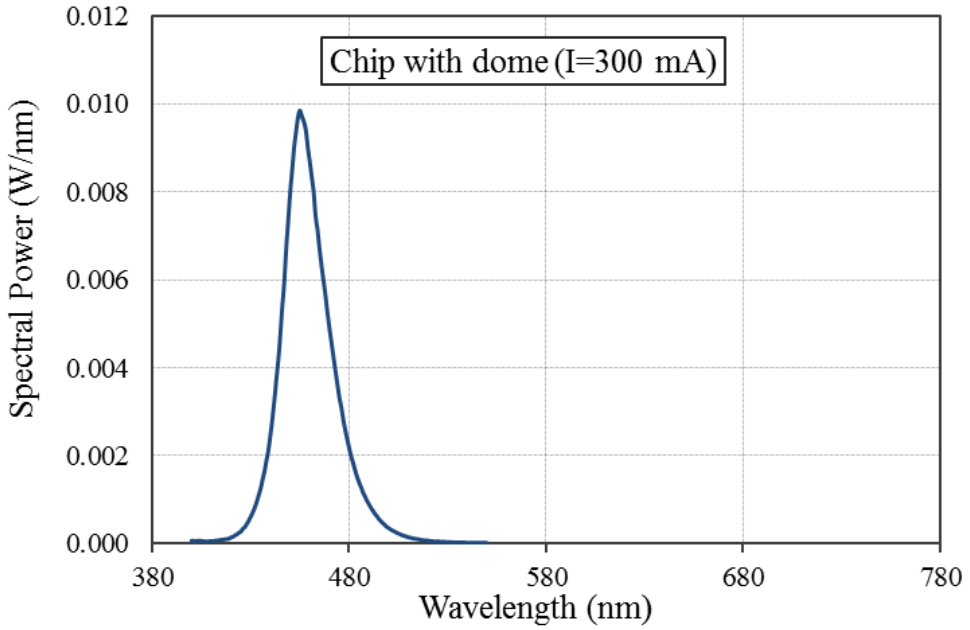


**Figure 3-6:** Spectral power distribution of blue LED with dome for 300 mA DC

In Table 3-3, the radiant and luminous fluxes are given for the driving current of 300 mA. Average luminous flux after glass dome is 15.16±0.04 lm, and radiant power is 290.9 mW.

**Table 3-3:** Measurement results of blue LED chip with a dome at 300 mA

| | *1* | *2* | *3* | *4* | *5* | *6* | *7* | *8* | *9* | *10* |
|---|---|---|---|---|---|---|---|---|---|---|
| Luminous Flux (Lm) | 15.2 | 15.2 | 15.2 | 15.2 | 15.2 | 15.1 | 15.2 | 15.2 | 15.1 | 15.2 |
| Radiant power (W) | 0.291 | 0.291 | 0.291 | 0.291 | 0.291 | 0.291 | 0.291 | 0.291 | 0.291 | 0.291 |

### 3.2.2. Measurements at 450 mA

In Figure 3-7, the spectral power distribution is given for the blue bare chip at 450 mA DC. The radiometric measurements have a peak wavelength of 455.2 nm, CCT of 22000, CRI of -52.0, center wavelength at 456.9 nm, and FWHM 25.5 nm. Its chromaticity results are 0.1456 x, 0.0402 y, 0.1826 u, and 0.0756 v.

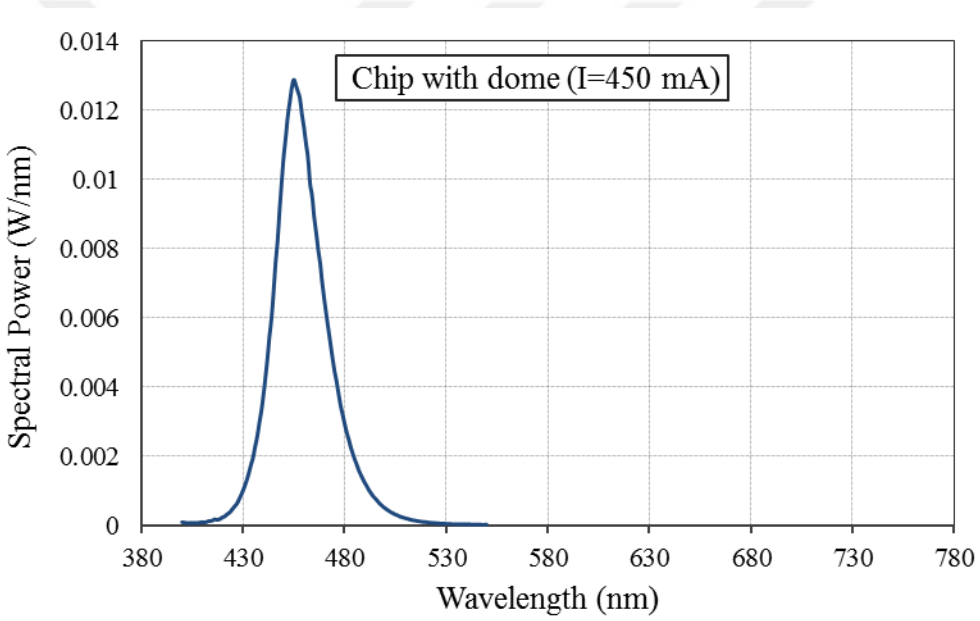


**Figure 3-7:** Spectral power distribution of blue LED with dome for 450 mA DC

In Table 3-4, the radiant and luminous fluxes are given for the driving current of 450 mA. Average luminous flux after glass dome is 20.42±0.05 lm, and radiant power is 394.4±0.5 mW.

**Table 3-4:** Measurement results of blue LED chip with dome at 450 mA

| | *1* | *2* | *3* | *4* | *5* | *6* | *7* | *8* | *9* | *10* |
|---|---|---|---|---|---|---|---|---|---|---|
| Luminous Flux (Lm) | 20.4 | 20.4 | 20.4 | 20.5 | 20.5 | 20.5 | 20.5 | 20.4 | 20.4 | 20.4 |

| | | | | | | | | | | |
|---|---|---|---|---|---|---|---|---|---|---|
| Radiant power (W) | 0.394 | 0.395 | 0.394 | 0.395 | 0.395 | 0.395 | 0.395 | 0.395 | 0.394 | 0.394 |

In the glass dome, luminous fluxes and radiant powers have reduced 2.57% and 2.68%, so for the both LED systems there are a small amount of loss rates, in fact both decrease rate should be equal in that phase. However we see that in the higher driving current power loss rate is higher than lower driving current. In the experiments all the factors affecting light extraction are effective such as optic and thermal management. In order to obtain loss rates in glass, we will compare the results after evaluating simulations in the next chapter.

**Table 3-5:** Luminous and radiant flux results and loss ratios

| | | 300 mA | 450 mA |
|---|---|---|---|
| LED chip | Lumen (Lm) | 15.6±0.04 | 21.0±0.05 |
| | Radiant power (mW) | 298.6±0.5 | 405.3±0.4 |
| Glass dome | Lumen (Lm) | 15.2±0.04 | 20.4±0.05 |
| | Radiant power (mW) | 290.9 | 394.4±0.5 |
| Lumen decrease (%) | | 2.57±0.08 | 2.67±0.1 |
| Radiant power decrease (%) | | 2.57±0.5 | 2.69±0.9 |

## *3.3. Experiments with Remote Phosphor Coated LED Packages*

Phosphor is mostly used in LED packages in order to convert blue light to white light. Cerium doped yttrium aluminum garnet phosphors (YAG:Ce) are able to broaden the light spectrum in the visible region with high efficiencies. Blue light generated by gallium nitride (GaN) chips generally has the wavelength of 450-460 nm, and these light particles are mostly absorbed by such a highly efficient phosphor [36][37]

In addition to heat generation in the LED chips, phosphor conversion also leads to radiant power energy loss and heat in the phosphor layer in the LED packages. However, doped phosphors have a quantum efficiency of higher than 95 % in recent years [38]. However, radiant energy decrease and Stokes shift (SS) changes are inevitable during conversion process, because the conversion of spectrum results in wider emission spectrum.

The emission region of cerium doped YAG phosphor is between 500 nm and 700 nm which include green, yellow, orange, and red colors with different intensities. Yet, we can obtain energy efficient but low rendering white with blue and yellow emission of YAG:Ce.

In LED packages, heat is mainly produced in semiconductor materials. Particular reasons have been given in the semiconductor chapter. In addition to semiconductors, light particles converted in phosphor lead to heat up LED package due to Stokes shift and quantum efficiency [39]. Although the heat generation is higher on semiconductor materials compared to phosphor layer, phosphor particles can have higher temperature in white light emitting LED packages [40],[41],[42].

In our remote phosphor coated experimental setup, phosphor is placed away from blue LED chip and 2 main heat sources are placed away from each other, so temperature and extra heat production are decreased in remote system. In our package we coated phosphor silicon mixture inside the glass dome in order to increase light extraction efficiency (LEE) and decrease temperature in phosphor and LED chip with heat dissipation.

Cerium doped yttrium aluminum garnet phosphor (YAG:Ce) has been prepared with a concentration of 16 % by weigh with a 1.5 mm thickness. After the phosphor coating, we repeated the measurements in the integrating sphere measurement system at 300 and 450 mA driving currents, and voltage, lumen, optical power, CRI, CCT and spectrum of the remote phosphor coated LED have been taken in the steady state conditions. The remote coated LED package can be seen in the Figure 3-8.

**Figure 3-8:** Remote phosphor coated LED package

### 3.3.1. Measurements at 300 mA

In Figure 3-9, the spectral power distribution is given for the remote phosphor coated LED package at 300 mA DC. The radiometric measurements have a peak wavelength of 544.5 nm, CCT of 4052, CRI of 53.8, center wavelength at 566.9 nm, and FWHM 116 nm. Its chromaticity results are 0.4187 x, 0.5315 y, 0.1961 u, and 0.3734 v.

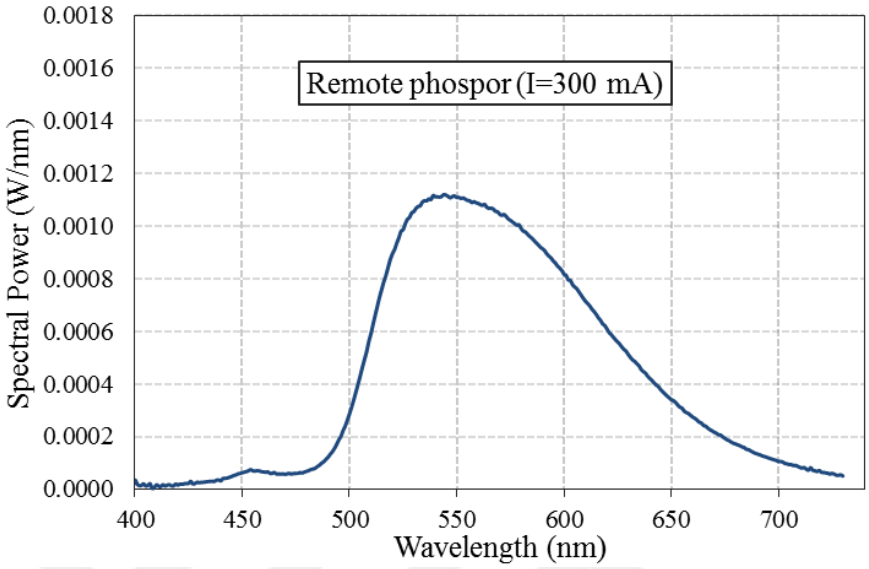


**Figure 3-9:** Spectral power distribution of remote phosphor coated LED for 300 mA DC

In Table 3-6, the radiant and luminous fluxes of remote phosphor coated LED are given for the driving current of 300 mA. Average luminous flux after remote phosphor is 62.55±0.03 lm, and radiant power is 148.7±0.9 mW.

**Table 3-6:** Measurement results for the remote phosphor coated LED package at 300 mA

| | *1* | *2* | *3* | *4* | *5* | *6* | *7* | *8* | *9* | *10* |
|---|---|---|---|---|---|---|---|---|---|---|
| Luminous Flux (Lm) | 62.6 | 62.6 | 62.6 | 62.6 | 62.6 | 62.6 | 62.6 | 62.6 | 62.5 | 62.6 |
| Radiant power (W) | 0.15 | 0.15 | 0.15 | 0.15 | 0.148 | 0.149 | 0.15 | 0.148 | 0.148 | 0.149 |

### 3.3.2. 450 mA Measurements

In Figure 3-10, the spectral power distribution is given for the remote phosphor coated LED package at 450 mA DC. The radiometric measurements have a peak wavelength of 544.5

nm, CCT of 4046, CRI of 54.2, center wavelength of 567 nm, and FWHM of 115.7 nm. Its chromaticity results are 0.4190 x, 0.5307 y, 0.1964 u, and 0.3733 v.

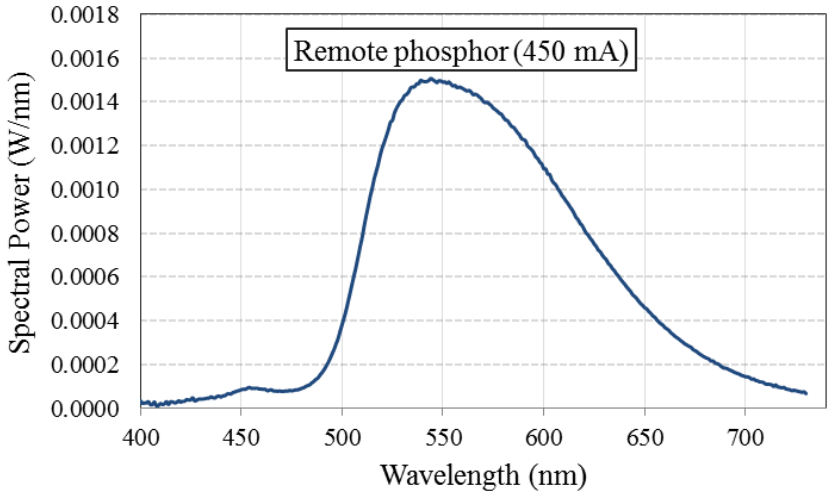


**Figure 3-10:** Spectral power distribution of remote phosphor coated LED for 450 mA DC

In Table 3-7, the radiant and luminous fluxes of remote phosphor coated LED are given for the driving current of 450 mA. Average luminous and radiant fluxes have been obtained 83.99 lm, 201.27±0.6 mW respectively.

**Table 3-7:** Measurement results for the remote phosphor coated LED package at 450 mA

| | *1* | *2* | *3* | *4* | *5* | *6* | *7* | *8* | *9* | *10* |
|---|---|---|---|---|---|---|---|---|---|---|
| Luminous Flux (Lm) | 84.0 | 84.0 | 84.0 | 84.0 | 84.0 | 84.0 | 84.0 | 84.0 | 84.0 | 84.0 |
| Radiant power (W) | 0.201 | 0.200 | 0.201 | 0.201 | 0.202 | 0.201 | 0.200 | 0.201 | 0.201 | 0.200 |

After phosphor coating, radiant power has decreased 49% in the remote phosphor layer. The loss is due to quantum efficiency, reflections, and Stokes shift. The peak wavelength

was close to 455 nm before phosphor coating, and then the peak became about 545 nm. Here, the conversion efficiency in Stokes shift is the ratio of wavelengths of photons at 455 nm to 545 nm which equals to 83%.

**Table 3-8:** Lumen increase rates after phosphor coating in both driving currents

| | | *300 mA* | *450 mA* |
|---|---|---|---|
| Chip With Glass | Lumen (Lm) | 15.16±0.04 | 20.42±0.05 |
| | Radiant power (mW) | 290.9 | 394.4±0.4 |
| Phosphor coated | Lumen (Lm) | 62.56±0.03 | 84 |
| | Radiant power (mW) | 148.7±0.9 | 201.3±0.6 |
| Lumen increase in P-layer | | 413±0.07 % | 411%±0.05 % |
| Radiant power efficiency | | 51±0.9 % | 51±0.1 % |
| Luminous efficacy | | 421 | 417 |

However, radiant energies of the chip with the glass dome are about 291 and 394 mW, and decreased to 148.7 and 201.3 mW in remote phosphor for the given driving currents respectively. We can conclude that the Stokes shift loss is about 17 %, and the rest loss which is about 32% goes to other factors such as reflection and Fresnel losses, quantum efficiency etc. Luminous efficacies have been obtained 421 and 417 lm/W for the given driving currents respectively (see Table 3-8).

## *3.4. Experiments with Phosphor Coated LED Chips*

There are mainly 2 phosphor coating methods in LED packages, which are remote phosphor and coating on LED chip. The remote phosphor can be higher efficient than the latter one due to lower operating temperature. In addition, optical extraction efficiency can

be increased as well. Moreover, color and intensity stability in the remote phosphor can be supplied, thus glare and iso-CCT distribution problems can be solved in remote phosphor case. [43], [44].

However, white light emitting phosphor coated LED chip is compact sized, thus they are mostly used in lighting industry. In this study, we want to see the losses in the phosphor coating of LED chip. CREE ez1000 blue chips and YAG:Ce phosphor with different concentrations of 7%, 10%, and 12% have been used in the experiments.

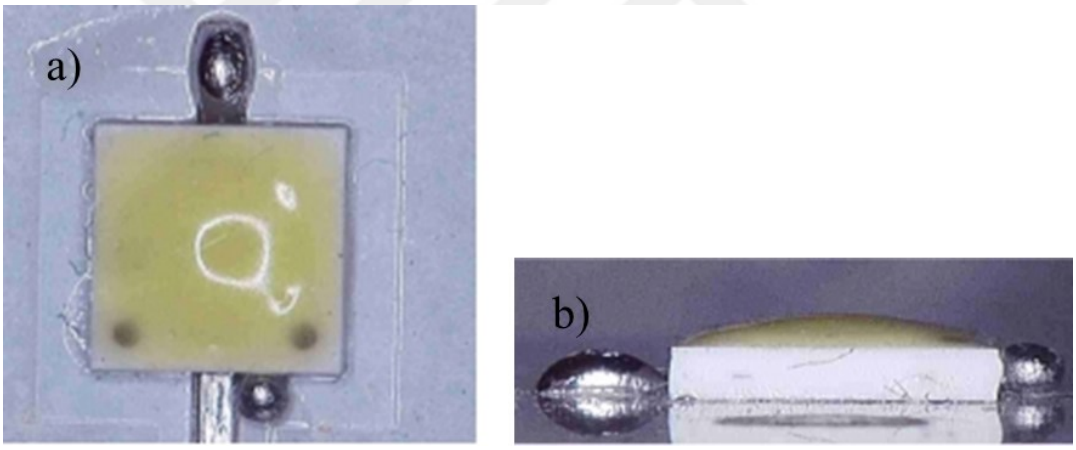


**Figure 3-11:** Phosphor coated LED a) top view b) side view

Phosphor coated LED chips have been tested under driving currents of 150, 300, and 450 mA in order. The initial radiant powers of blue LED chips are 199, 251, and 257 mW at 150 mA driving current for the blue chips. After phosphor coating, radiant powers decreased to 93.0 (7%C), 118 (10%C), and 105 mW (12%C). Radiant flux reduced 53, 53, and 59% in the given concentrations of phosphor coating respectively (Figure 3-12).

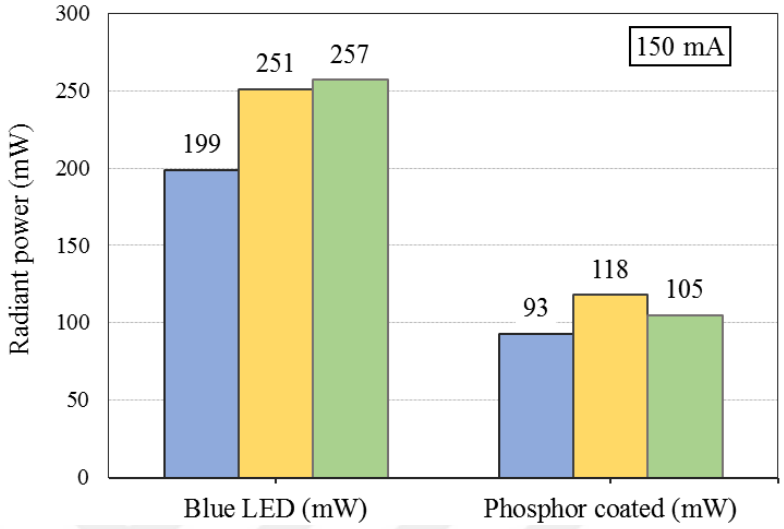


**Figure 3-12:** Radiant powers of blue LED and phosphor coated LEDs in 150 mA

The luminous flux results of blue chips are 5.5, 9.5, and 9.4 lumens at 150 mA driving current. However, phosphor has increased the lumen outputs to 24, 36, and 36 lm for the given concentrations respectively. The luminous enhancements correspond to more than 530, 370, and 380 per cent in phosphor coating. Optimum point for phosphor concentration seems about 10-12% to get highest luminous efficiency in the first step of experiments.

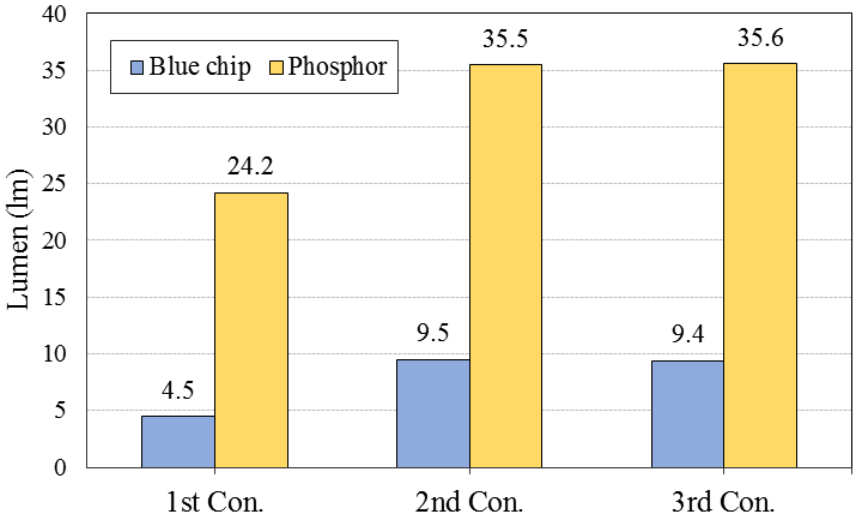

**Figure 3-13:** Luminous fluxes for blue LED and phosphor coated LED at 150 mA DC

In the 300 mA driving current, radiant powers have decreased from 320, 408, and 413 mW to 162, 202, and 181 mW. We have observed 49%, 50%, and 56% radiant energy decrease in the phosphor coating in the second driving current. The lumen outputs increased from 7.7, 16.3, and 16.3 lm to 43, 63.1, and 63.3 lm, so the luminous efficiency enhancements are almost 560, 390, and 390 per cent for the given concentrations respectively.

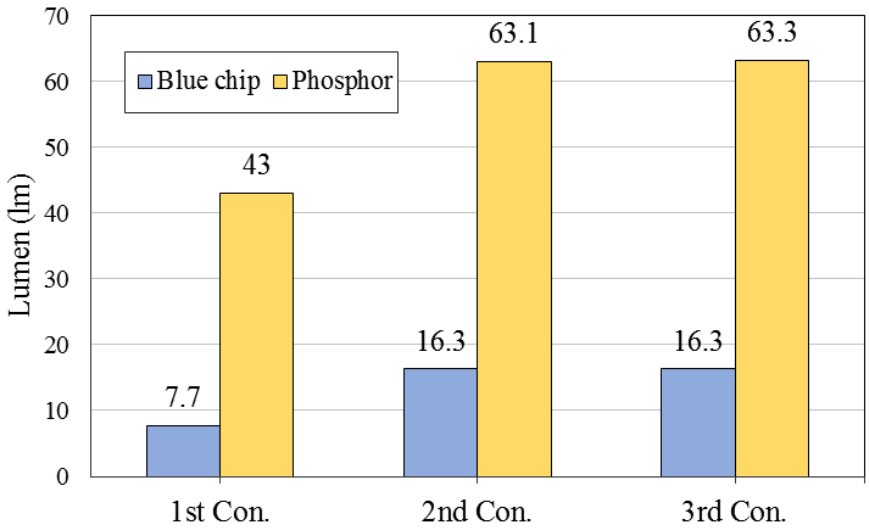


**Figure 3-14:** Luminous fluxes for blue LEDs and phosphor coated LEDs at 300 mA DC

In 450 mA driving current condition, radiant powers were 421, 543, and 548 mW before phosphor coating. They reduced to 218, 265, and 240 mW after coating on LED chip. Radiant energies decreased by 48, 51, and 56%, but luminous flux rates increased by 550, 370, and 380%.

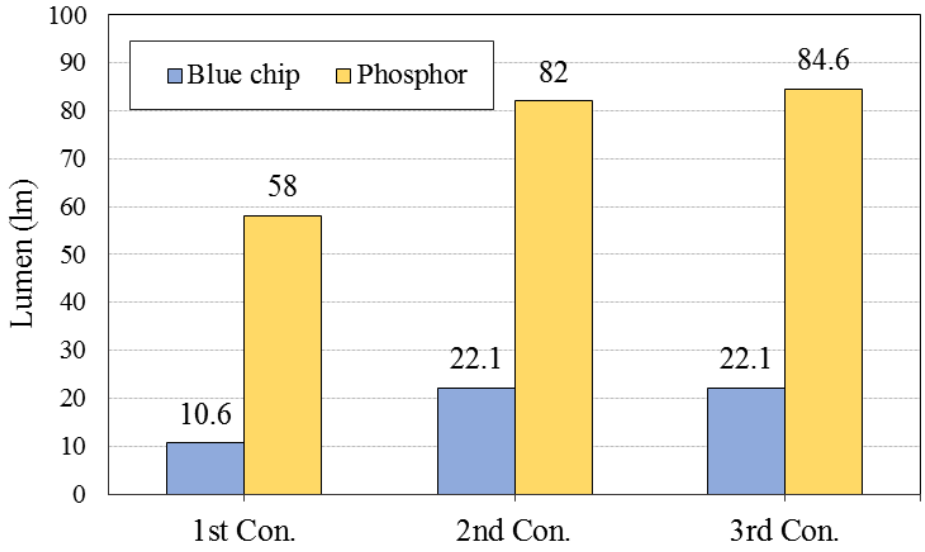


**Figure 3-15:** Luminous fluxes for blue LEDs and phosphor coated LEDs at 450 mA

Radiant energy for the first concentration of phosphor – silicon mixture has almost 50% energy efficiency. Second phosphor concentration has almost 48% and final concentration is 43% efficient. Lumen enhancements have been obtained 548%, 377%, and 383% for the given phosphor concentrations, and the luminous efficacies of coated LEDs are 244, 308, and 347 lm/W. In the remote phosphor coated LED, we had obtained 62.5 and 84 lumens corresponding to 421 and 417 lm/W efficacies in the 300 and 450 mA driving currents (see Table 3-9).

**Table 3-9:** Lumen enhancement ratios and efficacies

| *Concentration (%)* | *Lumen Enhancement* | *Luminous Efficacy of Coated LED* |
|---|---|---|
| 7 | 548% | 264 |
| 10 | 377% | 308 |
| 12 | 383% | 347 |

In remote phosphor experiment with 16% phosphor-silicon concentration we have obtained 51% energy efficiency in the remote phosphor. Yet, luminous flux rates at 300-450 mA driving currents are comparably close in both conformal and remote phosphor cases.

In the next part of the experiments, immersion cooling effects are studied for the combined effects of optic and thermal. Later on, the results will be compared with the optical analysis.

## *3.5. Experiments with Liquid Cooling Integrated Remote Phosphor Coated Light Emitting Diode*

We want to enhance the optical light extraction and thermal heat dissipation in the remote phosphor coated LED package [45]. In this part of the experimental study, we will study the effects of prosed method with dielectric liquid [46][47]. The gap between remote phosphor and blue GaN based semiconductor has been filled with a optically transparent liquid, so that refractive index matching can be increased in our package. Moreover, the immersion cooling can increase heat transfer between semiconductor and remote phosphor [40][42]. Then, the reflection and absorption losses will be evaluated after comparing experimental results of the immersion cooling with the simulations of optical effects.

Absorption coefficients of a transparent liquid of Nusil Silicon Technology LS5238 in the range 400-700 nm were measured by a spectrometer [48]. Absorbance of transparent liquid was measured as almost 0. Then, it has been assumed to be 0 in the simulations and experiments. Then, the liquid was injected through the two holes in the PCB, and then 2 valves were closed respectively in order to prevent air bubbles in the liquid. Air bubbles

would cause major loss in the light output in the upper surface of the LED. Back reflection of light would be occurred in the bubbles due to the refractive index variances between liquid-air gap and air gap-remote phosphor. The liquid injected remote phosphor coated pcLED is given in Figure 3-16. The liquid in the setup has direct contact with the 2 heat sources which are the chip and phosphor layer in our model. Thus, the liquid leads to natural convection between chip-liquid and liquid-phosphor layer. It will change thermal behavior of the LED package that we will evaluate later.

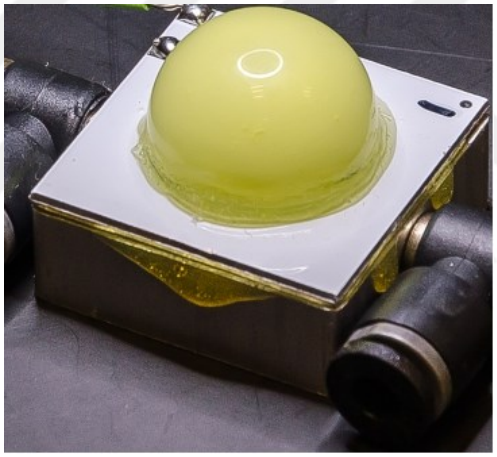

**Figure 3-16:** Remote phosphor coated liquid injected LED package

### 3.5.1. Measurements at 300 mA

In Figure 3-17 , the spectral power distributions are given for the liquid coolant integrated LED at 300 mA driving current. Radiometric results have a peak wavelength of 544.5 nm, CCT 4098, CRI 55, center wavelength of 567 nm, and a FWHM of 116 nm. Its chromaticity results are 0.4149 x, 0.5283 y, 0.195 u, 0.3725 v.

In the following table, measurement results of the radiant power and luminous flux for the liquid coolant integrated LED are given for the driving current of 300 mA. Average luminous flux and radiant power are 79.0±0.05 lumens and 180 mW respectively.

**Table 3-10:** Measurement results of remote phosphor coated liquid coolant integrated LED package at 300 mA

| | *1* | *2* | *3* | *4* | *5* | *6* | *7* | *8* | *9* | *10* |
|---|---|---|---|---|---|---|---|---|---|---|
| Luminous Flux (Lm) | 78.9 | 78.9 | 78.9 | 78.9 | 78.8 | 78.9 | 78.8 | 78.8 | 78.8 | 78.8 |
| Radiant power (W) | 0.180 | 0.180 | 0.180 | 0.180 | 0.180 | 0.180 | 0.180 | 0.180 | 0.180 | 0.180 |

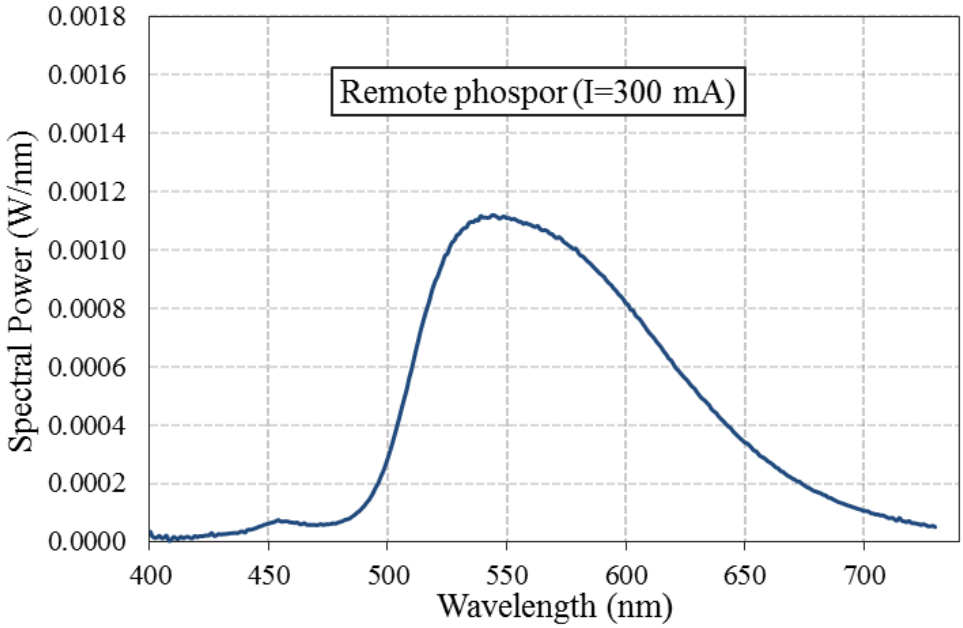


**Figure 3-17**: Spectral power distribution of liquid coolant integrated LED for 300 mA DC

### 3.5.2. Measurements at 450 mA

In Figure 3-18, spectral power distributions are given for 450 mA driving current. The measurement spectrum has a peak wavelength of 545 nm, CCT of 4092, CRI of 56, center

wavelength of 567 nm, and FWHM OF 116 nm. Its chromaticity results are 0.415 x, 0.527 y, 0.1954 u, 0.3723 v. In Table 3-11, the measurement result of the radiant and luminous flux for the liquid injected LED are given for 450 mA. Average fluxes are 105.0 lumens, and 254±1 mW.

**Table 3-11:** Measurement results of remote liquid injected LED package at 450 mA

| | *1* | *2* | *3* | *4* | *5* | *6* | *7* | *8* | *9* | *10* |
|---|---|---|---|---|---|---|---|---|---|---|
| Luminous Flux (Lm) | 105 | 105 | 105 | 105 | 105 | 105 | 105 | 105 | 105 | 105 |
| Radiant power (W) | 0.252 | 0.253 | 0.254 | 0.254 | 0.255 | 0.255 | 0.255 | 0.255 | 0.253 | 0.253 |

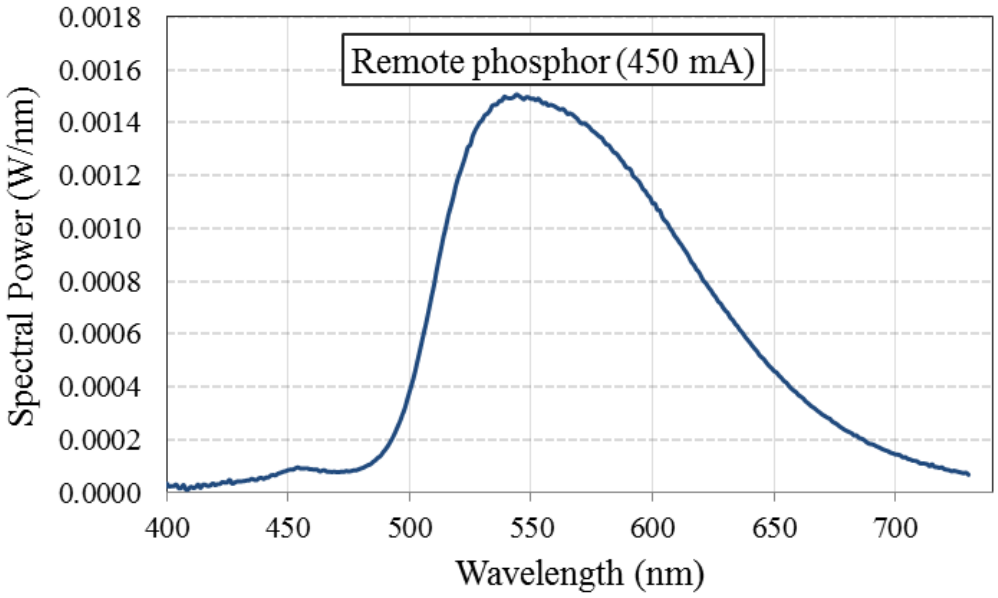


**Figure 3-18:** SPD of liquid injected LED for 450 mA DC

After liquid injection, radiant and luminous fluxes have increased in both driving currents. In the 300 mA driving current, lumen is increased from 63 to 79 which corresponds to

25.9% efficiency enhancement. In the higher current, it is increased from 84 to 105 lumens which corresponds to 25% more efficiency.

In Table 3-10 and Table 3-11, radiant power enhancements are also given. Here, the enhancement ratios are relatively different (21% and 26.2%) because the results of the spectrum is measured between 350 nm and 1000 nm, and there are some fluctuations at the longer wavelength of the spectrum.

There are 2 main reasons to increase fluxes here; they are basically better matching refractive index and thermal reasons. Optical effects will be evaluated in the simulation part. However, thermal effects of the immersion cooling decreases temperature, and thus the performance of the semiconductor chip increases according to data sheet of the CREE ez1000 chip (Figure 3-19). Operating chip temperature can reach up to 150 °C in LED packages. The temperature change of 50 °C can enhance the relative light intensity 10% according to the figure. Moreover, the cooling effects in the remote phosphor should be considered at this point, we can assert that the immersion cooling reduces the phosphor temperature, and thus the color conversion becomes more effective [32].

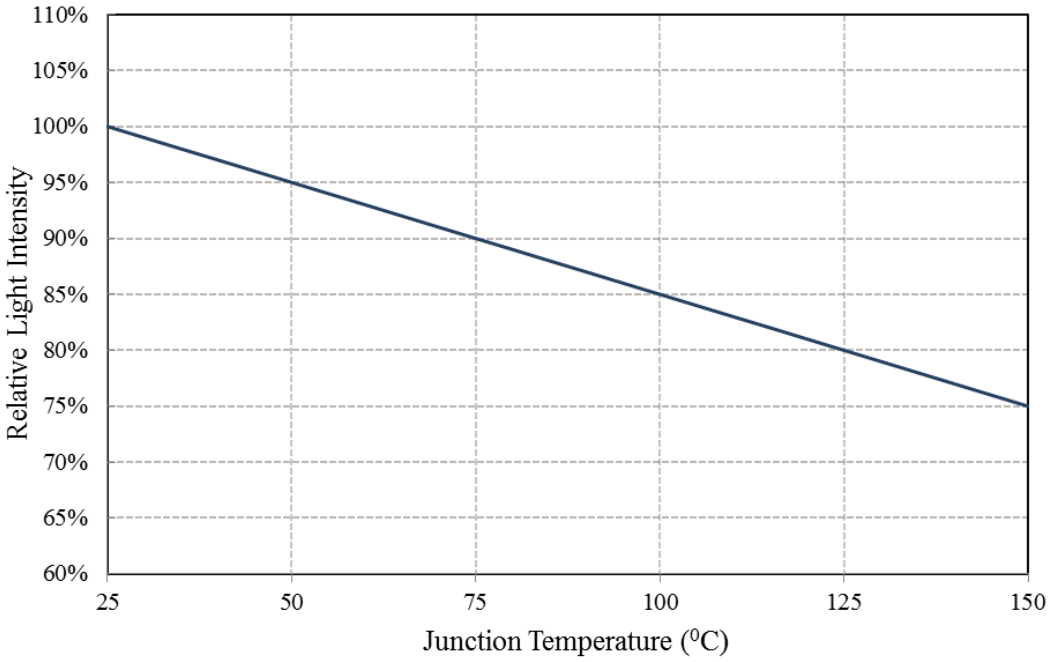


**Figure 3-19**: Relative light intensity with junction temperature of CREE LED chip [32]

Furthermore, the enhancement in the lower current is 1% higher than 450 mA. The optical reflections and absorptions should be same in two experimental setups, but the operating temperatures are the factors here increasing or decreasing the flux rates.

**Table 3-12:** Effect of liquid injection in lumen output

| | | *300 mA* | *450 mA* |
|---|---|---|---|
| Phosphor coated | Lumen (Lm) | 62.6±0.03 | 84 |
| | Radiant power (mW) | 148.7±0.9 | 201.3±0.6 |
| Liquid injected | Lumen (Lm) | 78.8±0.05 | 105 |
| | Radiant power (mW) | 180 | 254±1 |
| Lumen increase after injection | | 25.9±0.11% | 25.0% |
| Radiant power increase | | 21.0±0.6% | 26.2±0.6% |

# CHAPTER IV

# OPTICAL RAY TRACING SIMULATIONS IN BLUE AND COLOR CONVERTED LIGHT EMITTING DIODES

Simulations of the LED package have been performed by means of a commercially available optical simulation program (Lighttools) [49]. The program can be used for modeling light sources, ray tracing, reflector designs, fiber optics, automotive lighting, indoor-outdoor lighting, LED package design and phosphor blue light conversion. LED chips (CREE, OSRAM, and NICHIA etc.) and many other materials (silicon, glass, composites) can be found from the catalog.

Ray tracing simulations in LED packages basically contains spatial distribution and luminous flux calculations. Phosphor modeling can also be made, and phosphor properties can be optimized for accurate phosphor conversion calculations. In our study we mainly focused on luminous flux simulations in order to get the enhancements and losses in LED packages. In addition, the other spatial diagrams will be evaluated in this chapter. Some effects such as Stokes shift and reflections will be obtained in this part. Thus, only optical effects in the LED package will be considered in these simulations.

Spectral power distributions (SPD) of blue LEDs contains wavelengths between 450-460 nm with a Gaussian distribution, yet blackbody light sources have continuous SPD diagrams like halogen lamps (Figure 4-1). White light converted LEDs generally have two peaks in their spectrums, which first peak of blue wavelengths belongs to blue LED chip,

and the second one is yellow's peak which generally produced by the cerium doped yttrium aluminum garnet (YAG:Ce) phosphor with a peak of 555 nm. 2 types of phosphors which are green and red are generally used for high quality light in LEDs. However, when it comes to efficiency blue chips and yellow phosphors are preferred. In electrical devices with a screen like TVs and cell phones generally 3 color (red, green, blue) (RGB) LED sources are utilized to obtain millions of colors in each pixel of the screen. Sample spectrum of halogen, fluorescent, pcLED, and RGB LED were given in Figure 4-1.

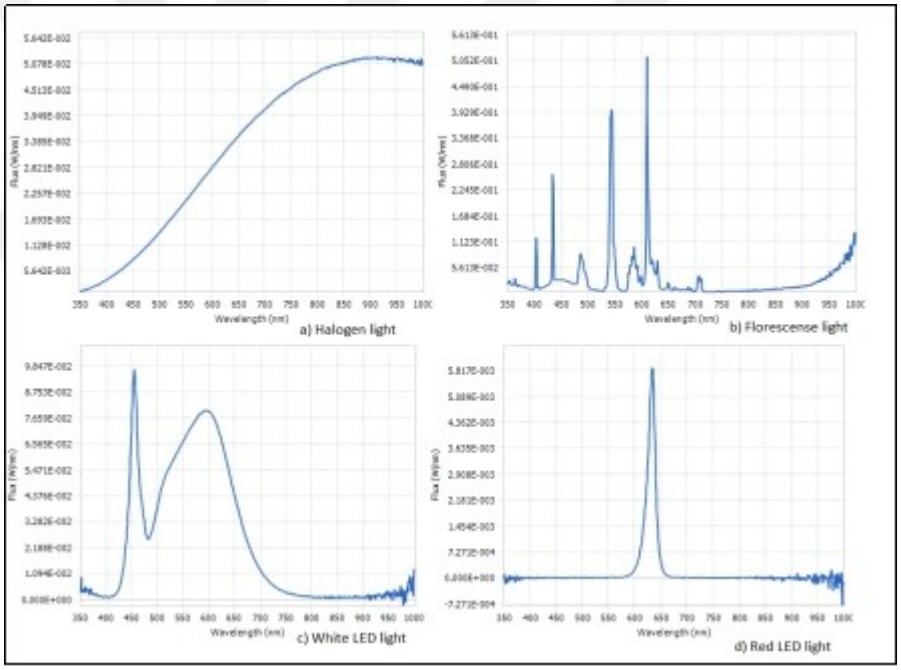


**Figure 4-1:** SPD diagrams a) Incandescent b) Fluorescent c) pcLED d) Red LED

Though, fluorescent light sources have been mainly used in general lighting whose SPD contains peaks and generates low quality white light. Such SPD data can be measured by spectroradiometers and can be imported to ray scattering simulations.

## *4.1. Blue LED Simulations*

Firstly, the chip and the ceramic enclosure are modeled in conformity with an LED as in Figure 4-2, and then emittance aim sphere, material, spectrum, and emitting surfaces of the chip were adjusted in the simulation program accordingly. Refractive index of the semiconductor blue LED die was set to 2.42 (Figure 4-2). Ceramic enclosure has a reflectance of 0.8 (Table 4-1).

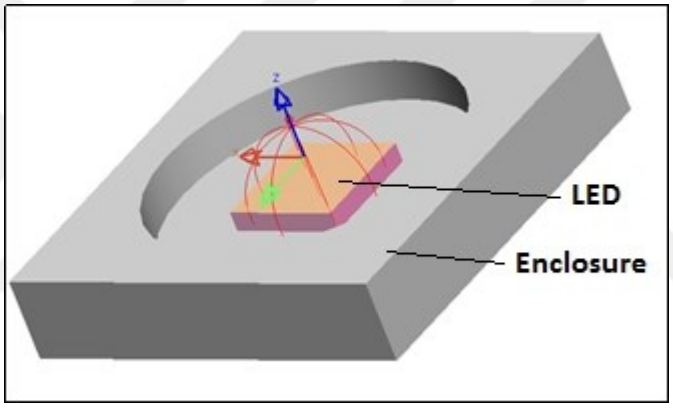


**Figure 4-2:** Blue LED chip and enclosure

The spectral power distribution data of the blue chip was measured by integrating sphere (LabSphere Illumia 610) mentioned in Chapter 3 [33]. In our model, spectral radiant power distribution (SPD) is the initial input of the simulations of the blue LED which contains spectrum data of the chips between the range 350-1000 nm.

The SPD data have a peak wavelength of 455 nm, FWHM of 25 nm and luminous flux of 15.6 lm for 300 mA. The SPD inputs are peak wavelength of 455 nm, FWHM of 25 nm, luminous flux of 20.98 lm. Then, these data were imported to simulation as the light source, and we successfully obtained the experimental findings.

**Table 4-1:** Parameters used in the simulations

| | *n* | *k* | *Re* | *Tr* |
|---|---|---|---|---|
| Chip | 2.42 | - | - | - |
| Enclosure | - | - | 0.8 | |
| PCB | - | - | 0.7 | - |
| Glass | 1.52 | 0 | - | 0.9 |
| Phosphor | 1.6 | 1.80E-06 | - | - |
| Liquid | 1.38 | 0 | - | 1 |
| Air | 1 | 0 | - | 1 |

## *4.2. Analysis of Blue Chip*

Polar diagrams of intensity, color diagrams, intensity diagrams, and CIE chart will be evaluated in this chapter of the thesis. Polar diagrams are given for almost every light source in datasheets, and it is the most fundamental chart of light measurement results in addition to lumen. Color diagrams give information about the color of the light, and intensity diagrams gives information about the light distribution over 2D-3D surfaces. CIE diagrams define colors and links between the wavelengths in electromagnetic visible spectrum [50].

The polar diagrams of white LEDs which have luminous fluxes of 15.16 and 20.98 are given in Figure 4-3. Their light distributions are close to Lambertian in the 0-180 planes, and in that plane their intensities are about 5 and 7 cd [lm/sr]. Thus, we can observe that 1/3 of the lumen numerically gives light intensity for Lambertian distribution. For example, 1000 lm Lambertian light source can give about 350 cd in the normal angle of the luminaire.

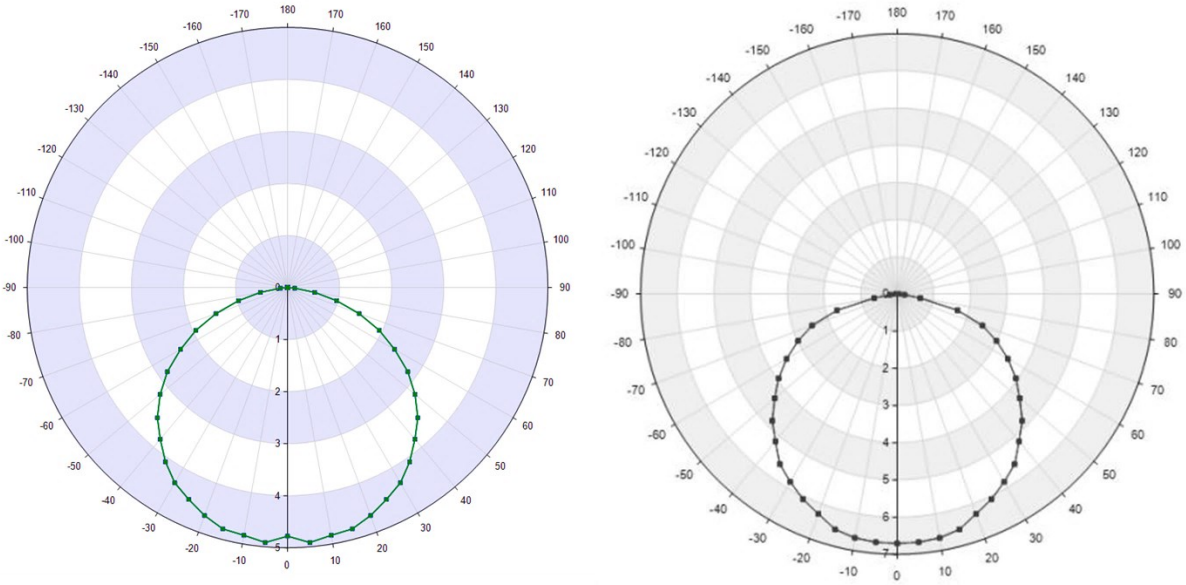

**Figure 4-3:** Polar diagram of spatial distribution (cd) of 300 mA and 450 mA in 0-180 plane

Color diagrams show that the color distributed in all directions is blue, and it is distributed in spherical coordinate system of 0 to 90 degree angles. Both diagrams are similar in the following figure due to same initial SPDs.

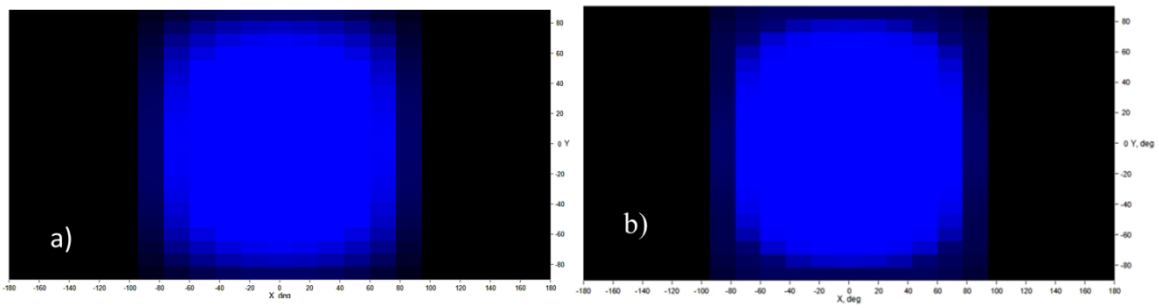


**Figure 4-4:** Color diagram of 455 nm blue LED simulations a) 300 mA b) 450 mA

Luminous intensity distributions for 300 and 450 mA are given in Figure 4-5. Maximum intensities achieved in both simulations in normal angles of LED surfaces which are 0-0 degrees. Highest luminous intensities are 4.9 and 6.6 candelas for the given currents

respectively. We see that the light intensity becomes half at the green region, so the beam angle is about 120 degree for this LED.

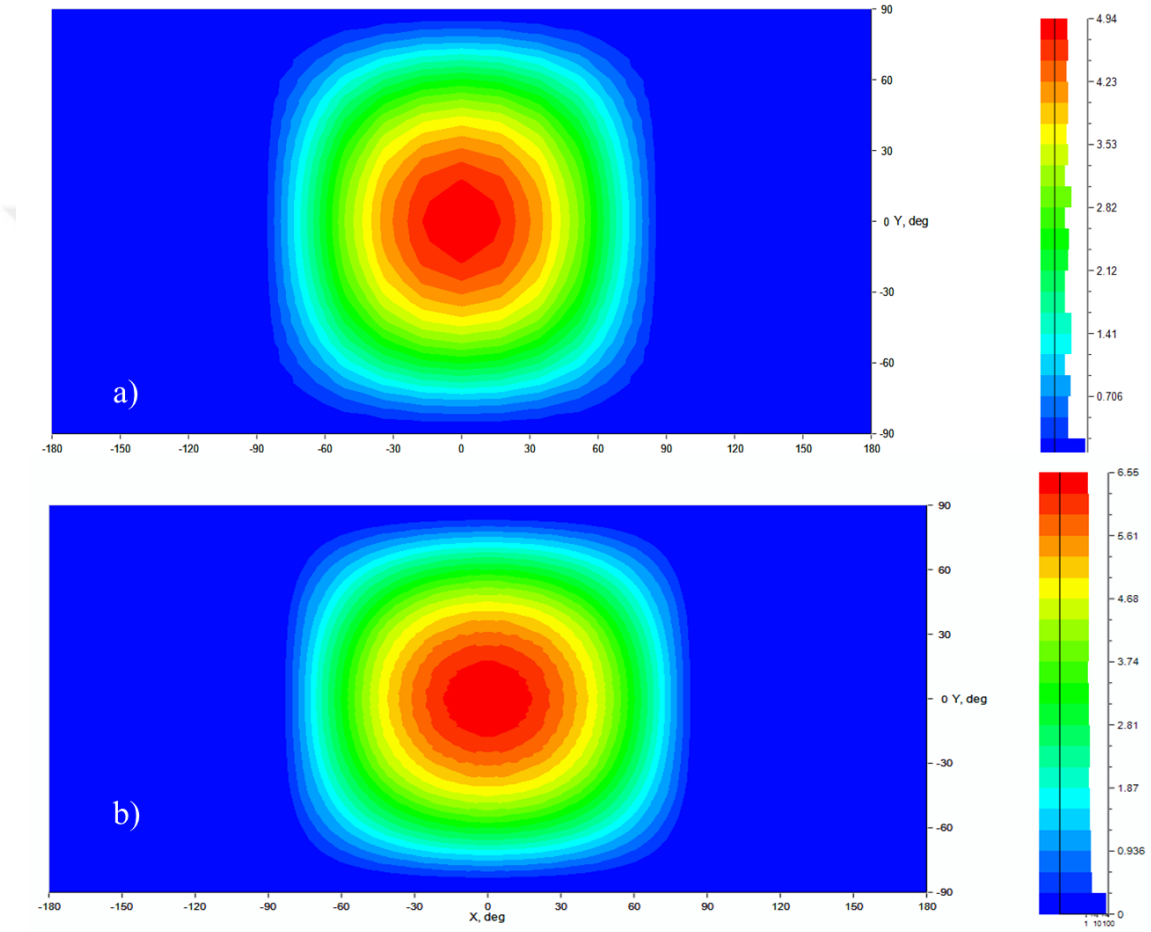


**Figure 4-5:** Luminous intensity distributions in far field receiver for both light LEDs

CIE xy chromatic coordinates are given for the blue chip simulations in Figure 4-6. The x coordinate is about 0.15, and y is about 0.4 for both simulations. We can calculate such optical parameters as CRI and CCT values with the aid of these x and y.

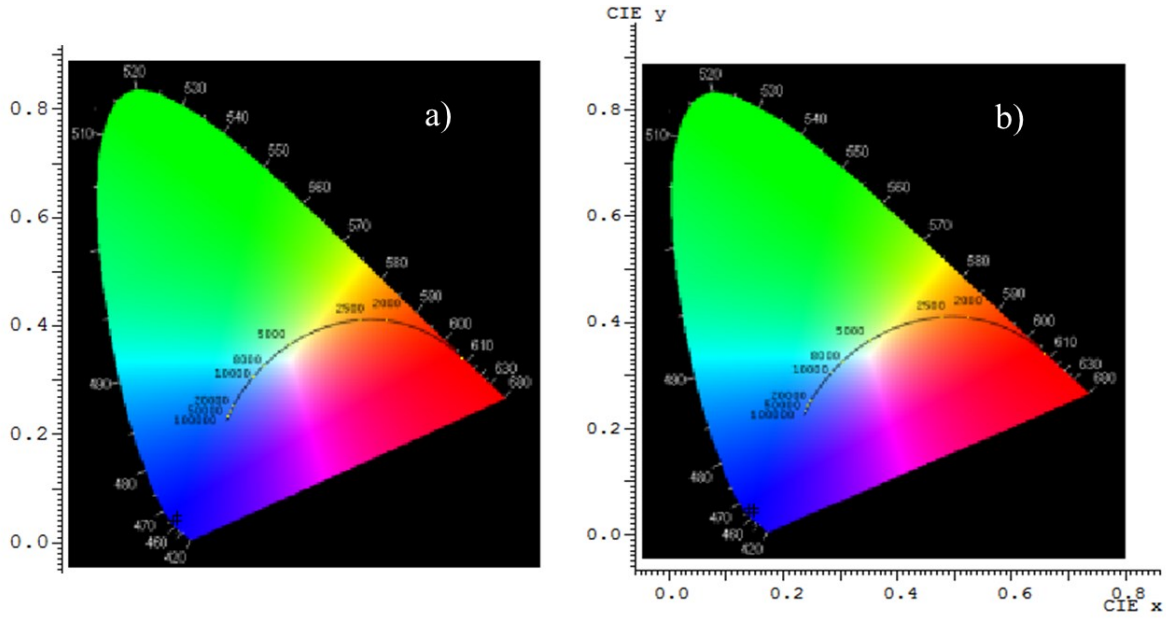


**Figure 4-6:** CIE color triangle of blue chip

## *4.3. Simulations with Glass Dome Mounted LEDs*

Generally glass like materials and silicon composites are used in light luminaires for protection or light distribution. We want to see optical losses and compare them with the experimental findings. In the packaged LED, optical results can differ due thermal effects in the running system.

Glass dome was modeled and optical properties of PCB and glass dome material was set to experimental model (Figure 4-7). The printed circuit board (PCB) has dimensions of 3x3 $cm^2$ and 1 mm thickness. Its optical behavior is set to simple mirror with a 70% reflectance and 30% absorbance. Its material was defined as aluminum. Optical property of the glass dome (2 cm diameter and 1.5 mm thickness) was defined as smooth optical which has 10% absorbance (at 1.5 mm) and Fresnel Losses (due to reflection in both sides of glass which is expected to be nearly 8%).

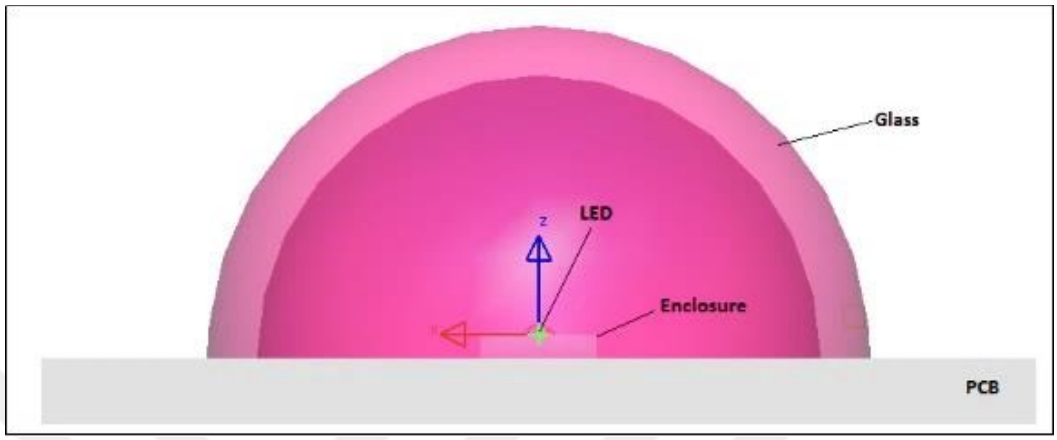


**Figure 4-7:** Model of LED with glass dome

Generally, glass materials have less absorbance than the given above, but the absorbance may increase due to hand made construction as in our sample. Refractive index of the glass is set to 1.52 according to borosilicate glass, indexed as BK7 in Schott library. Its imaginary refractive index is 0 (Table 4-1).

Lumen outputs decreased from 15.6 and 20.98 to 14.55 and 19.61 lm for the given powers respectively, also radiant powers of the 2 systems conformably decreased to 279.2 and 378.8 mW for the given DC currents. Optical losses in the glass dome of the LED package have been found 6.49% and 6.53% for the luminous and optical powers (Table 4-2).

**Table 4-2:** Simulation results for LED chip with glass dome

| | | *300 mA* | *450 mA* |
|---|---|---|---|
| LED chip | Lumen(Lm) | 15.56 | 20.98 |
| | Radiant power(mW) | 298.6 | 405.33 |
| Glass dome | Lumen (Lm) | 14.55 | 19.61 |
| | Radiant power(mW) | 279.2 | 378.8 |
| Lumen decrease (%) | | 6.49 | 6.53 |
| Radiant power decrease (%) | | 6.49 | 6.54 |

In comparison to experimental results, the loss is higher in the simulations. However, it is less than the analytical results of reflection losses at normal incidence. In the experimental result, the lumen decrease rates (2.6%) for glass dome are lower than the expected fluxes of simulations.

Thermal heat dissipation here can lead enhancement in the packaged LED system. Thermal measurements with infrared cameras or thermocouples are necessary for the junction temperatures of the LED in order to see temperature differences after glass dome mounting. Moreover, when we compare the results of simulation with Fresnel reflection rates, luminous fluxes almost decreased 6.5% in simulation and 8.33% in Fresnel reflection analysis (Table 4-3). In Fresnel reflection calculations only the inner and outer surface of the glass dome are considered. Normal reflection at one surface of the glass is about 4.17% and for the both sides of the glass dome this rate becomes about 8.33%. Back reflected light from glass turns to the PCB, and then some of these photons can pass through the glass. The simulation results thus include rays of back reflections, and we obtain rate of 6.5% in simulations which is lower than Fresnel losses.

**Table 4-3:** Experimental, computational and theoretical Fresnel loss rates for LED with a glass dome

| | *Experimental* | | *Simulation* | | *Fresnel loss for normal incidence* | |
|---|---|---|---|---|---|---|
| | *300 mA* | *450 mA* | *300 mA* | *450 mA* | *300 mA* | *450 mA* |
| Lumen decrease (%) | 2.57 | 2.67 | 6.49 | 6.53 | 8.33 | 8.33 |
| Radiant power decrease (%) | 2.57 | 2.69 | 6.49 | 6.54 | 8.33 | 8.33 |

## *4.4. Analysis of Blue Chip with a Glass Dome*

Polar, color, intensity distribution, and color chromaticity coordinates are almost the same with the blue chip simulations because light intensities, and spectrum has not changed during computations. However, this phase of study gives information about the reflection loss rates of some packaging elements in LEDs such as lenses (PMMA, refractive index of 1.49) , protective glass, and silicon [51]. The reflection loss can be about 8% in glass dome.

## *4.5. Simulations of Light Conversion in Phosphor Layer*

In Chapter 3, some of the phosphor parameters have been mentioned [28]. In accordance with the LED package, the thickness of hemispherical remote phosphor is set to 1.5 mm, and the type of phosphor layer was defined homogeneously in the model [38][52]. The refractive index of mixture has been calculated as 1.6 according to linearity formula. Mean free path of phosphor particles and distribution of unconverted rays have been determined by Mie Theory [53]. Concentration of the YAG:CE phosphor and silicon mixture by weight percentage is set to 16%. Phosphor density was given as 4.4 mg/mm$^3$. Real refractive index (n) and imaginary refractive index (k) of phosphor particles are 1.8 and $1.8 \times 10^{-6}$ respectively [54]. Particle size ratios of phosphor particles are chosen to be 9 μm, 11 μm, 13 μm, and 15 μm with the relative concentrations of 20%, 30%, 30%, and 20% respectively [55]. Lighttools model was shown in Figure 4-8 [56], [57], [53], [52].

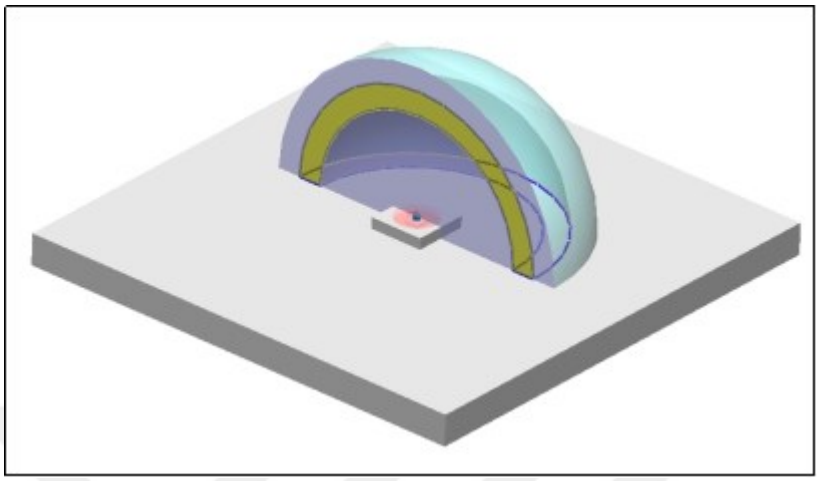

**Figure 4-8:** Schematic of the pcLED model in Lighttools

The excitation and emission data of the phosphor are configured in Lighttools according to the previous studies about phosphor, Jeon et al etc. [58]. The blue LEDs have an emittance region between 420 and 480 nm. The excitation spectrum involves the spectrum between 422-546 nm with peak intensity at 460 nm Figure 4-9. The emission spectrum of remote phosphor used in the simulations is given in Figure 4-10. It involves the region between 475-600 nm with peak intensity at 550 nm. These data will be given in the appendix parts of this thesis, because we think that phosphor conversion spectrums can be useful.

To be able to accurately compare optical effects, luminous fluxes of the light emitter surface in the simulation have been modified to get accurate optical effects, and then the phosphor successfully has been modeled. Explanations on this topic will be made in the conclusions so that optical and thermal effects should be evaluated separately from each other.

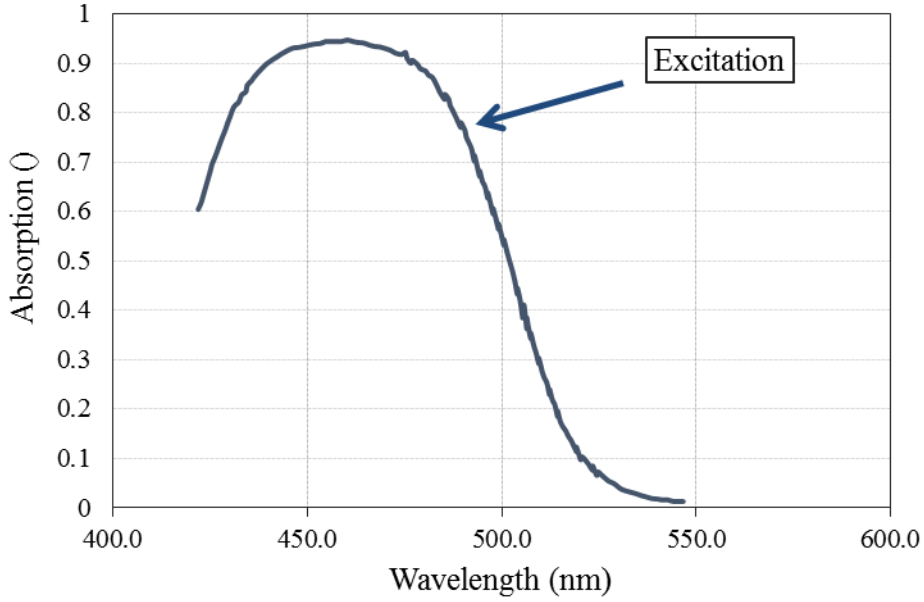


**Figure 4-9:** Excitation spectrum of phosphor

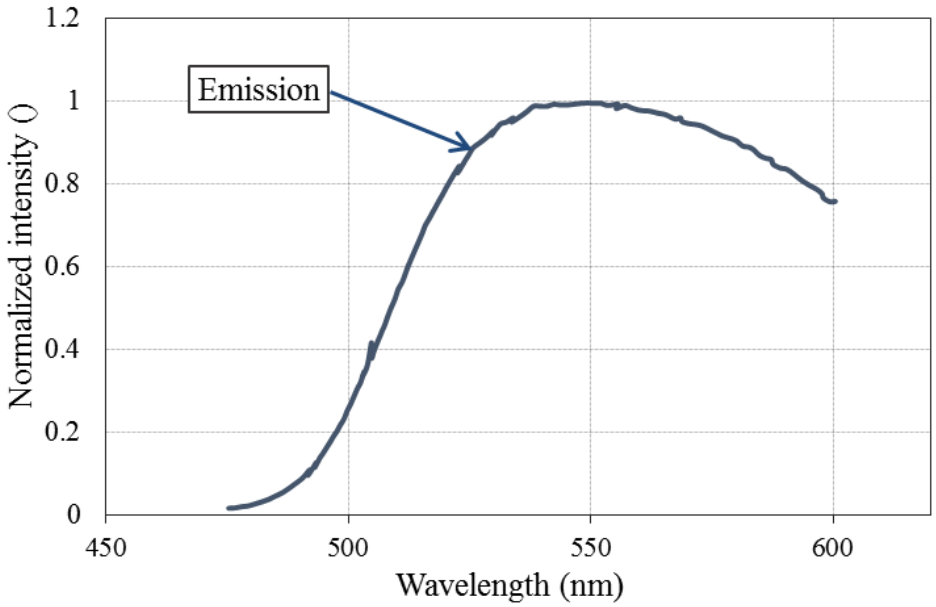


**Figure 4-10:** Relative emission spectrum of phosphor

## *4.6. Analysis of Remote Phosphor Converted LED*

Mie scattering defines the light intensity of scatter angles around spherical particles. Mie calculators and optic simulation programs like Lighttools assume that Mie particles have spherical shapes. Scattered photons mostly go in the direction of forward scattering. Logarithmic Mie scattering distribution of yellow light at 566 nm is given in Figure 4-11.

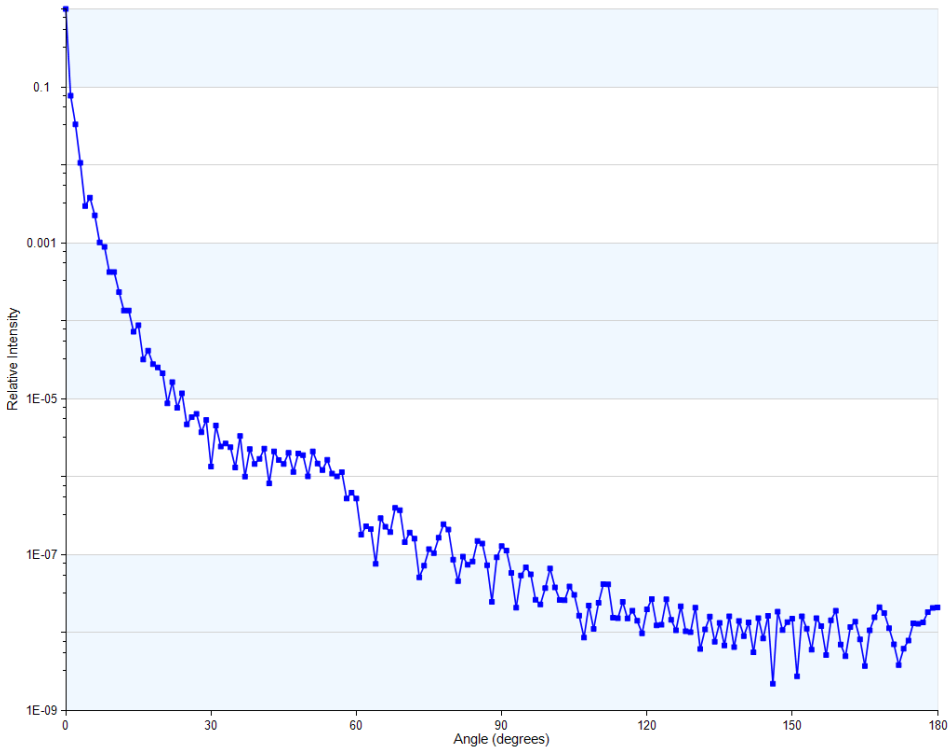


**Figure 4-11:** Mie scattering distribution for 566 nm yellow light

Luminous fluxes were 15.2 and 20.4 lumen respectively before remote phosphor coating. After light conversion process in phosphor, luminous fluxes increased to 62.5 and 84 lumen. That equals to more than 3 times lumen increase due to light conversion. However, radiant fluxes decreased almost 49% in this step (see Table 4-4).

**Table 4-4:** Optical simulation results of remote phosphor

| *Simulation results* | | *300 mA* | *450 mA* |
|---|---|---|---|
| Before phosphor coating | Lumen(Lm) | 15.2 | 20.4 |
| | Radiant power(mW) | 291 | 394 |
| After phosphor coating | Lumen (Lm) | 62.5 | 84.0 |
| | Radiant power(mW) | 148.7 | 201.3 |
| Lumen increase (%) | | 312 | 311 |
| Radiant power decrease (%) | | 48.8 | 48.9 |

SPD diagrams results of simulation are given for remote coated white-LED (wLED) in Figure 4-12. SPD diagrams in the figure contain the wavelength data between 400-740 nm. Phosphor simulations first were compromised with experimental results of different LEDs, and then similar SPD diagrams are obtained with the experimental results. Moreover, lumen calibrations are also necessary during simulations in order to get correct results in this step.

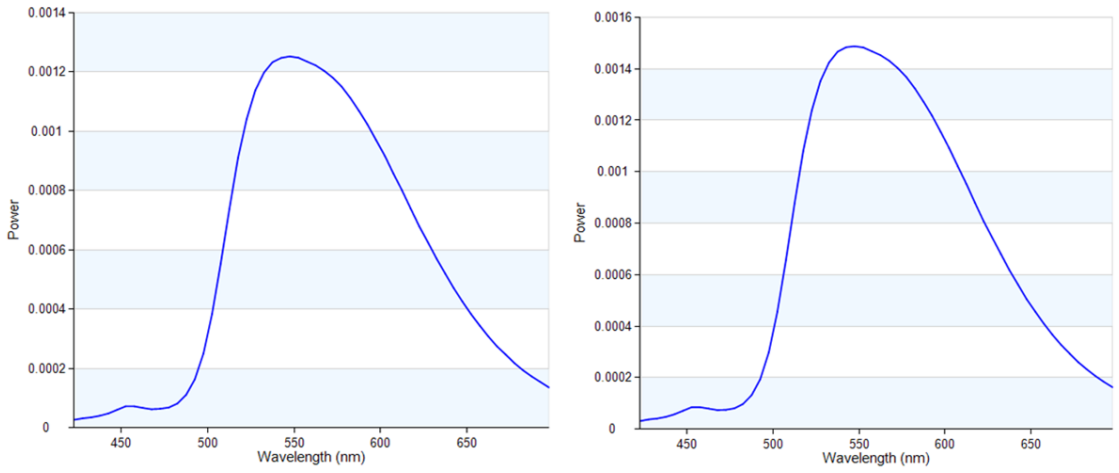


**Figure 4-12:** SPD diagrams of LED with remote phosphor (at 1 nm intervals)

The polar diagrams of the pcLED which have luminous fluxes of 62.5 and 84 are given in Figure 4-13; their distributions are close to Lambertian in the 0-180. The maximum light intensities in the simulations of two LEDs are 21 and 28 cd respectively.

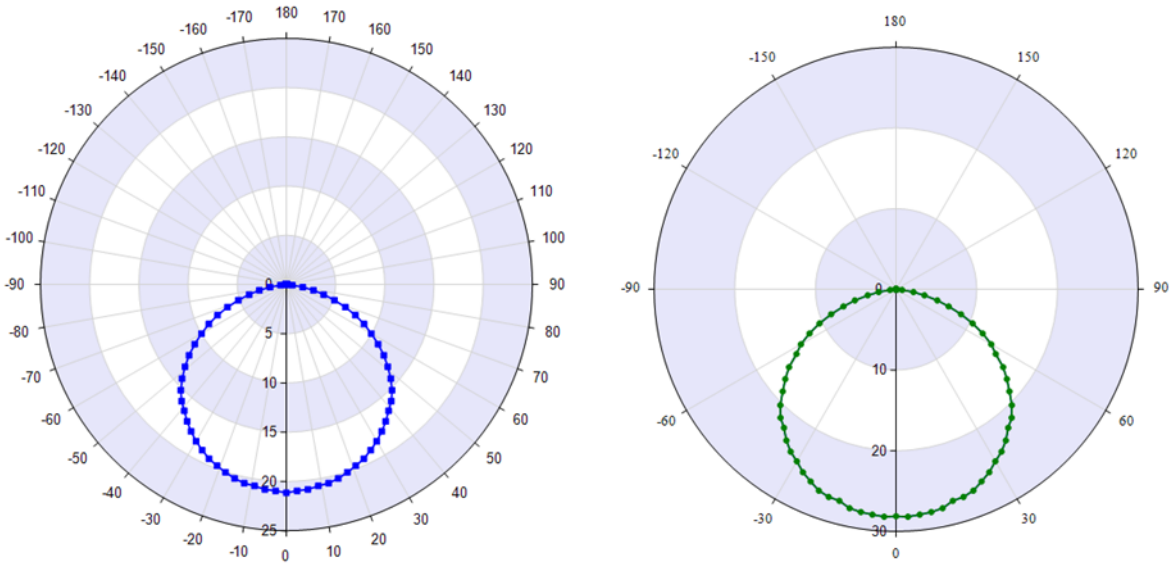


**Figure 4-13:** Polar diagrams of pcLED

Color chart diagrams of the simulations are given in Figure 4-14. We have seen in phosphor coating chapter that 10 or 12% phosphor concentration is optimal for pcLEDs. In the remote phosphor experiments and simulations we see that 16% of phosphor concentration is very high for pcLEDs due to little photons at the blue wavelengths. Thus, we have obtained here yellowish color chart rather than white light.

CIE xy chromatic coordinates for pcLED simulations are given in Figure 4-15. The x coordinate is about 0.4, and y is about 0.5 for both simulations. Chromatic coordinates shifted from blue to green. Computer aided tools can calculate CCT by that coordinates, but

during this thesis we cannot show the calculation. We mostly focus on the efficiency enhancement in this thesis.

In Figure 4-16, luminous intensity distributions in far field receiver for both light LEDs are given. In the first simulation, 18-21 cd light intensity is achieved between 0 to 30 degrees, and it becomes half at about 60 degrees. As we can see from the figures, after that point of half angle on, the intensity rates decrease in Lambertian source.

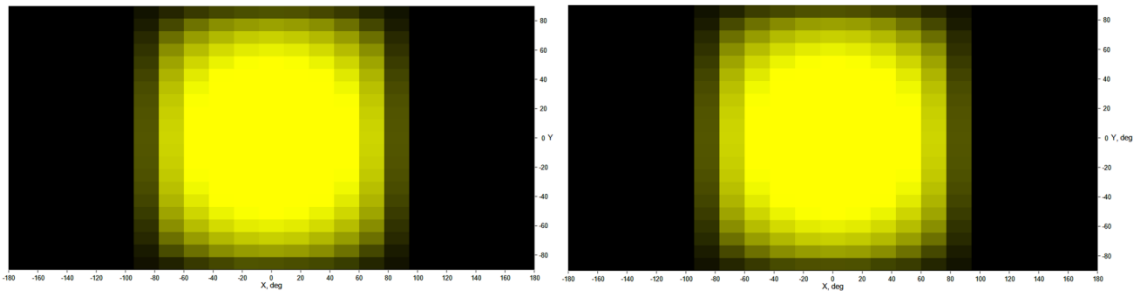

**Figure 4-14:** Color charts of pcLED simulations a) 300 mA b) 450 mA

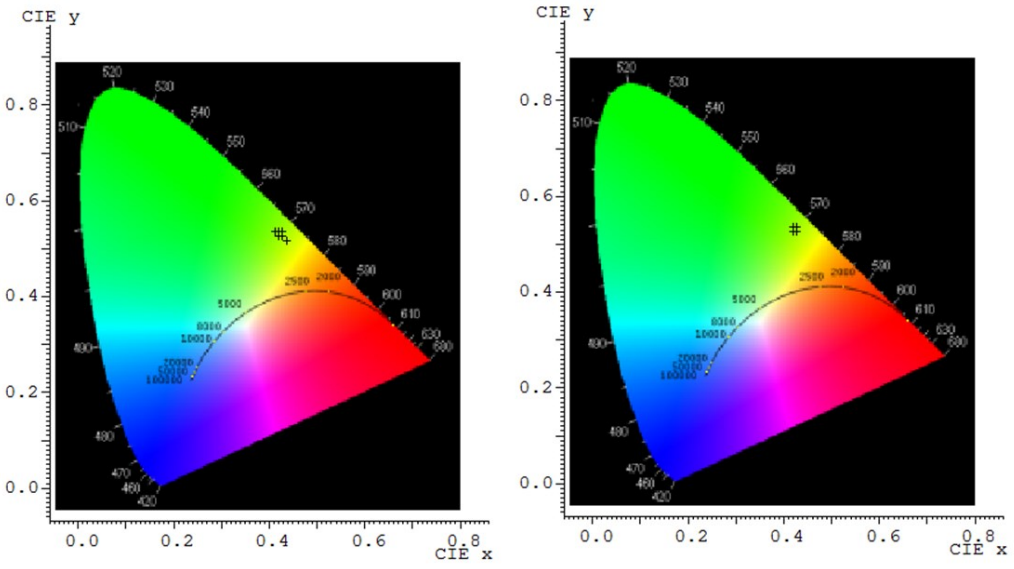


**Figure 4-15:** CIE chromatic coordinates of the pcLED

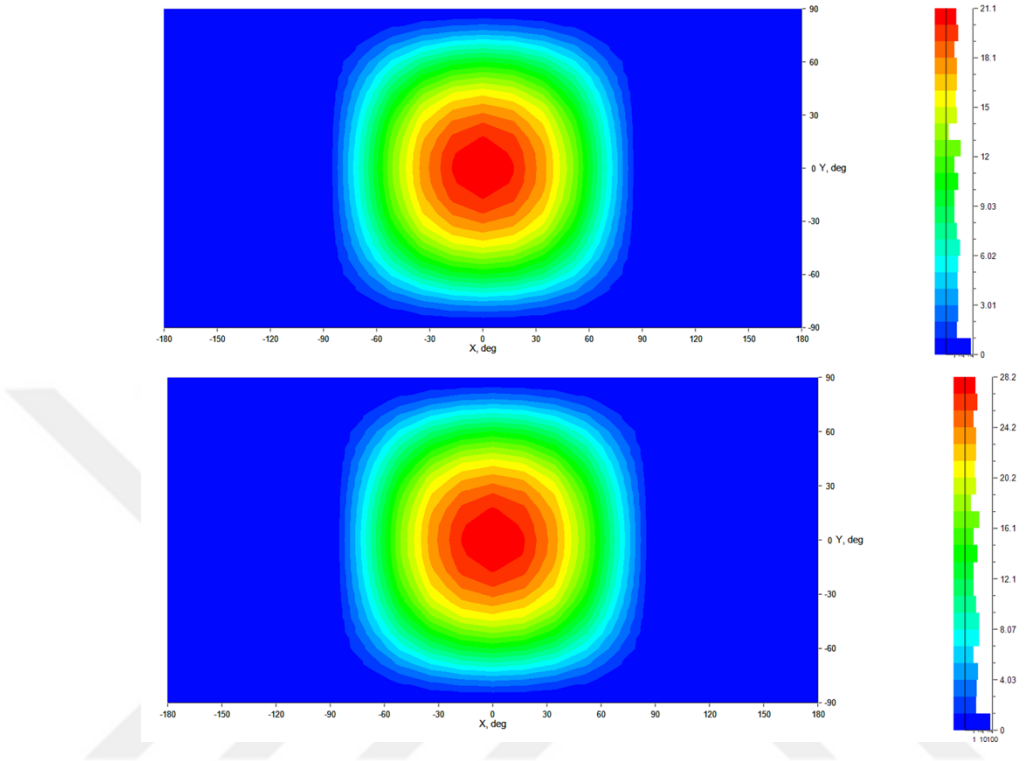


**Figure 4-16:** Luminous intensity distributions in far field receiver for both light LEDs

## *4.7. Simulations of Liquid Injection Remote Phosphor Coated LEDs*

In the simulation model, a hemispherical optically transparent material was created at the free space, and defined as transparent liquid. This liquid has a radius of 7 mm. Optical property is chosen as smooth optical material, which has Fresnel reflections and absorbance. The rays which are transmitted and internally reflected have been traced in the simulations. The smooth optical material (Liquid5238) has been defined as completely homogeneous. It has given a constant refractive index of 1.38. Absorption type was defined by transmittance over length, and then Monte Carlo tracing of 20 million rays were then started for each simulations.

## *4.8. Analysis of Liquid Injection in pcLED*

In the simulations of liquid injection, luminous fluxes increased from 62.5 and 84 to 70.7 and 95.0 for the given driving currents (see Table 4-5). Reflections between emitter, air, and remote phosphor occur due to the refractive index mismatching. The performance hence can be increased by 13.1% compromising the indices.

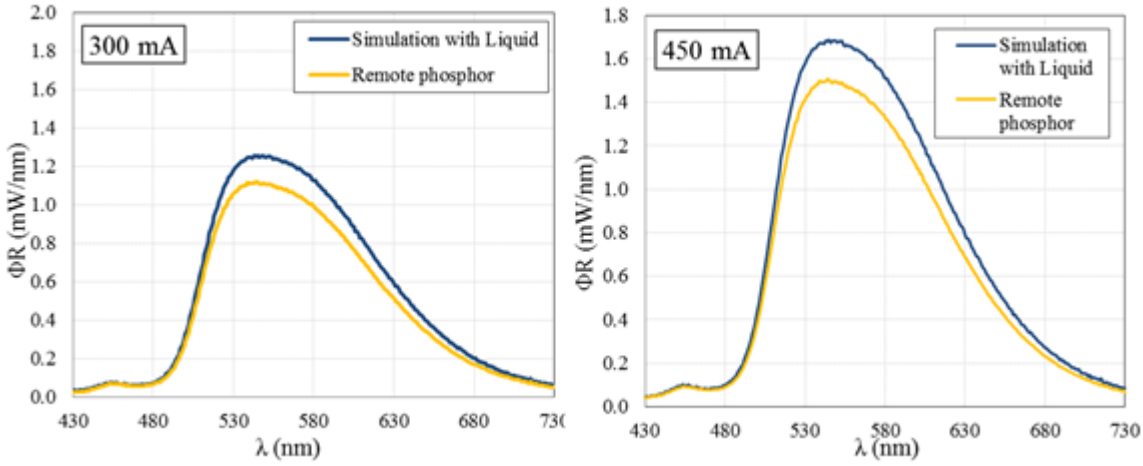


**Figure 4-17:** SPD diagrams of LED with liquid injection (at 1 nm intervals)

**Table 4-5**: Simulation results of liquid injection

| *Simulation results* | | *300 mA* | *450 mA* |
|---|---|---|---|
| Remote phosphor | Lumen(Lm) | 62.5 | 84 |
| | Radiant power(mW) | 298.6 | 405.3 |
| Liquid injected | Lumen (Lm) | 70.7 | 95.0 |
| | Radiant power(mW) | 337.7 | 458.4 |
| Lumen increase (%) | | 13.1 | 13.1 |
| Radiant power increase (%) | | 13.1 | 13.1 |

## *4.9. Complete Analysis of Liquid Injected pcLED Packages*

As we have shown previously, remote phosphor LEDs can reach higher luminous efficacies than phosphor coated LED packages due to thermal and optical reasons. Semiconductor based light emitters have high refractive indices of more than 2, and this causes most of the light particles to reflect back into the semiconductor materials. However, when we add a material which has a mediate refractive index like silicon or dielectric liquid between the mediums of semiconductors and ambient, Fresnel losses are diminished. Thus, we have put a transparent material with a refractive index of 1.38, and reflection losses further decreased by almost 13% in the simulations.

In addition to reflection losses in the semiconductor, in the glass dome and phosphor layers reflection losses are about 10% as we have shown in the first chapter. Injecting a liquid in a remote phosphor helps to lessen these rates of reflections in the remote phosphor and domes.

Thus, luminous fluxes have increased to 70.7 and 95 lm in the simulations due to decreasing reflections. Correspondingly, radiant fluxes have increased to 337.7 and 458.4 mW. Luminous and radiant flux increase rates become 13.1% in the simulations.

However, when we compare the experimental and simulation results, luminous fluxes has increased by 26 and 25% in the given currents of 300 and 450 mA respectively. In this chapter, we have showed that 13% enhancement can be achieved due to only optical

effects. There is 13% and 12 % more light enhancement in the experiments than the simulations.

In the experiments there are thermal reasons as well as optical effects which can enhance light extraction in the liquid injected remote phosphor coated LEDs. The dielectric liquid increases the thermal heat dissipation in the semiconductor chip and remote phosphor. The combined thermal enhancements in the chip and remote phosphor have been found 13 and 12% for the immersion cooling applied LEDs at 300 and 450 mA driving currents.

In fact, we cannot distinguish thermal effects of immersion cooling which boost luminous flux between the LED chip and remote phosphor. However, we can only assert that the temperature has been decreased a lot by the liquid injection. We have found previously that the losses in the semiconductor and phosphor are 96% and 50% respectively (LEE ratio of GaN based semiconductor is about 4% according to Equation (2-1) [5], in the remote phosphor layer radiant power reduction is about 50%).

## *4.10. Optimization of Liquid Coolant with Simulations*

We have used an optically transparent material which has a refractive index of 1.38[48] in the experiments and simulations. When the out medium is assumed to be air with a refractive index close to 1, reflection losses become highest in such a packaging model, and when the refractive index increases we can reach the highest extraction efficiency instead of 13%.

In the simulation, total luminous flux is added as optimization constraint, and refractive index of the liquid is defined as optimization variable. The simulations of liquid injected pcLED at 300 mA driving current have been completed, and the results are given in Figure 4-18. The luminous flux was 62.5 for the remote phosphor coated LED. After liquid injection it increased to 70.7 lm. However, at the index of refraction of 1.98, luminous flux of 75.5 lm has been obtained.

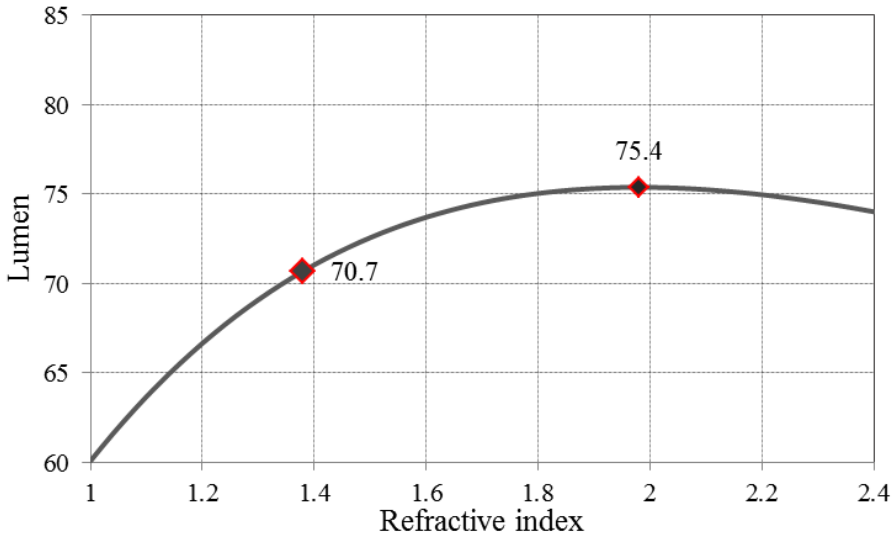


**Figure 4-18**: Optimization of lumen for liquid injected pcLED at 300 mA

At the 450 mA simulations, optical output raised from 84 to 95 lm in the liquid injected LED, and then in the optimizations the highest optical performance has been achieved when the refractive index increased to 1.98.

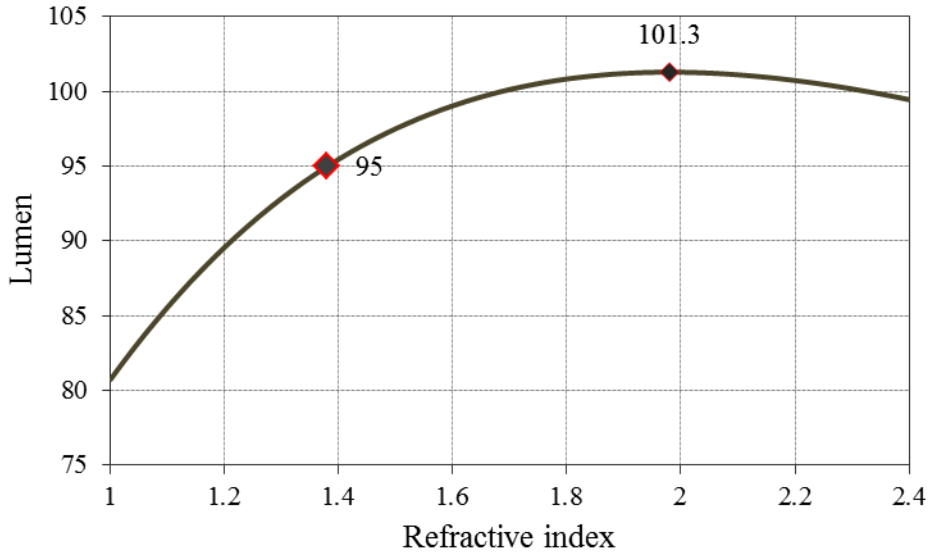


**Figure 4-19:** Optimization of lumen for liquid injected pcLED at 450 mA DC

The optical enhancement effects have been found to be 13.1% for the simulations of LS5238 liquid in both driving currents. Optimization results give that almost 20% light extraction efficiency can be achieved with the help of a liquid which has a refractive index 1.98 (see Table 4-6).

**Table 4-6:** Optimization of luminous flux rates

| | *Remote phosphor (Lm)* | *Liquid injected (Lm)* | *Performance (%)* |
|---|---|---|---|
| *300 mA* | 62.5 | 70.7 | 13.1% |
| *450 mA* | 84 | 95 | 13.1% |
| *300 mA* | 62.5 | 75.4 | 20.6% |
| *450 mA* | 84 | 101.3 | 20.6% |

# CHAPTER V

# CONCLUSIONS AND FUTURE RESEARCH

The small portion of the electromagnetic spectrum is visible, but in the outside of that portion there is a wide range invisible. We –humankind- has always had the curiosity about the nature, because of that physics was previously called as the philosophy of nature in the past. Photons here are the window which can open us to universe.

Photons are not completely a particle nor a wave. Since the beginning of the $20^{th}$ century we have known this nature of photons. However, previously candles and oil lamps have been used for a long time for lighting. In the 1882 Edison invented a commercially viable light bulb in 1879 [59] and the first visible LED (red) was developed in 1962 by Nick Holonyak, in General Electric company [60].

Light emitting diodes, to date, have been widely used in displays units, signage applications, and cell phones. Moreover, many LED applications have focused on the general lighting market due to their compact size, long life, high efficiency and luminous flux rates. However, high power LEDs are still exposed to high temperatures in chip and phosphor level due to optical and thermal reasons. Hence, we have proposed an immersion cooling method for blue GaN based LED with glass dome, phosphor coating, remote phosphor, and injected liquid coolant. Optical effects of each element in the packaging procedure have been shown and we have tried to enhance luminous efficiency.

## *5.1. Summary of the Current Study*

In the final part of the simulations, we have compared the experiments with the simulations, and distinguished the optical effects and combined thermal effects in liquid injected remote phosphor coated LED package. By liquid injection, luminous efficiency has been enhanced by 25.5%, and we showed optical and thermal enhancement rates are about 13, 12.5% respectively (see Figure 5-1).

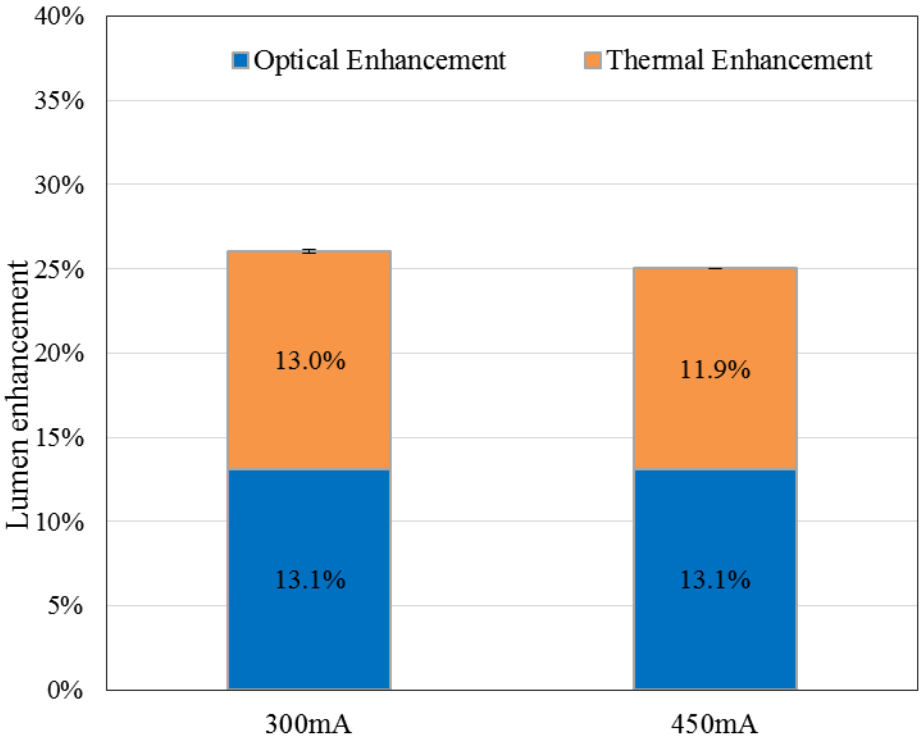


**Figure 5-1:** Lumen enhancement ratios of optical and thermal effects

Then, to enhance further luminous efficiency optimization has been done for the refractive of liquid. Optimization variable has been varied between the values of 1 (refractive index of air) and 2.4 (refractive index of GaN semiconductor). Almost at the midpoint of the

refractive indices (1.98) of GaN and phosphor mixture we have obtained the highest efficiency. We can additionally enhance optical performance 20% by using such a theoretical transparent liquid with a total amount of 33% due to optical and thermal reasons.

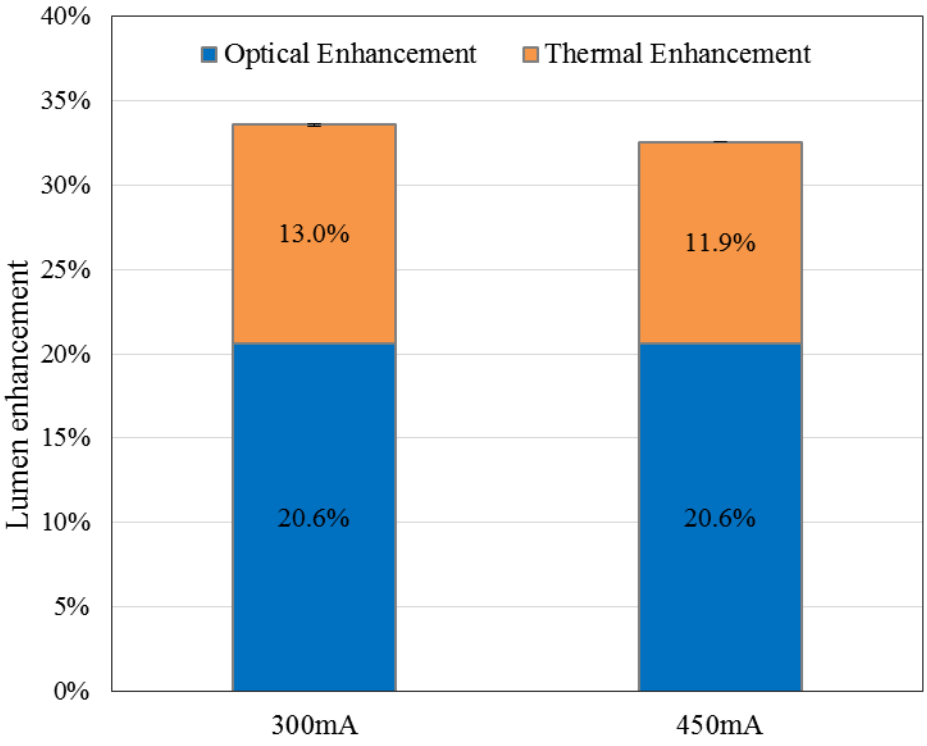


**Figure 5-2:** Lumen enhancement ratios of optical and thermal effects

## *5.2. Recommendation for the Future Work*

For the future work, we showed that light extraction efficiency (LEE) and thermal performance of phosphor converted LED packages can be improved by refractive index matching and liquid coolant. The current result shows that the innovative liquid injection

into remote phosphor coated LED is appropriate for both optical and thermal performance of a LED package. The results here can be used in further work in future:

- Light extraction can further be enhanced in LED chips, because EQE of semiconductor chips have very low efficiency. The current theoretical rate of is about 4%. This value has recently increased to almost 50%, but it can still be improved by surface texturing, refractive index matching, and coating by other materials.
- In any optical system including glass, semiconductor, liquid, or silicon which photon extraction rate is important the method can be applied in order to enhance efficiency of system and thermal performance e.g. lasers, radars, x-ray or gamma imaging.
- As proposed in the optimization part of this study, new liquid coolants can be invented with higher refractive indices.

# APPENDIX A

## *Photopic and Scotopic Functions*

| *Wavelength (nm)* | *Photopic Vision()* | *Scotopic Vision()* | *Wavelength (nm)* | *Photopic Vision ()* | *Scotopic Vision()* |
|---|---|---|---|---|---|
| *380* | 0.00004 | 0.00059 | 581 | 0.85986 | 0.11430 |
| *381* | 0.00004 | 0.00067 | 582 | 0.84939 | 0.10780 |
| *382* | 0.00005 | 0.00075 | 583 | 0.83862 | 0.10150 |
| *383* | 0.00005 | 0.00085 | 584 | 0.82758 | 0.09560 |
| *384* | 0.00006 | 0.00097 | 585 | 0.81630 | 0.08990 |
| *385* | 0.00006 | 0.00111 | 586 | 0.80479 | 0.08450 |
| *386* | 0.00007 | 0.00127 | 587 | 0.79308 | 0.07930 |
| *387* | 0.00008 | 0.00145 | 588 | 0.78119 | 0.07450 |
| *388* | 0.00009 | 0.00167 | 589 | 0.76915 | 0.06990 |
| *389* | 0.00011 | 0.00192 | 590 | 0.75700 | 0.06550 |
| *390* | 0.00012 | 0.00221 | 591 | 0.74475 | 0.06130 |
| *391* | 0.00013 | 0.00255 | 592 | 0.73242 | 0.05740 |
| *392* | 0.00015 | 0.00294 | 593 | 0.72000 | 0.05370 |
| *393* | 0.00017 | 0.00339 | 594 | 0.70750 | 0.05020 |
| *394* | 0.00019 | 0.00392 | 595 | 0.69490 | 0.04690 |
| *395* | 0.00022 | 0.00453 | 596 | 0.68222 | 0.04380 |
| *396* | 0.00025 | 0.00524 | 597 | 0.66947 | 0.04090 |
| *397* | 0.00028 | 0.00605 | 598 | 0.65667 | 0.03816 |
| *398* | 0.00032 | 0.00698 | 599 | 0.64384 | 0.03558 |
| *399* | 0.00036 | 0.00806 | 600 | 0.63100 | 0.03315 |
| *400* | 0.00040 | 0.00929 | 601 | 0.61816 | 0.03087 |
| *401* | 0.00043 | 0.01070 | 602 | 0.60531 | 0.02874 |
| *402* | 0.00047 | 0.01231 | 603 | 0.59248 | 0.02674 |
| *403* | 0.00052 | 0.01413 | 604 | 0.57964 | 0.02487 |
| *404* | 0.00057 | 0.01619 | 605 | 0.56680 | 0.02312 |
| *405* | 0.00064 | 0.01852 | 606 | 0.55396 | 0.02147 |
| *406* | 0.00072 | 0.02113 | 607 | 0.54114 | 0.01994 |
| *407* | 0.00083 | 0.02405 | 608 | 0.52835 | 0.01851 |
| *408* | 0.00094 | 0.02730 | 609 | 0.51563 | 0.01718 |
| *409* | 0.00107 | 0.03089 | 610 | 0.50300 | 0.01593 |
| *410* | 0.00121 | 0.03484 | 611 | 0.49047 | 0.01477 |

| | | | | | |
|---|---|---|---|---|---|
| *411* | 0.00136 | 0.03916 | 612 | 0.47803 | 0.01369 |
| *412* | 0.00153 | 0.04390 | 613 | 0.46568 | 0.01269 |
| *413* | 0.00172 | 0.04900 | 614 | 0.45340 | 0.01175 |
| *414* | 0.00194 | 0.05450 | 615 | 0.44120 | 0.01088 |
| *415* | 0.00218 | 0.06040 | 616 | 0.42908 | 0.01007 |
| *416* | 0.00245 | 0.06680 | 617 | 0.41704 | 0.00932 |
| *417* | 0.00276 | 0.07360 | 618 | 0.40503 | 0.00862 |
| *418* | 0.00312 | 0.08080 | 619 | 0.39303 | 0.00797 |
| *419* | 0.00353 | 0.08850 | 620 | 0.38100 | 0.00737 |
| *420* | 0.00400 | 0.09660 | 621 | 0.36892 | 0.00682 |
| *421* | 0.00455 | 0.10520 | 622 | 0.35683 | 0.00630 |
| *422* | 0.00516 | 0.11410 | 623 | 0.34478 | 0.00582 |
| *423* | 0.00583 | 0.12350 | 624 | 0.33282 | 0.00538 |
| *424* | 0.00655 | 0.13340 | 625 | 0.32100 | 0.00497 |
| *425* | 0.00730 | 0.14360 | 626 | 0.30934 | 0.00459 |
| *426* | 0.00809 | 0.15410 | 627 | 0.29785 | 0.00424 |
| *427* | 0.00891 | 0.16510 | 628 | 0.28659 | 0.00391 |
| *428* | 0.00977 | 0.17640 | 629 | 0.27562 | 0.00361 |
| *429* | 0.01066 | 0.18790 | 630 | 0.26500 | 0.00334 |
| *430* | 0.01160 | 0.19980 | 631 | 0.25476 | 0.00308 |
| *431* | 0.01257 | 0.21190 | 632 | 0.24489 | 0.00284 |
| *432* | 0.01358 | 0.22430 | 633 | 0.23533 | 0.00262 |
| *433* | 0.01463 | 0.23690 | 634 | 0.22605 | 0.00242 |
| *434* | 0.01572 | 0.24960 | 635 | 0.21700 | 0.00224 |
| *435* | 0.01684 | 0.26250 | 636 | 0.20816 | 0.00206 |
| *436* | 0.01801 | 0.27550 | 637 | 0.19955 | 0.00190 |
| *437* | 0.01921 | 0.28860 | 638 | 0.19116 | 0.00176 |
| *438* | 0.02045 | 0.30170 | 639 | 0.18297 | 0.00162 |
| *439* | 0.02172 | 0.31490 | 640 | 0.17500 | 0.00150 |
| *440* | 0.02300 | 0.32810 | 641 | 0.16722 | 0.00138 |
| *441* | 0.02429 | 0.34120 | 642 | 0.15965 | 0.00128 |
| *442* | 0.02561 | 0.35430 | 643 | 0.15228 | 0.00118 |
| *443* | 0.02696 | 0.36730 | 644 | 0.14513 | 0.00109 |
| *444* | 0.02835 | 0.38030 | 645 | 0.13820 | 0.00101 |
| *445* | 0.02980 | 0.39310 | 646 | 0.13150 | 0.00093 |
| *446* | 0.03131 | 0.40600 | 647 | 0.12502 | 0.00086 |
| *447* | 0.03288 | 0.41800 | 648 | 0.11878 | 0.00079 |

| | | | | | |
|---|---|---|---|---|---|
| *448* | 0.03452 | 0.43100 | 649 | 0.11277 | 0.00073 |
| *449* | 0.03623 | 0.44300 | 650 | 0.10700 | 0.00068 |
| *450* | 0.03800 | 0.45500 | 651 | 0.10148 | 0.00063 |
| *451* | 0.03985 | 0.46700 | 652 | 0.09619 | 0.00058 |
| *452* | 0.04177 | 0.47900 | 653 | 0.09112 | 0.00054 |
| *453* | 0.04377 | 0.49000 | 654 | 0.08626 | 0.00050 |
| *454* | 0.04584 | 0.50200 | 655 | 0.08160 | 0.00046 |
| *455* | 0.04800 | 0.51300 | 656 | 0.07712 | 0.00043 |
| *456* | 0.05024 | 0.52400 | 657 | 0.07283 | 0.00039 |
| *457* | 0.05257 | 0.53500 | 658 | 0.06871 | 0.00036 |
| *458* | 0.05498 | 0.54600 | 659 | 0.06477 | 0.00034 |
| *459* | 0.05746 | 0.55700 | 660 | 0.06100 | 0.00031 |
| *460* | 0.06000 | 0.56700 | 661 | 0.05740 | 0.00029 |
| *461* | 0.06260 | 0.57800 | 662 | 0.05396 | 0.00027 |
| *462* | 0.06528 | 0.58800 | 663 | 0.05067 | 0.00025 |
| *463* | 0.06804 | 0.59900 | 664 | 0.04755 | 0.00023 |
| *464* | 0.07091 | 0.61000 | 665 | 0.04458 | 0.00021 |
| *465* | 0.07390 | 0.62000 | 666 | 0.04176 | 0.00020 |
| *466* | 0.07702 | 0.63100 | 667 | 0.03908 | 0.00018 |
| *467* | 0.08027 | 0.64200 | 668 | 0.03656 | 0.00017 |
| *468* | 0.08367 | 0.65300 | 669 | 0.03420 | 0.00016 |
| *469* | 0.08723 | 0.66400 | 670 | 0.03200 | 0.00015 |
| *470* | 0.09098 | 0.67600 | 671 | 0.02996 | 0.00014 |
| *471* | 0.09492 | 0.68700 | 672 | 0.02808 | 0.00013 |
| *472* | 0.09905 | 0.69900 | 673 | 0.02633 | 0.00012 |
| *473* | 0.10337 | 0.71000 | 674 | 0.02471 | 0.00011 |
| *474* | 0.10788 | 0.72200 | 675 | 0.02320 | 0.00010 |
| *475* | 0.11260 | 0.73400 | 676 | 0.02180 | 0.00010 |
| *476* | 0.11753 | 0.74500 | 677 | 0.02050 | 0.00009 |
| *477* | 0.12267 | 0.75700 | 678 | 0.01928 | 0.00008 |
| *478* | 0.12799 | 0.76900 | 679 | 0.01812 | 0.00008 |
| *479* | 0.13345 | 0.78100 | 680 | 0.01700 | 0.00007 |
| *480* | 0.13902 | 0.79300 | 681 | 0.01590 | 0.00007 |
| *481* | 0.14468 | 0.80500 | 682 | 0.01484 | 0.00006 |
| *482* | 0.15047 | 0.81700 | 683 | 0.01381 | 0.00006 |
| *483* | 0.15646 | 0.82800 | 684 | 0.01283 | 0.00005 |
| *484* | 0.16272 | 0.84000 | 685 | 0.01192 | 0.00005 |

| | | | | | |
|---|---|---|---|---|---|
| *485* | 0.16930 | 0.85100 | 686 | 0.01107 | 0.00005 |
| *486* | 0.17624 | 0.86200 | 687 | 0.01027 | 0.00004 |
| *487* | 0.18356 | 0.87300 | 688 | 0.00953 | 0.00004 |
| *488* | 0.19127 | 0.88400 | 689 | 0.00885 | 0.00004 |
| *489* | 0.19942 | 0.89400 | 690 | 0.00821 | 0.00004 |
| *490* | 0.20802 | 0.90400 | 691 | 0.00762 | 0.00003 |
| *491* | 0.21712 | 0.91400 | 692 | 0.00709 | 0.00003 |
| *492* | 0.22673 | 0.92300 | 693 | 0.00659 | 0.00003 |
| *493* | 0.23686 | 0.93200 | 694 | 0.00614 | 0.00003 |
| *494* | 0.24748 | 0.94100 | 695 | 0.00572 | 0.00003 |
| *495* | 0.25860 | 0.94900 | 696 | 0.00534 | 0.00002 |
| *496* | 0.27018 | 0.95700 | 697 | 0.00500 | 0.00002 |
| *497* | 0.28229 | 0.96400 | 698 | 0.00468 | 0.00002 |
| *498* | 0.29505 | 0.97000 | 699 | 0.00438 | 0.00002 |
| *499* | 0.30858 | 0.97600 | 700 | 0.00410 | 0.00002 |
| *500* | 0.32300 | 0.98200 | 701 | 0.00384 | 0.00002 |
| *501* | 0.33840 | 0.98600 | 702 | 0.00359 | 0.00002 |
| *502* | 0.35469 | 0.99000 | 703 | 0.00335 | 0.00001 |
| *503* | 0.37170 | 0.99400 | 704 | 0.00313 | 0.00001 |
| *504* | 0.38929 | 0.99700 | 705 | 0.00293 | 0.00001 |
| *505* | 0.40730 | 0.99800 | 706 | 0.00274 | 0.00001 |
| *506* | 0.42563 | 1.00000 | 707 | 0.00256 | 0.00001 |
| *507* | 0.44431 | 1.00000 | 708 | 0.00239 | 0.00001 |
| *508* | 0.46339 | 1.00000 | 709 | 0.00224 | 0.00001 |
| *509* | 0.48294 | 0.99800 | 710 | 0.00209 | 0.00001 |
| *510* | 0.50300 | 0.99700 | 711 | 0.00195 | 0.00001 |
| *511* | 0.52357 | 0.99400 | 712 | 0.00182 | 0.00001 |
| *512* | 0.54451 | 0.99000 | 713 | 0.00170 | 0.00001 |
| *513* | 0.56569 | 0.98600 | 714 | 0.00159 | 0.00001 |
| *514* | 0.58697 | 0.98100 | 715 | 0.00148 | 0.00001 |
| *515* | 0.60820 | 0.97500 | 716 | 0.00138 | 0.00001 |
| *516* | 0.62935 | 0.96800 | 717 | 0.00129 | 0.00001 |
| *517* | 0.65031 | 0.96100 | 718 | 0.00120 | 0.00001 |
| *518* | 0.67088 | 0.95300 | 719 | 0.00112 | 0.00001 |
| *519* | 0.69084 | 0.94400 | 720 | 0.00105 | 0.00000 |
| *520* | 0.71000 | 0.93500 | 721 | 0.00098 | 0.00000 |
| *521* | 0.72819 | 0.92500 | 722 | 0.00091 | 0.00000 |

| | | | | | |
|---|---|---|---|---|---|
| *522* | 0.74546 | 0.91500 | 723 | 0.00085 | 0.00000 |
| *523* | 0.76197 | 0.90400 | 724 | 0.00079 | 0.00000 |
| *524* | 0.77784 | 0.89200 | 725 | 0.00074 | 0.00000 |
| *525* | 0.79320 | 0.88000 | 726 | 0.00069 | 0.00000 |
| *526* | 0.80811 | 0.86700 | 727 | 0.00064 | 0.00000 |
| *527* | 0.82250 | 0.85400 | 728 | 0.00060 | 0.00000 |
| *528* | 0.83631 | 0.84000 | 729 | 0.00056 | 0.00000 |
| *529* | 0.84949 | 0.82600 | 730 | 0.00052 | 0.00000 |
| *530* | 0.86200 | 0.81100 | 731 | 0.00048 | 0.00000 |
| *531* | 0.87381 | 0.79600 | 732 | 0.00045 | 0.00000 |
| *532* | 0.88496 | 0.78100 | 733 | 0.00042 | 0.00000 |
| *533* | 0.89549 | 0.76500 | 734 | 0.00039 | 0.00000 |
| *534* | 0.90544 | 0.74900 | 735 | 0.00036 | 0.00000 |
| *535* | 0.91485 | 0.73300 | 736 | 0.00034 | 0.00000 |
| *536* | 0.92373 | 0.71700 | 737 | 0.00031 | 0.00000 |
| *537* | 0.93209 | 0.70000 | 738 | 0.00029 | 0.00000 |
| *538* | 0.93992 | 0.68300 | 739 | 0.00027 | 0.00000 |
| *539* | 0.94723 | 0.66700 | 740 | 0.00025 | 0.00000 |
| *540* | 0.95400 | 0.65000 | 741 | 0.00023 | 0.00000 |
| *541* | 0.96026 | 0.63300 | 742 | 0.00021 | 0.00000 |
| *542* | 0.96601 | 0.61600 | 743 | 0.00020 | 0.00000 |
| *543* | 0.97126 | 0.59900 | 744 | 0.00019 | 0.00000 |
| *544* | 0.97602 | 0.58100 | 745 | 0.00017 | 0.00000 |
| *545* | 0.98030 | 0.56400 | 746 | 0.00016 | 0.00000 |
| *546* | 0.98409 | 0.54800 | 747 | 0.00015 | 0.00000 |
| *547* | 0.98742 | 0.53100 | 748 | 0.00014 | 0.00000 |
| *548* | 0.99031 | 0.51400 | 749 | 0.00013 | 0.00000 |
| *549* | 0.99281 | 0.49700 | 750 | 0.00012 | 0.00000 |
| *550* | 0.99495 | 0.48100 | 751 | 0.00011 | 0.00000 |
| *551* | 0.99671 | 0.46500 | 752 | 0.00010 | 0.00000 |
| *552* | 0.99810 | 0.44800 | 753 | 0.00010 | 0.00000 |
| *553* | 0.99911 | 0.43300 | 754 | 0.00009 | 0.00000 |
| *554* | 0.99975 | 0.41700 | 755 | 0.00008 | 0.00000 |
| *555* | 1.00000 | 0.40200 | 756 | 0.00008 | 0.00000 |
| *556* | 0.99986 | 0.38640 | 757 | 0.00007 | 0.00000 |
| *557* | 0.99930 | 0.37150 | 758 | 0.00007 | 0.00000 |
| *558* | 0.99833 | 0.35690 | 759 | 0.00006 | 0.00000 |

| | | | | | |
|---|---|---|---|---|---|
| *559* | 0.99690 | 0.34270 | 760 | 0.00006 | 0.00000 |
| *560* | 0.99500 | 0.32880 | 761 | 0.00006 | 0.00000 |
| *561* | 0.99260 | 0.31510 | 762 | 0.00005 | 0.00000 |
| *562* | 0.98974 | 0.30180 | 763 | 0.00005 | 0.00000 |
| *563* | 0.98644 | 0.28880 | 764 | 0.00005 | 0.00000 |
| *564* | 0.98272 | 0.27620 | 765 | 0.00004 | 0.00000 |
| *565* | 0.97860 | 0.26390 | 766 | 0.00004 | 0.00000 |
| *566* | 0.97408 | 0.25190 | 767 | 0.00004 | 0.00000 |
| *567* | 0.96917 | 0.24030 | 768 | 0.00003 | 0.00000 |
| *568* | 0.96386 | 0.22910 | 769 | 0.00003 | 0.00000 |
| *569* | 0.95813 | 0.21820 | 770 | 0.00003 | 0.00000 |
| *570* | 0.95200 | 0.20760 | 771 | 0.00003 | 0.00000 |
| *571* | 0.94545 | 0.19740 | 772 | 0.00003 | 0.00000 |
| *572* | 0.93850 | 0.18760 | 773 | 0.00002 | 0.00000 |
| *573* | 0.93116 | 0.17820 | 774 | 0.00002 | 0.00000 |
| *574* | 0.92346 | 0.16900 | 775 | 0.00002 | 0.00000 |
| *575* | 0.91540 | 0.16020 | 776 | 0.00002 | 0.00000 |
| *576* | 0.90701 | 0.15170 | 777 | 0.00002 | 0.00000 |
| *577* | 0.89828 | 0.14360 | 778 | 0.00002 | 0.00000 |
| *578* | 0.88920 | 0.13580 | 779 | 0.00002 | 0.00000 |
| *579* | 0.87978 | 0.12840 | 780 | 0.00001 | 0.00000 |

# APPENDIX B

## *YAG:Ce Phosphor Excitation Spectrum*

| *Wavelength (nm)* | *Excitation ()* | *Wavelength (nm)* | *Excitation ()* |
|---|---|---|---|
| 422 | 0.604 | 494 | 0.671 |
| 423 | 0.619 | 494 | 0.682 |
| 423 | 0.638 | 495 | 0.661 |
| 424 | 0.657 | 496 | 0.65 |
| 425 | 0.676 | 496 | 0.627 |
| 425 | 0.694 | 496 | 0.638 |
| 426 | 0.708 | 497 | 0.617 |
| 427 | 0.722 | 498 | 0.595 |
| 427 | 0.738 | 498 | 0.606 |
| 428 | 0.752 | 498 | 0.586 |
| 429 | 0.766 | 499 | 0.564 |
| 430 | 0.782 | 499 | 0.575 |
| 430 | 0.796 | 500 | 0.554 |
| 431 | 0.811 | 501 | 0.532 |
| 432 | 0.822 | 501 | 0.543 |
| 433 | 0.836 | 501 | 0.518 |
| 434 | 0.842 | 502 | 0.499 |
| 434 | 0.855 | 503 | 0.48 |
| 436 | 0.864 | 503 | 0.461 |
| 437 | 0.875 | 504 | 0.433 |
| 438 | 0.887 | 504 | 0.445 |
| 439 | 0.898 | 505 | 0.417 |
| 441 | 0.906 | 505 | 0.385 |
| 442 | 0.913 | 505 | 0.398 |
| 444 | 0.92 | 506 | 0.41 |
| 445 | 0.926 | 506 | 0.363 |
| 446 | 0.931 | 506 | 0.385 |
| 448 | 0.932 | 507 | 0.369 |
| 449 | 0.934 | 507 | 0.343 |
| 451 | 0.937 | 507 | 0.354 |
| 452 | 0.939 | 508 | 0.328 |

| | | | |
|---|---|---|---|
| 453 | 0.94 | 509 | 0.314 |
| 455 | 0.944 | 509 | 0.292 |
| 456 | 0.944 | 509 | 0.303 |
| 457 | 0.944 | 510 | 0.278 |
| 459 | 0.944 | 511 | 0.264 |
| 460 | 0.947 | 512 | 0.253 |
| 462 | 0.944 | 512 | 0.229 |
| 463 | 0.942 | 512 | 0.24 |
| 464 | 0.941 | 513 | 0.219 |
| 466 | 0.937 | 514 | 0.208 |
| 467 | 0.934 | 514 | 0.185 |
| 469 | 0.933 | 514 | 0.196 |
| 470 | 0.93 | 515 | 0.175 |
| 471 | 0.926 | 516 | 0.164 |
| 473 | 0.92 | 516 | 0.156 |
| 474 | 0.918 | 517 | 0.145 |
| 475 | 0.922 | 518 | 0.135 |
| 476 | 0.911 | 519 | 0.114 |
| 477 | 0.9 | 519 | 0.123 |
| 477 | 0.906 | 520 | 0.098 |
| 478 | 0.897 | 521 | 0.104 |
| 479 | 0.889 | 522 | 0.092 |
| 480 | 0.884 | 523 | 0.076 |
| 481 | 0.876 | 523 | 0.085 |
| 482 | 0.871 | 524 | 0.066 |
| 483 | 0.856 | 525 | 0.073 |
| 484 | 0.842 | 526 | 0.063 |
| 485 | 0.827 | 528 | 0.054 |
| 485 | 0.837 | 529 | 0.049 |
| 486 | 0.827 | 530 | 0.04 |
| 487 | 0.815 | 532 | 0.035 |
| 487 | 0.804 | 533 | 0.032 |
| 488 | 0.791 | 534 | 0.029 |
| 489 | 0.77 | 536 | 0.025 |
| 489 | 0.78 | 537 | 0.022 |
| 490 | 0.764 | 539 | 0.019 |
| 491 | 0.751 | 540 | 0.018 |

| | | | |
|---|---|---|---|
| 492 | 0.739 | 541 | 0.016 |
| 492 | 0.726 | 543 | 0.016 |
| 493 | 0.702 | 544 | 0.013 |
| 493 | 0.714 | 546 | 0.013 |
| 494 | 0.693 | 547 | 0.013 |

# APPENDIX C

## *YAG:Ce Phosphor Emission Spectrum*

| *Wavelength (nm)* | *Emission ()* | *Wavelength (nm)* | *Emission ()* |
|---|---|---|---|
| 475 | 0.017 | 524 | 0.861 |
| 477 | 0.018 | 525 | 0.874 |
| 478 | 0.021 | 526 | 0.888 |
| 479 | 0.023 | 527 | 0.9 |
| 481 | 0.028 | 528 | 0.913 |
| 482 | 0.033 | 530 | 0.93 |
| 484 | 0.039 | 529 | 0.919 |
| 485 | 0.047 | 531 | 0.945 |
| 486 | 0.055 | 533 | 0.951 |
| 488 | 0.066 | 534 | 0.961 |
| 489 | 0.078 | 534 | 0.951 |
| 491 | 0.091 | 535 | 0.964 |
| 492 | 0.11 | 537 | 0.976 |
| 492 | 0.097 | 538 | 0.989 |
| 493 | 0.128 | 540 | 0.989 |
| 493 | 0.116 | 541 | 0.989 |
| 494 | 0.139 | 542 | 0.994 |
| 495 | 0.151 | 544 | 0.992 |
| 496 | 0.164 | 545 | 0.992 |
| 496 | 0.177 | 547 | 0.994 |
| 497 | 0.191 | 548 | 0.996 |
| 498 | 0.203 | 549 | 0.997 |
| 498 | 0.218 | 551 | 0.996 |
| 499 | 0.234 | 552 | 0.996 |
| 500 | 0.252 | 554 | 0.991 |
| 500 | 0.268 | 556 | 0.994 |
| 501 | 0.287 | 555 | 0.983 |
| 502 | 0.306 | 557 | 0.991 |
| 503 | 0.322 | 558 | 0.985 |
| 503 | 0.347 | 560 | 0.98 |
| 503 | 0.335 | 561 | 0.978 |
| 504 | 0.363 | 562 | 0.977 |
| 505 | 0.417 | 564 | 0.972 |

| | | | |
|---|---|---|---|
| 505 | 0.38 | 565 | 0.969 |
| 505 | 0.399 | 567 | 0.958 |
| 506 | 0.424 | 568 | 0.961 |
| 506 | 0.41 | 569 | 0.952 |
| 507 | 0.443 | 570 | 0.947 |
| 508 | 0.462 | 572 | 0.945 |
| 508 | 0.482 | 573 | 0.941 |
| 509 | 0.506 | 574 | 0.933 |
| 508 | 0.493 | 576 | 0.925 |
| 510 | 0.525 | 577 | 0.917 |
| 510 | 0.546 | 579 | 0.912 |
| 511 | 0.563 | 580 | 0.906 |
| 512 | 0.581 | 581 | 0.893 |
| 512 | 0.607 | 583 | 0.89 |
| 512 | 0.594 | 584 | 0.882 |
| 513 | 0.626 | 585 | 0.87 |
| 514 | 0.645 | 586 | 0.863 |
| 515 | 0.664 | 587 | 0.86 |
| 515 | 0.683 | 588 | 0.849 |
| 516 | 0.701 | 589 | 0.84 |
| 517 | 0.715 | 590 | 0.837 |
| 517 | 0.73 | 592 | 0.826 |
| 518 | 0.745 | 593 | 0.816 |
| 519 | 0.76 | 594 | 0.807 |
| 519 | 0.774 | 595 | 0.797 |
| 520 | 0.79 | 597 | 0.788 |
| 521 | 0.804 | 598 | 0.778 |
| 521 | 0.818 | 598 | 0.767 |
| 523 | 0.844 | 599 | 0.758 |
| 523 | 0.828 | 600 | 0.759 |

# BIBLIOGRAPHY


[1] R. González, "Light2015," 2015. [Online]. Available: http://www.light2015.org/Home/About/Latest-News/January2016/Inspired-by-Light-Book.html. [Accessed: 10-Aug-2018].

[2] "Photo-Electric Effect." [Online]. Available: https://www.britannica.com/science/photoelectric-effect. [Accessed: 01-Dec-2018].

[3] NASA, "The Electromagnetic Spectrum," *National Association of Broadcasters: Engineering Handbook*, 2013. [Online]. Available: http://imagine.gsfc.nasa.gov/science/toolbox/emspectrum1.html. [Accessed: 07-Dec-2018].

[4] C. Crockett, "What is the electromagnetic spectrum?," *EarthSky Communications Inc.*, 2017. [Online]. Available: http://earthsky.org/space/what-is-the-electromagnetic-spectrum. [Accessed: 01-Dec-2018].

[5] E. F. Schubert, *Light-emitting diodes, second edition*, Second., vol. 9780521865, no. 2. Cambridge: Cambridge University Press, 2006.

[6] "Refractive index." [Online]. Available: https://en.wikipedia.org/wiki/Refractive_index. [Accessed: 07-Dec-2018].

[7] P. University, "Meteo300 Fundamentals of Atmospheric Science." [Online]. Available: https://www.e-education.psu.edu/meteo300/node/785. [Accessed: 07-Dec-2018].

[8] Dr. Simon A. Carn, "Scattering_Lecture_Slides.Pdf." [Online]. Available: pages.mtu.edu/~scarn/teaching/GE4250/scattering_lecture_slides.pdf. [Accessed: 03-Jul-2018].

[9] Bureau Central de la CIE, "CIE Procedings," 1951, vol. 1, p. 37.

[10] B. C. de la CIE, "CIE Proceedings," 1957.

[11] D. Schreuder, *Outdoor lighting: Physics, vision and perception*. 2008.

[12] S. Liu and X. Luo, *LED Packaging for Lighting Applications*. Singapore: John Wiley & Sons (Asia) Pte Ltd, 2011.

[13] Engineering ToolBox, "Illuminance - Recommended Light Level," 2004. [Online]. Available: https://www.engineeringtoolbox.com/light-level-rooms-d_708.html. [Accessed: 07-Dec-2018].

[14] International Electrotechnical Commission, “IEC 61966-2-1: Multimedia systems and equipment - Colour measurement and management - Part 2-1: Colour management - Default RGB colour space - sRGB,” p. 51, 1999.

[15] H. I. Kahvecioglu, E. Tamdogan, and M. Arik, “Investigation of combined optical and thermal effects on phosphor converted light-emitting diodes with liquid immersion cooling,” *Opt. Eng.*, vol. 57, no. 5, 2018.

[16] F. M. Steranka *et al.*, “High Power LEDs - Technology Status and Market Applications,” *Phys. status solidi*, vol. 194, no. 2, pp. 380–388, Dec. 2002.

[17] M. R. Krames *et al.*, “Status and Future of High-Power Light-Emitting Diodes for Solid-State Lighting,” *J. Disp. Technol.*, vol. 3, no. 2, pp. 160–175, Jun. 2007.

[18] Y. Narukawa *et al.*, “Recent progress of high efficiency white LEDs,” *Phys. status solidi*, vol. 204, no. 6, pp. 2087–2093, Jun. 2007.

[19] M. Suzuki, T. Uenoyama, and A. Yanase, “First-principles calculations of effective-mass parameters of AlN and GaN,” *Phys. Rev. B*, vol. 52, no. 11, pp. 8132–8139, Sep. 1995.

[20] J.-W. Pan and C.-S. Wang, “Light extraction efficiency of GaN-based LED with pyramid texture by using ray path analysis,” *Opt. Express*, vol. 20, no. S5, p. A630, Sep. 2012.

[21] Y.-K. Ee, P. Kumnorkaew, R. A. Arif, H. Tong, J. F. Gilchrist, and N. Tansu, “Light extraction efficiency enhancement of InGaN quantum wells light-emitting diodes with polydimethylsiloxane concave microstructures,” *Opt. Express*, vol. 17, no. 16, p. 13747, Aug. 2009.

[22] H. Ichikawa and T. Baba, “Efficiency enhancement in a light-emitting diode with a two-dimensional surface grating photonic crystal,” *Appl. Phys. Lett.*, vol. 84, no. 4, pp. 457–459, Jan. 2004.

[23] J. W. Pan, S. H. Tu, W. S. Sun, C. M. Wang, and J. Y. Chang, “Integration of Non-Lambertian LED and Reflective Optical Element as Efficient Street Lamp,” *Opt. Express*, vol. 18, no. S2, p. A221, Jun. 2010.

[24] Wikipedia, “List of semiconductor materials.” [Online]. Available: https://en.wikipedia.org/wiki/List_of_semiconductor_materials. [Accessed: 01-Dec-2018].

[25] T.-Y. Seong, J. Han, H. Amano, and H. Morkoc, Eds., *III-Nitride Based Light Emitting Diodes and Applications*, vol. 126. Dordrecht: Springer Netherlands, 2013.

[26] X. Luo and R. Hu, “Calculation of the phosphor heat generation in phosphor-converted light-emitting diodes,” *Int. J. Heat Mass Transf.*, vol. 75, pp. 213–217, Aug. 2014.

[27] S.-W. Jeon *et al.*, “Improvement of phosphor modeling based on the absorption of Stokes shifted light by a phosphor,” *Opt. Express*, vol. 22, no. S5, p. A1237, 2014.

[28] M. Zachau, D. Becker, D. Berben, T. Fiedler, F. Jermann, and F. Zwaschka, “Phosphors for solid state lighting,” 2008, p. 691010.

[29] P. F. Smet, A. B. Parmentier, and D. Poelman, “Selecting Conversion Phosphors for White Light-Emitting Diodes,” *J. Electrochem. Soc.*, vol. 158, no. 6, p. R37, 2011.

[30] S. Shionoya, W. M. Yen, and H. Yamamoto, *Phosphor handbook*. 2006.

[31] F. P. Wenzl *et al.*, “Impact of extinction coefficient of phosphor on thermal load of color conversion elements of phosphor converted LEDs,” *J. Rare Earths*, vol. 32, no. 3, pp. 201–206, Mar. 2014.

[32] Cree, “EZ1000-n LED Chips.” [Online]. Available: https://www.cree.com/led-chips/products/ez-n-leds/ez1000-n. [Accessed: 01-Dec-2018].

[33] Labshphere, “Illumia Plus 610.” [Online]. Available: https://www.labsphere.com/labsphere-products-solutions/light-metrology/illumia-plus-systems/illumia-plus-600-610/.

[34] Schott, “Borosilicate glass.” [Online]. Available: https://www.schott.com/borofloat/english/index.html. [Accessed: 01-Dec-2018].

[35] Wikipedia, “Borosilicate_glass.” [Online]. Available: https://www.wikizero.com/en/Borosilicate_glass. [Accessed: 01-Dec-2018].

[36] C. Sommer *et al.*, “On The Effect of Light Scattering in Phosphor Converted White Light-emitting Diodes,” *Adv. Photonics Renew. Energy*, p. SOTuB5, 2010.

[37] R. Yu, S. Jin, S. Cen, and P. Liang, “Effect of the phosphor geometry on the luminous flux of phosphor-converted light-emitting diodes,” *IEEE Photonics Technol. Lett.*, vol. 22, no. 23, pp. 1765–1767, 2010.

[38] P. Gorrotxategi, M. Consonni, and A. Gasse, “Optical efficiency characterization of LED phosphors using a double integrating sphere system,” *J. Solid State Light.*, vol. 2, no. 1, p. 1, Feb. 2015.

[39] L. Guide, *Advanced Physics Module User’s Guide*. 2014.

[40] M. Arik, J. Petroski, and S. Weaver, “Thermal challenges in the future generation solid state lighting applications: light emitting diodes,” in *ITherm 2002. Eighth Intersociety Conference on Thermal and Thermomechanical Phenomena in Electronic Systems (Cat. No.02CH37258)*, pp. 113–120.

[41] M. Arik, C. A. Becker, S. E. Weaver, and J. Petroski, “Thermal management of LEDs: package to system,” 2004, p. 64.

[42] M. Arik, S. Weaver, C. Becker, M. Hsing, and A. Srivastava, “Effects of Localized Heat Generations Due to the Color Conversion in Phosphor Particles and Layers of High Brightness Light Emitting Diodes,” in *2003 International Electronic Packaging Technical Conference and Exhibition, Volume 1*, 2003, pp. 611–619.

[43] K. J. Chen *et al.*, “Effect of the Thermal Characteristics of Phosphor for the Conformal and Remote Structures in White Light-Emitting Diodes,” *IEEE Photonics J.*, vol. 5, no. 5, pp. 8200508–8200508, Oct. 2013.

[44] J. Ryckaert, S. Leyre, P. Hanselaer, and Y. Meuret, “Determination of the optimal amount of scattering in a wavelength conversion plate for white LEDs,” *Opt. Express*, vol. 23, no. 24, p. A1629, Nov. 2015.

[45] E. Tamdogan, “IMMERSION COOLING OF SUSPENDED AND COATED NANO-PHOSPHOR PARTICLES FOR EXTENDING THE LIMITS OF OPTICAL EXTRACTION OF LIGHT EMITTING DIODES,” Özyeğin, 2017.

[46] E. Tamdogan and M. Arik, “Natural Convection Immersion Cooling With Enhanced Optical Performance of Light-Emitting Diode Systems,” *J. Electron. Packag.*, vol. 137, no. 4, p. 041006, Oct. 2015.

[47] E. Tamdogan and M. Arik, “Effect of Direct Liquid Cooling on the Light Emitting Diode Local Hot Spots: Natural Convection Immersion Cooling,” in *Proceedings of the 15th International Heat Transfer Conference*, 2014.

[48] Http://lookpolymers.com, “LS-5238 Silicone Optical Fluid.” [Online]. Available: http://lookpolymers.com/polymer_NuSil-Lightspan-LS-5238-Silicone-Optical-Fluid.php. [Accessed: 01-Dec-2018].

[49] Synopsys, “Lighttools.” [Online]. Available: https://optics.synopsys.com/lighttools/. [Accessed: 01-Dec-2018].

[50] Wikipedia, “CIE 1931 color space.” [Online]. Available: https://en.wikipedia.org/wiki/CIE_1931_color_space%0A%0A. [Accessed: 01-Dec-2018].

[51] Refractiveindex.info, “Optical constants of (C5H8O2)n (Poly(methyl methacrylate), PMMA).” [Online]. Available: https://refractiveindex.info/?shelf=organic&book=poly(methyl_methacrylate)&page=Szczurowski. [Accessed: 01-Dec-2018].

[52] Z. Liu, S. Liu, K. Wang, and X. Luo, “Optical Analysis of Phosphor’s Location for High-Power Light-Emitting Diodes,” *IEEE Trans. Device Mater. Reliab.*, vol. 9, no. 1, pp. 65–73, Mar. 2009.

[53] V. Y. F. Leung, A. Lagendijk, T. W. Tukker, A. P. Mosk, W. L. IJzerman, and W. L. Vos, “Interplay between multiple scattering, emission, and absorption of light in the phosphor of a white light-emitting diode,” *Opt. Express*, vol. 22, no. 7, p. 8190, Apr. 2014.

[54] R. Hu, X. Luo, H. Zheng, and S. Liu, “Optical constants study of YAG:Ce phosphor layer blended with SiO2 particles by Mie theory for white light-emitting diode package,” *Front. Optoelectron.*, vol. 5, no. 2, pp. 138–146, Jun. 2012.

[55] Intematix, “NYAG4354.” [Online]. Available: http://www.intematix.com/uploads/phosphor-datasheets/Aluminate/%0AGAL550-02-13.pdf. [Accessed: 01-Dec-2018].

[56] Michael Zollers, “Phosphor Modeling in LightTools.” [Online]. Available: https://www.synopsys.com/content/dam/synopsys/optical-solutions/documents/datasheets/modeling-phosphors-in-lighttools.pdf. [Accessed: 01-Dec-2018].

[57] J. Wang, J. C. C. Lo, S. W. R. Lee, F. Yun, and M. Tao, “Modeling and Parametric Study of Light Scattering, Absorption and Emission of Phosphor in a White Light-Emitting Diode,” in *Volume 2: Advanced Electronics and Photonics, Packaging Materials and Processing; Advanced Electronics and Photonics: Packaging, Interconnect and Reliability; Fundamentals of Thermal and Fluid Transport in Nano, Micro, and Mini Scales*, 2015, p. V002T02A046.

[58] S.-W. Jeon *et al.*, “Improvement of phosphor modeling based on the absorption of Stokes shifted light by a phosphor,” *Opt. Express*, vol. 22, no. S5, p. A1237, Aug. 2014.

[59] MICHELE WEHRWEIN ALBION, *THE FLORIDA LIFE OF THOMAS EDISON*. University Press of Florida, 2008.

[60] N. Holonyak and S. F. Bevacqua, “COHERENT (VISIBLE) LIGHT EMISSION FROM Ga(As 1− x P x ) JUNCTIONS,” *Appl. Phys. Lett.*, vol. 1, no. 4, pp. 82–83, Dec. 1962.

# VITA

**Halil İbrahim Kahvecioğlu**

**Research Areas:** Optics, Optical Analysis, Optical Measurement Systems, Light Sources, Solid-state lighting, Light Emitting Diodes, Energy Efficiency, Light conversion materials, and Spectroscopy

**Undergraduate:** Physics, Boğaziçi University, 2013

Halil İbrahim Kahvecioğlu received his B.Sc. in Physics from Boğaziçi University, Istanbul, 2013. He joined to Özyeğin University, Mechanical Engineering department for his M.Sc under the supervision of Mehmet Arık, and worked as optical engineer in Evateg Center, Özyeğin University. He was also responsible from optical measurement systems in Evateg Optic Laboratory. His research interests contain optical analysis, optical measurement systems, energy efficiency, lighting fixture modelling, solid-state lighting, blue and white light LEDs, light conversion materials, and spectroscopy.

---

Darkness cannot drive out darkness: only light can do that.

- Martin Luther King Jr.